

Testing Forecast Rationality for Measures of Central Tendency*

Timo Dimitriadis[†]

Andrew J. Patton[‡]

Patrick Schmidt[§]

This Version: May 24, 2022

First Version: February 15, 2019

Abstract

Rational respondents to economic surveys may report as a point forecast any measure of the central tendency of their (possibly latent) predictive distribution, for example the mean, median, mode, or any convex combination thereof. We propose tests of forecast rationality when the measure of central tendency used by the respondent is unknown. These tests require us to overcome an identification problem when the measures of central tendency are equal or in a local neighborhood of each other, as is the case for (exactly or nearly) symmetric and unimodal distributions. As a building block, we also present novel tests for the rationality of mode forecasts. We apply our tests to survey forecasts of individual income, Greenbook forecasts of U.S. GDP, and random walk forecasts for exchange rates. We find that the Greenbook and random walk forecasts are best rationalized as mean, or near-mean forecasts, while the income survey forecasts are best rationalized as mode forecasts.

Keywords: forecast evaluation, weak identification, survey forecasts, mode forecasts

J.E.L. Codes: C53, E37

*We thank Tilmann Gneiting, Adam Rosen, Melanie Schienle, as well as seminar participants at Duke University, KIT Karlsruhe, HITS Heidelberg, Universitt Hohenheim, CSS Workshop in Zrich, HKMetrics Workshop in Mannheim, ISI World Statistics Congress in Kuala Lumpur, and the 2019 Statistische Woche in Trier.

[†]Heidelberg Institute for Theoretical Studies, Heidelberg, Germany and University of Hohenheim, Germany, e-mail: timo.dimitriadis@h-its.org

[‡]Department of Economics, Duke University, Durham, USA, e-mail: andrew.patton@duke.edu

[§]Heidelberg Institute for Theoretical Studies, Heidelberg, Germany and Goethe University Frankfurt, Frankfurt, Germany, e-mail: p.schmidt@econ.uni-frankfurt.de

1 Introduction

Economic surveys are a rich source of information about future economic conditions. Most economic surveys, however, are vague about the specific statistical quantity the respondent is expected to report. For example, the New York Federal Reserve’s labor market survey asks respondents “What do you believe your annual earnings will be in four months?” A reasonable response to this question is the respondent reporting her *expectation* of future earnings, or her median, or her mode; all common measures of the central tendency of a distribution. When these measures coincide, as they do for symmetric unimodal distributions, this ambiguity does not affect the information content of the forecast. When these measures can differ, the specific measure adopted by the respondent can influence its use in other applications, and testing rationality of forecasts becomes difficult.

We consider the class of general central tendency measures defined by the set of convex combinations of the mean, median, and mode,¹ and we propose tests of forecast rationality that can be employed when the specific measure of central tendency used by the respondent is unknown. Similar to [Elliott et al. \(2005\)](#), we propose a testing framework that nests the mean as a special case, but unlike [Elliott et al. \(2005\)](#) we allow for alternative forecasts within the class of general measures of central tendency, rather than measures that represent other aspects of the predictive distribution (such as non-central quantiles or expectiles). Further, we face an identification problem: for symmetric distributions, the combination weight vector is unidentified, while for “mildly” asymmetric distributions, the weight vector is only weakly identified. Economic variables may or may not be asymmetrically distributed, and a valid testing approach must accommodate these measures of central tendency being equal, unequal, or in a local neighborhood of each other. We use the work of [Stock and Wright \(2000\)](#) to obtain asymptotically valid confidence sets for the combination weights and to test forecast rationality for a general measure of central tendency.

Before implementing the above test for rationality for a general forecast of central tendency, we must first overcome a lack of rationality tests for mode forecasts.² Rationality tests for mean

¹These are the three measures of central tendency described in standard introductory statistics textbooks, e.g. [McClave et al. \(2017\)](#). Our approach can be extended to consider a broader set of measures of centrality; we discuss this in Section 3.

²We use the phrase “mode forecasts,” or similar, as shorthand for the forecaster reporting the mode of her predictive distribution as her point forecast.

forecasts go back to at least [Mincer and Zarnowitz \(1969\)](#), see [Elliott and Timmermann \(2016\)](#) for a recent survey, while rationality tests for quantile forecasts (nesting median forecasts as a special case) are considered in [Christoffersen \(1998\)](#) and [Gaglianone et al. \(2011\)](#). A critical impediment to similar tests for mode forecasts is that the mode is not an “elicitable functional” ([Heinrich, 2014](#)), meaning that it cannot be obtained as the solution to an expected loss minimization problem.³ We obtain a test for mode forecast rationality by first proposing novel results on the *asymptotic elicibility* of the mode. We define a functional to be asymptotically elicitable if there exists a sequence of elicitable functionals that converges to the target functional. We consider the (elicitable) “generalized modal interval,” defined in detail in Section 2.2, and show that it converges to the mode for the class of strongly unimodal probability distributions. We combine these results with recent work on mode regression ([Kemp and Silva, 2012](#); [Kemp et al., 2019](#)) to obtain mode forecast evaluation tests analogous to well-known tests for mean and median forecasts.

We apply our proposed new tests in three important economic applications. We firstly analyze over 3,000 individual income survey responses from the Survey of Consumer Expectations conducted by the Federal Reserve Bank of New York. We find that we can reject rationality with respect to the mean or median, however we cannot reject rationality when interpreting these as mode forecasts, suggesting that survey participants report the anticipated *most likely* outcome (the mode) rather than the average or median. (Interestingly, only convex combinations very close to the mode are rationalizable; these survey respondents appear to report the mode or a functional very close to it.) When allowing for cross-respondent heterogeneity, we find that forecasts from survey respondents with income below the median and who are either employed in the private sector (as opposed to the government, non-profit or other sectors) or who are likely to change jobs in the coming period cannot be rationalized using any measure of central tendency. In contrast, forecasts from respondents with income above the median, regardless of the industry in which they work or their likelihood of changing jobs, can be rationalized using many different centrality measures.

³[Gneiting \(2011\)](#) provides an overview of elicibility and identifiability of statistical functionals and shows that several important functionals such as variance, Expected Shortfall, mode, minimum and maximum are not elicitable. [Fissler and Ziegel \(2016\)](#) introduce the concept of higher-order elicibility, which facilitates the elicitation of vector-valued (stacked) functionals such as the variance and Expected Shortfall, though not the mode ([Dearborn and Frongillo, 2019](#)).

We next analyze the Federal Reserve staff’s “Greenbook” forecasts of quarterly U.S. GDP. Consistent with these forecasts being constructed using econometric models, which generally focus on the mean, we find that we cannot reject rationality with respect to the mean, however we can reject with respect to the median and mode. Finally, we revisit the famous result of [Meese and Rogoff \(1983\)](#) that exchange rates are approximately unpredictable when evaluated by the squared-error loss function, i.e. the lagged exchange rate is an optimal mean forecast. For the USD/EUR and JPY/EUR exchange rates we find evidence consistent with this: the lagged exchange rate is not rejected as a mean forecast, while it is rejected when taken as a mode or median forecast. For the GBP/EUR exchange rate, on the other hand, we find we cannot reject rationality with respect to *any* of convex combination of these measures of central tendency; the random walk forecast is consistent with rationality under any of these measures.

We evaluate the finite sample performance of the new mode rationality test and of the proposed method for obtaining confidence sets for the measures of centrality through an extensive simulation study. We use cross-sectional and time-series data generating processes with a range of levels of asymmetry. We find that our proposed mode forecast rationality test has satisfactory size properties, even in small samples, and exhibits strong power across different misspecification designs, sample sizes, and skewness parameters. Our simulation design also provides us with a unified framework for considering the three identification cases that arise in our proposed rationality test for a general centrality forecast: strongly identified (skewed data), where the mean, median and mode differ; unidentified (symmetric unimodal data), where all centrality measures coincide; and weakly identified (mildly skewed data), where the centrality measures differ but are close to each other. We find that in the symmetric case, the resulting confidence sets contain (correctly) the entire set of convex combinations of mean, median and mode. In the asymmetric cases, our rationality test is able to identify the combination weights corresponding to the issued centrality forecast.

Our paper is related to the large literature on forecasting under asymmetric loss, see [Granger \(1969\)](#), [Christoffersen and Diebold \(1997\)](#), [Patton and Timmermann \(2007\)](#) and [Elliott et al. \(2008\)](#) amongst others. The work in these papers is motivated by the fact that forecasters may wish to use a loss function other than the omnipresent squared-error loss function. The use of asymmetric loss

functions generally leads to point forecasts that differ from the mean (though this is not always true, see [Gneiting, 2011](#) and [Patton, 2018](#)), and generally these point forecasts are not interpretable as measures of central tendency. For example, [Christoffersen and Diebold \(1997\)](#) show that the linex loss function implies an optimal point forecast that is a weighted sum of the mean and variance, while [Elliott et al. \(2008\)](#) find that their sample of macroeconomic forecasters report an expectile with asymmetry parameter around 0.4. Instead of moving from the mean to a forecast that is not a measure of location, we instead consider moving only *within* the general set of location measures defined by convex combinations of the mean, median, and mode.

Our paper is also related to experimental work on eliciting centrality measures from survey respondents. In an early psychological study, [Peterson and Miller \(1964\)](#) found that participants can accurately predict the mode and median, if incentivized correctly, but are unable to report accurate estimates of the mean. Other work on eliciting centrality measures includes [Hossain and Okui \(2013\)](#) for the mean, [Dufwenberg and Gneezy \(2000\)](#) and [Kirchkamp and Reiß \(2011\)](#) for the median, and [Charness and Dufwenberg \(2006\)](#) and [Sapienza et al. \(2013\)](#) for the modal interval.

The remainder of the paper is structured as follows. In [Section 2](#) we propose new forecast rationality tests for the mode based on the concepts of asymptotic elicitable and identifiable. [Section 3](#) presents forecast rationality tests for general measures of central tendency, allowing for weak identification. [Section 4](#) presents a simulation results on the finite-sample properties of the proposed tests, and [Section 5](#) presents empirical applications using survey forecasts of earnings, Greenbook forecasts of GDP growth, and the random-walk forecast for exchange rates. Proofs are presented in the appendix, and additional details are presented in a supplemental appendix.

2 Eliciting and Evaluating Mode Forecasts

2.1 General Forecast Rationality Tests

Let $Z_t = (Y_t, X_t, \tilde{\mathbf{h}}_t)$ be a stochastic process defined on a common probability space $(\Omega, \mathcal{F}, \mathbb{P})$. Y_{t+1} denotes the (scalar) variable of interest, $\tilde{\mathbf{h}}_t$ denotes a vector of variables known to the forecaster at the time she issues her point forecast for Y_{t+1} , which is denoted X_t . We define the information set

$\mathcal{F}_t = \sigma\{Y_s, X_s, \tilde{\mathbf{h}}_s; s \leq t\}$ as the σ -field containing all information known to the forecaster at time t . We assume the econometrician can observe an \mathcal{F}_t -measureable $(k \times 1)$ vector \mathbf{h}_t . We denote the distribution of Y_{t+1} given \mathcal{F}_t by F_t . Whenever they exists, we denote the corresponding densities by f_t and the expectations by $E_t[\cdot] = E[\cdot|\mathcal{F}_t]$. We use \mathcal{P} to denote a class of distributions.

We start by considering rationality tests (also known as calibration tests; [Nolde and Ziegel, 2017](#)) for the mean, i.e. we assume that the forecasts X_t are one-step ahead *mean* forecasts for Y_{t+1} . We are interested in testing if these forecasts are rational, which would imply the null hypothesis:

$$\mathbb{H}_0 : X_t = \mathbb{E}[Y_{t+1}|\mathcal{F}_t] \ \forall t \text{ a.s.} \quad (2.1)$$

This is carried out by considering the “identification function,” which for the mean is simply the difference between the forecast and the realized value, i.e., the forecast error:⁴

$$V_{Mean}(X_t, Y_{t+1}) = X_t - Y_{t+1} \equiv \varepsilon_t. \quad (2.2)$$

Under the above null hypothesis and subject to certain standard regularity conditions, it is straight forward to show that $T^{-1/2} \sum_{t=1}^T V_{Mean}(X_t, Y_{t+1}) \mathbf{h}_t \xrightarrow{d} \mathcal{N}(0, \Omega_{Mean})$, and that

$$J_T = \frac{1}{T} \left(\sum_{t=1}^T V_{Mean}(X_t, Y_{t+1}) \mathbf{h}_t^\top \right) \hat{\Omega}_{T, Mean}^{-1} \left(\sum_{t=1}^T V_{Mean}(X_t, Y_{t+1}) \mathbf{h}_t \right) \xrightarrow{d} \chi_k^2 \quad (2.3)$$

as $T \rightarrow \infty$. This asymptotic result facilitates testing whether given forecasts X_t are rational mean forecasts for the realizations Y_{t+1} . Specifically, the statistic in equation (2.3) can be used to test whether the identification function $V_{Mean}(X_t, Y_{t+1})$ is correlated with the instrument vector \mathbf{h}_t . Under the null of forecast rationality, this correlation should be zero. Like most other tests in the literature, this is only a test of a necessary condition for forecast rationality, and the conclusion may be sensitive to the choice of instruments, \mathbf{h}_t .

The test statistic in equation (2.3) is only informative about forecast rationality if the forecasts

⁴In econometrics the forecast error is usually defined as $Y_{t+1} - X_t$, that is, as the negative of the identification function in equation (2.2). Given the important role that forecast identification functions play in this paper, we use the definition for ε_{t+1} given in equation (2.2), and we refer to ε_{t+1} as the forecast error.

are interpreted as forecasts for the *mean* of Y_{t+1} . The decision-theoretic framework of identification functions and consistent loss functions, see [Gneiting \(2011\)](#) for discussion, is fundamental for generalizations to other measures of central tendency, such as the median and the mode.

For a general real-valued functional $\Gamma : \mathcal{P} \rightarrow \mathbb{R}$, a strict identification function $V_\Gamma(Y, x)$ is defined by being zero in expectation, if and only if x equals the functional $\Gamma(F)$. Strict identification functions are generally obtained as the derivatives of strictly consistent loss functions, which are defined as having the functional $\Gamma(F)$ as their unique minimizer (in expectation). A functional is called *identifiable* if a strict identification function exists, and is called *elicitable* if a strictly consistent loss function exists. See [Gneiting \(2011\)](#) for a general introduction to elicibility and identifiability.

The forecast error $X_t - Y_{t+1}$ is a strict identification function for the mean, and a strict identification function for the median is given by the step function

$$V_{Med}(X_t, Y_{t+1}) = \mathbb{1}_{\{Y_{t+1} > X_t\}} - \mathbb{1}_{\{Y_{t+1} \leq X_t\}}. \quad (2.4)$$

Hence, we can obtain a test of median forecast rationality by simply replacing V_{Mean} by V_{Med} in equation (2.3).

2.2 The Mode Functional

In contrast to the mean and the median, rationality tests for mode forecasts are more challenging to consider. The underlying reason is that there do not exist identification functions for the mode for absolutely continuous distributions ([Heinrich, 2014](#); [Dearborn and Frongillo, 2019](#)). For our discussion below, we make the following distinction in the notion of *unimodality*.

Definition 2.1. *We say that an absolutely continuous distribution is (a) weakly unimodal if it has a unique and well-defined mode, and (b) strongly unimodal if it is weakly unimodal and does not have further local modes.*

[Heinrich \(2014\)](#) and [Dearborn and Frongillo \(2019\)](#) show that there do not exist any strictly consistent loss or strict identification functions for the mode for the class of weakly unimodal

distributions. While this does not imply that there do not exist any such functions for the class of strongly unimodal distributions, none have yet been found.

As pointed out in [Gneiting \(2011\)](#), it is sometimes stated informally that the mode is an optimal point forecast under the following loss function $L_\delta(x, Y) = \mathbb{1}_{\{|x-Y| \leq \delta\}}$ for some fixed $\delta > 0$. In fact, this loss function elicits the midpoint of the modal interval (also known as the modal midpoint, or MMP) of length 2δ . The MMP is defined as the midpoint of the interval of length 2δ that contains the highest probability,

$$\text{MMP}_\delta(P) := \sup_{x \in \mathbb{R}} P(Y \in [x - \delta, x + \delta]) \quad (2.5)$$

In a similar manner, [Eddy \(1980\)](#), [Kemp and Silva \(2012\)](#) and [Kemp et al. \(2019\)](#) propose estimation of the (conditional) mode through estimating the modal interval with an asymptotically shrinking length. We formalize these ideas in the decision-theoretical framework through the following definition.

Definition 2.2. *We say that the functional $\Gamma : \mathcal{P} \rightarrow \mathbb{R}$ is asymptotically elicitable (identifiable) relative to \mathcal{P} if there exists a sequence of elicitable (identifiable) functionals $\Gamma_k : \mathcal{P} \rightarrow \mathbb{R}$, $k \in \mathbb{N}$, such that $\Gamma_k(P) \rightarrow \Gamma(P)$ for all $P \in \mathcal{P}$.*

For any $\delta > 0$ small enough, the modal midpoint is well-defined for all distributions with unique and well-defined mode and it holds that $\lim_{\delta \downarrow 0} \text{MMP}_\delta(P) = \text{Mode}(P)$ ([Gneiting, 2011](#)). This establishes *asymptotic elicibility* for the mode functional for the class of weakly unimodal probability distributions with Lebesgue densities. Unfortunately, this does not directly allow for asymptotic *identifiability* of the mode as any pseudo-derivative of the loss function L_δ equals zero. We establish asymptotic identifiability of the mode through the *generalized modal midpoint*.

Definition 2.3. *We define the generalized modal midpoint as the functional with parameter δ as the minimizer of the (expected) loss function*

$$\Gamma_\delta(P) = \arg \min_{x \in \mathbb{R}} \mathbb{E} [L_\delta^K(x, Y)], \quad \text{where} \quad L_\delta^K(x, Y) = -\frac{1}{\delta} K\left(\frac{x - Y}{\delta}\right), \quad (2.6)$$

where $K(\cdot)$ denotes some kernel function.

While the classical modal midpoint is nested in this definition by using a rectangular kernel for $K(u) = \mathbf{1}_{\{|u| \leq 1\}}$, this definition further allows for smooth generalizations. As the definition of Γ_δ in Definition 2.3 involves the argmin of a function, we first establish that this is well-defined and that it converges to the mode functional.

Proposition 2.4. *For the class of distributions \mathcal{P} consists of absolutely continuous unimodal distributions with bounded density and for any kernel function K which is positive, smooth, $\int K(u)du = 1$ and $\log(K(u))$ is a concave function, the functional Γ_δ induced by the loss function (2.6) is well-defined for all $\delta > 0$ and for $\delta \rightarrow 0$, it holds that $\Gamma_\delta(P) \rightarrow \text{Mode}(P)$ for all $P \in \mathcal{P}$.*

The proof of Proposition 2.4 is given in Appendix A.

If we further impose that the kernel K is strictly decreasing to the right and strictly increasing to the left of its maximum at zero, then $x = Y$ is the only critical point of $L_\delta^K(x, Y)$. Thus,

$$V_\delta^K(x, Y) = \frac{\partial}{\partial x} L_\delta^K(x, Y) = -\frac{1}{\delta^2} K' \left(\frac{x - Y}{\delta} \right) \quad (2.7)$$

is a strict identification function for Γ_δ . This establishes that the mode functional is both asymptotically identifiable and asymptotically elicitable for the class of absolutely continuous and strongly unimodal distributions with bounded density.

2.3 Forecast Rationality Tests for the Mode

Having established the asymptotic identifiability of the mode in the previous section, we now consider rationality testing of mode forecasts, i.e. testing the following null hypothesis,

$$\mathbb{H}_0 : X_t = \text{Mode}(Y_{t+1} | \mathcal{F}_t) \quad \forall t \text{ a.s.} \quad (2.8)$$

While classical, \sqrt{T} -consistent rationality tests based on strict identification functions are unavailable for the mode due to its non-identifiability, we next propose a rationality test for mode forecasts based on an asymptotically shrinking bandwidth parameter δ_T . Consider the (asymptotically valid)

identification function V_δ , multiplied by the instruments \mathbf{h}_t and with bandwidth δ_T ,

$$\psi(Y_{t+1}, X_t, \mathbf{h}_t, \delta_T) = V_{\delta_T}^K(X_t, Y_{t+1})\mathbf{h}_t = -\frac{1}{\delta_T^2}K'\left(\frac{X_t - Y_{t+1}}{\delta_T}\right)\mathbf{h}_t. \quad (2.9)$$

We make the following assumptions.

Assumption 2.5.

- (A1) *The sequence (Y_t, X_t, \mathbf{h}_t) is stationary and ergodic.*
- (A2) *It holds that $\mathbb{E}[\|\mathbf{h}_t\|^{2+\delta}] < \infty$.*
- (A3) *The matrix $\mathbb{E}[\mathbf{h}_t\mathbf{h}_t^\top]$ has full rank for all $t = 1, \dots, T$.*
- (A4) *The conditional distribution of $\varepsilon_t = X_t - Y_{t+1}$ given \mathcal{F}_t is absolutely continuous with density $f_t(\cdot)$ which is three times continuously differentiable with bounded derivatives.*
- (A5) *$K : \mathbb{R} \rightarrow \mathbb{R}$, $u \mapsto K(u)$ is a continuously differentiable kernel function such that: (i) $\int K(u)du = 1$, (ii) $\sup K(u) \leq c < \infty$, (iii) $\sup K'(u) \leq c < \infty$, (iv) $\int uK(u)du = 0$, (v) $\int u^2K(u)du = c < \infty$, (vi) $\int (K'(u))^2 du = M < \infty$.*
- (A6) *δ_T is a strictly positive and non-stochastic bandwidth such that for $T \rightarrow \infty$, (i) $T\delta_T \rightarrow \infty$, and (ii) $T\delta_T^7 \rightarrow 0$.*

The above assumptions are a combination of standard assumptions from rationality testing and nonparametric statistics. Condition (A1) facilitates the usage of a standard CLT and allows for both time-series and cross-sectional applications. For non-stationary data, this can be replaced by the assumption of an α -mixing process (see e.g. White (2001), Section 5.4) by slightly strengthening the moment condition (A2). In cross-sectional applications with independent observations, this assumption can be replaced (and weakened) by the classical Lindeberg condition (see e.g. White (2001), Section 5.2). Condition (A2) is a standard moment assumption in time-series applications. Notice that as the kernel function K' is bounded, we do not require existence of any moments of Y_t or X_t , which makes this more flexible than rationality testing for mean forecasts. The classical

full rank condition (A3) prevents the instruments from being perfectly colinear which in turn prevents the asymptotic covariance matrix from being singular. Assumption (A4) assumes a relatively smooth behavior of the conditional density function which is required to apply a Taylor expansion common to the nonparametric literature. The conditions (A5) are standard conditions on kernels in the nonparametric literature. We discuss additional details in Supplemental Appendix S.1. The bandwidth assumption (A6) implies that δ_T shrinks to zero at an appropriate rate. We discuss the choice of δ_T in Supplemental Appendix S.2.

Theorem 2.6. *Under $\mathbb{H}_0 : X_t = \text{Mode}(Y_{t+1}|\mathcal{F}_t)$ almost surely and Assumption 2.5, it holds that*

$$\delta_T^{3/2} T^{-1/2} \sum_{t=1}^T \psi(Y_{t+1}, X_t, \mathbf{h}_t, \delta_T) \xrightarrow{d} \mathcal{N}(0, \Omega_{Mode}) \quad (2.10)$$

as $T \rightarrow \infty$, where $\Omega_{Mode} = \mathbb{E} [\mathbf{h}_t \mathbf{h}_t^\top f_t(0)] \int K'(u)^2 du$.

The proof of Theorem 2.6 is given in Appendix A. As the identification functions are only *asymptotically* valid, we enhance the conventional approach with techniques known from the literature of nonparametric estimation. As a consequence, we do not obtain \sqrt{T} convergence of the random process but convergence at some slower rate captured by the factor $\delta_T^{3/2}$ in Equation (2.10). The limitations of condition (A6) imply that $\delta_T \propto T^{-\kappa}$ where $\kappa \in (1/7, 1)$. In practice, the fastest convergence is obtained by choosing $\delta_T \approx T^{-1/7}$ resulting in a convergence rates close to $T^{2/7}$.

The speed of convergence may be increased via the use of *higher-order* kernel functions, see e.g. Li and Racine (2006) for discussion. This would require a Taylor expansion of higher order in the proof of Lemma S.3.1. Using this method the speed of convergence can generally be made arbitrarily close to \sqrt{T} , however, at the cost of stricter smoothness assumptions on the density function and unstable kernel functions. The rate $\delta_T \approx T^{-1/7}$ is a strict bound in the absence of additional smoothness assumptions on the density f_t . Furthermore, the generalized modal midpoint from Definition 2.3 requires a log-concave kernel to be well-defined and unique (see the assumptions of Proposition 2.4). This assumption is automatically violated for higher-order kernels.

We utilize a Gaussian kernel in our analysis for two reasons. First, while infinite support kernels yield to slightly less efficient estimates in nonparametric literature (Li and Racine, 2006),

the identification function $V_\delta(Y, x)$ is a strict identification function if and only if K is infinitely supported and strictly increasing (decreasing) left (right) of its mode. Second, we do not observe a loss in test power compared to the relatively efficient quartic (or biweight) kernel. We refer to Supplemental Appendix S.1 for a further discussion of the kernel choice.

Following Kemp and Silva (2012) and Kemp et al. (2019), we estimate the covariance matrix by its sample counterpart,

$$\hat{\Omega}_{T, Mode} = \frac{1}{T} \sum_{t=1}^T \delta_T^{-1} K' \left(\frac{X_t - Y_{t+1}}{\delta_T} \right)^2 \mathbf{h}_t \mathbf{h}_t^\top. \quad (2.11)$$

The following theorem shows consistency of the asymptotic covariance estimator.

Theorem 2.7. *Given that Assumption 2.5 holds, it holds that*

$$\hat{\Omega}_{T, Mode} \xrightarrow{P} \Omega_{Mode}. \quad (2.12)$$

The proof of Theorem 2.7 is given in Appendix A. We can now define the Wald test statistic:

$$J_T = \left(\delta_T^{3/2} T^{-1/2} \sum_{t=1}^T \psi(Y_{t+1}, X_t, \mathbf{h}_t, \delta_T) \right)^\top \hat{\Omega}_{T, Mode}^{-1} \left(\delta_T^{3/2} T^{-1/2} \sum_{t=1}^T \psi(Y_{t+1}, X_t, \mathbf{h}_t, \delta_T) \right). \quad (2.13)$$

The following statement follows directly from Theorem 2.6 and Theorem 2.7.

Corollary 2.8. *Under $\mathbb{H}_0 : X_t = \text{Mode}(Y_{t+1} | \mathcal{F}_t) \forall t$ a.s. and Assumption 2.5, it holds that*

$$J_T \xrightarrow{d} \chi_k^2. \quad (2.14)$$

This corollary justifies an asymptotic test at level $\alpha \in (0, 1)$ which rejects \mathbb{H}_0 when $J_T > Q_k(1 - \alpha)$, where $Q_k(1 - \alpha)$ denotes the $(1 - \alpha)$ quantile of the χ_k^2 distribution.

We now turn to the behavior of our test statistic J_T under the alternative hypothesis. For this, we consider the alternative hypothesis:

$$\mathbb{H}_A : |f'_t(0)| \geq \varepsilon \quad \text{a.s. for some } \varepsilon > 0 \quad \text{and for all } t = 1, \dots, T. \quad (2.15)$$

The following theorem characterizes the behavior of our mode rationality test under this alternative hypothesis.

Theorem 2.9. *If $\mathbb{E}[\mathbf{h}_t] \neq 0$ and $T\delta_T^3 \rightarrow \infty$, then under Assumption 2.5 and the alternative hypothesis, \mathbb{H}_A ,*

$$\mathbb{P}(J_T \geq c) \rightarrow 1 \quad (2.16)$$

for any constant $c \in \mathbb{R}$.

The assumption $\mathbb{E}[\mathbf{h}_t] \neq 0$ is trivially fulfilled when the vector of instruments contain a constant. The assumption $T\delta_T^3 \rightarrow \infty$ is fulfilled using our bandwidth choice, described in Supplemental Appendix S.2. While our mode rationality test has asymptotically correct size for the class of weakly unimodal distributions, it only has power against points of non-flat conditional density f_t . (This can be interpreted as uniform power against the class of strongly unimodal distributions.) This can be seen as a drawback of our test as it cannot reject forecasts which are far in the tail, where the density is almost flat. However, this test is intended to be applied to forecasts of some measure of central tendency, and such forecasts will lie broadly in the central region of the distribution where this concern does not arise.

3 Evaluating Forecasts of Measures of Central Tendency

We define the class of measures of central tendency as the set defined by convex combinations of the mean, median and mode,⁵ and we next propose identification-robust tests of whether *any* element of the class is consistent with forecast rationality.

Our approach is related to, but distinct from, Elliott et al. (2005). These authors consider the case that a respondent’s point forecast corresponds to some quantile (or expectile) of her predictive distribution. They employ a parametric loss function (“lin-lin” for quantiles, “quad-quad” for expectiles), $L(Y, X; \alpha)$ with a scalar unknown parameter (α) characterizing the asymmetry of the

⁵We focus on these three measures as foundational centrality measures, but our testing approach can easily be extended to include other measures, e.g. the trimmed mean, Huber’s (1964) robust centrality measure, Barendse’s (2017) “interquantile expectation,” and others.

loss. Elliott et al. (2005) then use GMM to estimate the asymmetry parameter that best describes the sequence of forecasts and realizations, and test whether forecast rationality holds at the estimated probability level. In contrast, we work with weighted averages of identification functions, not parametric loss functions, and we are forced to accommodate the fact that our unknown parameter may be unidentified or weakly identified, which precludes point estimation.

Our analysis begins by considering the $(3 \times k)$ matrix $\psi_{t,T}$ defined below, the rows of which are comprised of the strict identification functions for the mean and median, and the asymptotically valid choice for the mode (as discussed in the previous section), multiplied by the \mathcal{F}_t -measurable $(k \times 1)$ vector of instruments \mathbf{h}_t . We normalize each of these using positive definite matrices, $\widehat{\mathbf{W}}_{T,\text{Mean}}$, $\widehat{\mathbf{W}}_{T,\text{Med}}$ and $\widehat{\mathbf{W}}_{T,\text{Mode}}$, which may depend on the sample. For example, one could use the identity matrix, the square-root of the inverse sample covariance matrix, or some other matrix.

$$\psi_{t,T} = T^{-1/2} \begin{pmatrix} \mathbf{h}_t^\top & \widehat{\mathbf{W}}_{T,\text{Mean}} & \varepsilon_t \\ \mathbf{h}_t^\top & \widehat{\mathbf{W}}_{T,\text{Med}} & \mathbb{1}_{\{\varepsilon_t > 0\}} - \mathbb{1}_{\{\varepsilon_t < 0\}} \\ \mathbf{h}_t^\top & \widehat{\mathbf{W}}_{T,\text{Mode}} & \delta_T^{-1/2} K' \left(\frac{-\varepsilon_t}{\delta_T} \right) \end{pmatrix} \quad (3.1)$$

where $\varepsilon_t = X_t - Y_{t+1}$ denotes the forecast error.

For any weight vector $\theta \in \Theta = \{\theta \in \mathbb{R}^3 : \|\theta\|_1 = 1, \theta \geq 0\}$, we define the k -dimensional random variable $\phi_{t,T}(\theta)$ as a combination of the three individual (normalized and interacted with the instrument vector) identification functions:

$$\phi_{t,T}(\theta) = \theta^\top \psi_{t,T}, \quad (3.2)$$

It is important to note that the convex combination of identification functions defined by the vector θ does not necessarily lead to a forecast that is the *same* convex combination of the underlying measures of central tendency. (For example, an equal-weighted combination of the identification functions will *not* generally lead to a forecast that is an equal-weighted combination of the mean, median and mode; it will generally be some other convex combination.) At the vertices the weights are clearly identical, but for non-degenerate combinations the weights will generally differ, though

they will also lie in the three-dimensional unit simplex, Θ .

Consider the GMM objective function based on the above convex combination:

$$S_T(\theta) = \left[\sum_{t=1}^T \phi_{t,T}(\theta) \right]^\top \widehat{\Sigma}_T^{-1}(\theta) \left[\sum_{t=1}^T \phi_{t,T}(\theta) \right], \quad (3.3)$$

where $\widehat{\Sigma}_T^{-1}(\theta)$ denotes an $O_p(1)$ positive definite weighting matrix, which may depend on the parameter θ . Unlike the problem in [Elliott et al. \(2005\)](#), the unknown parameter in our framework (the weight vector θ) cannot be assumed to be well identified. For symmetric distributions, the combination weights applied to the mean and median identification functions are unidentified, and for symmetric unimodal distributions the entire vector is unidentified. For distributions that exhibit only mild asymmetry a weak identification problem arises. The distribution of economic variables may or may not exhibit asymmetry, and so this identification problem is a first-order concern.

The possibility that the true parameter θ_0 is unidentified or weakly identified implies that the objective function $S_T(\theta)$ may be flat or almost flat in a neighborhood of θ_0 , ruling out consistent estimation of θ_0 . [Stock and Wright \(2000\)](#) show that, under regularity conditions, we can nevertheless construct asymptotically valid confidence bounds for θ_0 , by showing that the objective function S_T evaluated at θ_0 continues to exhibit an asymptotic χ^2 distribution. This facilitates the construction of asymptotically valid confidence bounds even in a setting where the parameter vector may be strongly identified, weakly identified, or unidentified.

For the technical treatment of this approach, we define the counterpart of $\phi_{t,T}(\theta)$ that depends on the probability limits of the weighting matrices: $\tilde{\phi}_{t,T}(\theta) = \theta^\top \tilde{\psi}_{t,T}$, where

$$\tilde{\psi}_{t,T} = T^{-1/2} \begin{pmatrix} \mathbf{h}_t^\top & \mathbf{W}_{\text{Mean}} & \varepsilon_t \\ \mathbf{h}_t^\top & \mathbf{W}_{\text{Med}} & \mathbb{1}_{\{\varepsilon_t > 0\}} - \mathbb{1}_{\{\varepsilon_t < 0\}} \\ \mathbf{h}_t^\top & \mathbf{W}_{\text{Mode}} & \delta_T^{-1/2} K' \left(\frac{-\varepsilon_t}{\delta_T} \right) \end{pmatrix}, \quad (3.4)$$

and where \mathbf{W}_{Mean} , \mathbf{W}_{Med} and \mathbf{W}_{Mode} , denote the probability limits of $\widehat{\mathbf{W}}_{T,\text{Mean}}$, $\widehat{\mathbf{W}}_{T,\text{Med}}$ and $\widehat{\mathbf{W}}_{T,\text{Mode}}$. We make the following assumption.

Assumption 3.1. *There exist $\theta_0 \in \Theta$ and sequences $\phi_{t,T}^*(\theta_0)$ and $u_{t,T}(\theta_0)$, such that*

$$\tilde{\phi}_{t,T}(\theta_0) := \phi_{t,T}^*(\theta_0) + u_{t,T}(\theta_0), \quad (3.5)$$

and

- (A) $\left\{ \phi_{t,T}^*(\theta_0), \mathcal{F}_{t+1} \right\}$ is a martingale difference sequence.
- (B) $\sum_{t=1}^T (u_{t,T}(\theta_0)\lambda)^2 \xrightarrow{P} 0$ and $\sum_{t=1}^T \mathbb{E} [\|u_{t,T}(\theta_0)\|^{2+\delta}] \rightarrow 0$
- (C) $\sum_{t=1}^T u_{t,T}(\theta_0)\tilde{\phi}_{t,T}(\theta_0) \xrightarrow{P} 0$ and $\sum_{t=1}^T \mathbb{E} [u_{t,T}(\theta_0)\tilde{\phi}_{t,T}(\theta_0)] \rightarrow 0$

The decomposition in equation (3.5) implies that the sequence $\tilde{\phi}_{t,T}(\theta_0)$ is an *approximate* or *asymptotic* martingale difference sequence (MDS) in the sense that $\tilde{\phi}_{t,T}(\theta_0)$ can be decomposed into a MDS $\phi_{t,T}^*(\theta_0)$ and some asymptotically vanishing sequence $u_{t,T}(\theta_0)$. While this assumption seems to be unintuitive at first sight, we first explain in the following why it is necessary and subsequently discuss its validity.

The above assumption of an approximate MDS is weaker than the standard MDS assumption,

$$\exists \theta_0 \in \Theta \text{ s.t. } \left\{ \tilde{\phi}_t(\theta_0), \mathcal{F}_{t+1} \right\} \text{ is a MDS.} \quad (3.6)$$

However, an exact MDS assumption as in (3.6) does not hold for the baseline case that X_t is a true mode forecast, as in this case the MDS assumption only holds asymptotically. We refer to the proof of Theorem 2.6 in Appendix A for details on this. Furthermore, the classically imposed (weaker) assumption

$$\exists \theta_0 \in \Theta \text{ s.t. } \mathbb{E} [\tilde{\phi}_t(\theta_0)] = 0, \quad (3.7)$$

is too weak for our case. Given (3.7), in order to apply CLT for stationary and ergodic (or strong mixing) assumptions without the MDS assumption, we need that moments of order $2 + \delta$ (or $r > 2$) are finite, which is not fulfilled for the mode case as these moments diverge arbitrarily slowly through the bandwidth parameter δ_T .

Assumption 3.1 is an intermediate case of classically-imposed conditions (3.6) and (3.7). It can easily be shown to hold for the three vertices, where the forecast is the mean, median or mode. Specifically, when X_t is a mean or median forecast (i.e. $\theta_0 = (1, 0, 0)$ or $\theta_0 = (0, 1, 0)$), set $u_{t,T}(\theta_0) = 0$ and $\{\tilde{\phi}_{t,T}(\theta_0), \mathcal{F}_{t+1}\}$ is obviously a MDS. When X_t is the true conditional mode of Y_{t+1} , (i.e. $\theta_0 = (0, 0, 1)$), set

$$u_{t,T}(\theta_0) = \mathbb{E}_t \left[\tilde{\phi}_{t,T}(\theta_0) \right] = (T\delta_T)^{-1/2} \mathbb{E}_t \left[K' \left(\frac{-\varepsilon_t}{\delta_T} \right) \right] \mathbf{h}_t^\top. \quad (3.8)$$

as in the proof of Theorem 2.6. The conditions on $u_{t,T}(\theta_0)$ in Assumption 3.1 are fulfilled by the arguments given in the proof of Theorem 2.6 and Lemma S.3.1 - Lemma S.3.4. When X_t is a convex combination of a mean and median forecast, i.e. $\theta_0 = (\xi, 1 - \xi, 0)$ for some $\xi \in [0, 1]$, we set $u_{t,T}(\theta_0) = 0$ and $\{\tilde{\phi}_{t,T}(\theta_0), \mathcal{F}_{t+1}\}$ is again a MDS. When X_t is a convex combination with non-zero weight on the mode Assumption 3.1 is difficult to verify.

We further impose the following regularity conditions on our process.

Assumption 3.2. (a) $\mathbb{E} [\varepsilon_t^2] < \infty$ and (b) $\widehat{\mathbf{W}}_{T,Mean} \xrightarrow{P} \mathbf{W}_{Mean}$, $\widehat{\mathbf{W}}_{T,Med} \xrightarrow{P} \mathbf{W}_{Med}$, and $\widehat{\mathbf{W}}_{T,Mode} \xrightarrow{P} \mathbf{W}_{Mode}$ for some positive definite matrices \mathbf{W}_{Mean} , \mathbf{W}_{Med} and \mathbf{W}_{Mode} .

Theorem 3.3 below presents the asymptotic distribution of the process $\sum_{t=1}^T \phi_{t,T}(\theta_0)$ at the true parameter θ_0 . The proof is given in Appendix A.

Theorem 3.3. *Given Assumption 2.5, Assumption 3.1 and Assumption 3.2, it holds that*

$$\sum_{t=1}^T \phi_{t,T}(\theta_0) \xrightarrow{d} \mathcal{N}(0, \Sigma(\theta_0)), \quad (3.9)$$

where

$$\begin{aligned} \Sigma(\theta_0) = & \mathbb{E} \left[\theta_{10}^2 \mathbf{W}_{Mean} \mathbf{h}_t \mathbf{h}_t^\top \mathbf{W}_{Mean} \varepsilon_t^2 + \theta_{20}^2 \mathbf{W}_{Med} \mathbf{h}_t \mathbf{h}_t^\top \mathbf{W}_{Med} (\mathbb{1}_{\{\varepsilon_t > 0\}} - \mathbb{1}_{\{\varepsilon_t < 0\}})^2 \right. \\ & + \theta_{30}^2 \mathbf{W}_{Mode} \mathbf{h}_t \mathbf{h}_t^\top \mathbf{W}_{Mode} f_t(0) \int K'(u)^2 du \\ & \left. + 2\theta_{10}\theta_{20} \mathbf{W}_{Mean} \mathbf{h}_t \mathbf{h}_t^\top \mathbf{W}_{Med} \varepsilon_t (\mathbb{1}_{\{\varepsilon_t > 0\}} - \mathbb{1}_{\{\varepsilon_t < 0\}}) \right]. \end{aligned} \quad (3.10)$$

Under the null hypothesis, Assumption 3.1 implies that $\phi_{t,T}(\theta_0)$ is an approximate MDS, i.e.

this sequence is approximately (asymptotically, as $T \rightarrow \infty$) uncorrelated. Consequently, we do not need to rely on HAC covariance estimation, and can instead estimate the asymptotic covariance matrix using the simple sample covariance matrix:

$$\widehat{\Sigma}_T(\theta) = \frac{1}{T} \sum_{t=1}^T \phi_{t,T}(\theta) \phi_{t,T}(\theta)^\top. \quad (3.11)$$

The next theorem shows consistency of the outer product covariance estimator.

Theorem 3.4. *Given Assumption 2.5, Assumption 3.1, Assumption 3.2, it holds that*

$$\widehat{\Sigma}_T(\theta) \xrightarrow{P} \Sigma(\theta_0). \quad (3.12)$$

Corollary 3.5. *Given Assumption 2.5, Assumption 3.1, Assumption 3.2, it holds that $S_T(\theta_0) \xrightarrow{d} \chi_k^2$ as $T \rightarrow \infty$.*

Following [Stock and Wright \(2000\)](#), this corollary allows to construct asymptotically valid confidence regions for θ_0 with coverage probability $(1 - \alpha)\%$ by considering the set

$$\{\theta_0 : S_T(\theta_0) \leq Q_k(1 - \alpha)\}, \quad (3.13)$$

where $Q_k(1 - \alpha)$ denotes the $(1 - \alpha)$ quantile of the χ_k^2 distribution.

Given the above results, we implement a test for forecast rationality for a general measure of central tendency by evaluating the GMM objective function using a dense grid of convex combination parameters $\theta_j \in \Theta$ for $j = 1, \dots, J$. An asymptotically valid confidence set is given by the values of θ_j for which $S_T(\theta_j) \leq Q_k(1 - \alpha)$. These values represent the centrality measures that “rationalize” the observed sequence of forecasts and realizations, in that rationality cannot be rejected for these measures of centrality. It is possible that the confidence set is empty, in which case we reject rationality at the α significance level for the *entire class* of general centrality measures.

4 Simulation Study

This section studies the finite-sample performance of the methods proposed above. Section 4.1 presents simulations for the mode rationality test and Section 4.2 analyzes the test for rationality for general measures of central tendency.

4.1 Rationality tests for mode forecasts

In order to evaluate the finite-sample properties of our mode rationality test, we simulate data from the following data generating processes (DGPs), which cover the standard data assumptions in the classical cases of possible applications. We consider two cross-sectional DGPs, one homoskedastic and the other heteroskedastic, and two time-series DGPs, a simple AR(1) and an AR(1)-GARCH(1,1). We simulate data using the following unified framework:

$$Y_{t+1} = Z_t^\top \zeta + \sigma_{t+1} \varepsilon_{t+1}, \quad \text{where} \quad \varepsilon_{t+1} \stackrel{iid}{\sim} \mathcal{SN}(0, 1, \gamma), \quad (4.1)$$

where $\mathcal{SN}(0, 1, \gamma)$ is a skewed standard Normal distribution, and Z_t denotes a vector of covariates (possibly including lagged values of Y_{t+1}), ζ denotes a parameter vector and σ_{t+1} denotes a conditional variance process. Using this general formulation, we consider four cases:

- (1) Homoskedastic cross-sectional data: $Z_t \sim \text{iid } \mathcal{N}((1, 1, -1, 2), \text{diag}(0, 1, 1, 0.1))$, where $\zeta = (1, 1, 1, 1)$ and $\sigma_{t+1} = 1$.
- (2) Heteroskedastic cross-sectional data: $Z_t \sim \text{iid } \mathcal{N}((1, 1, -1, 2), \text{diag}(0, 1, 1, 0.1))$, where $\zeta = (1, 1, 1, 1)$ and $\sigma_{t+1} = 0.5 + 1.5(t + 1)/T$.
- (3) AR(1) data: $Z_t = Y_t$ with $\zeta = 0.5$ and $\sigma_{t+1} = 1$.
- (4) AR(1)-GARCH(1,1) data: $Z_t = Y_t$, where $\zeta = 0.5$ and $\sigma_{t+1} = 0.1 + 0.8\sigma_t^2 + 0.1\sigma_t^2\varepsilon_t^2$.

All the above DGPs are based on a skewed Gaussian residual distribution with skewness parameter γ . This choice nests the case of a standard Gaussian distribution at $\gamma = 0$, and in this case all measures of centrality coincide. As the skewness parameter increases in magnitude, the measures of centrality increasingly diverge.

For the general DGP in (4.1), optimal one-step ahead mode forecasts are given by

$$X_t = \text{Mode}(Y_{t+1}|\mathcal{F}_t) = Z_t^\top \zeta + \sigma_{t+1} \text{Mode}(\varepsilon_t), \quad (4.2)$$

where $\text{Mode}(\varepsilon_t)$ depends on the skewness parameter γ .

We consider a range of skewness parameters, $\gamma \in \{0, 0.1, 0.25, 0.5\}$, and sample sizes $T \in \{100, 500, 2000, 5000\}$. In all cases we use 10,000 replications. In order to evaluate the size of our test in finite samples, we generate optimal mode forecasts through equation (4.2) and apply the mode forecast rationality test based on three choices of instruments: we use the instrument choices $\mathbf{h}_{t,1} = 1$ and $\mathbf{h}_{t,2} = (1, X_t)$ for all DGPs; for the two cross-sectional DGPs, our third choice of instruments is $\mathbf{h}_{t,3} = (1, X_t, Z_{t,1})$, while for the two time-series DGPs we use $\mathbf{h}_{t,3} = (1, X_t, Y_{t-1})$.⁶

Table 1 presents the finite-sample size of the tests under the different DGPs, sample sizes, instrument choices, and skewness parameters. In all cases we use a Gaussian kernel and a set the nominal size to 5%. Results for a biweight kernel and nominal test sizes of 1% and 10% are given in Table S.4 to Table S.8 in the supplementary appendix.

We find that our mode rationality test leads to finite-sample rejection rates close to the nominal test size, across all of the different choices of DGPs, instruments, skewness parameters. We find similar results for different significance levels and kernel choices, reported in tables in the supplementary appendix. Table 1 reveals that an increasing degree of skewness in the underlying conditional distribution negatively influences the tests' performance. This is explained by the fact that for an increasing skewness, we choose a smaller bandwidth parameter (following the rule of thumb described in Supplemental Appendix S.2) resulting in less efficient estimates. Consequently, for highly skewed distributions, the mode rationality test requires larger sample sizes in order to converge to the nominal test size.

To analyze the power of the test, we introduce two misspecification designs:

(a) **Bias:** $\tilde{X}_t = X_t + \kappa \sigma_X$, where $\sigma_X = \sqrt{\text{Var}(X_t)}$ for $\kappa \in (-1, 1)$, and

(b) **Noise:** $\tilde{X}_t = X_t + \mathcal{N}(0, \kappa \sigma_X^2)$, where $\sigma_X = \sqrt{\text{Var}(X_t)}$, for $\kappa \in (0, 1)$.

⁶Notice that the choice of instruments $(1, X_t, Y_t)$ is invalid for the AR-GARCH DGP for $\gamma = 0$ as then, X_t and Y_t are perfectly colinear. Consequently, we use the second lag Y_{t-1} as instrument here.

Table 1: Size of the mode rationality test in finite samples

	Instrument Set 1				Instrument Set 2				Instrument Set 3			
Skewness	0	0.1	0.25	0.5	0	0.1	0.25	0.5	0	0.1	0.25	0.5
Sample size	Panel A: Homoskedastic iid data											
100	4.2	4.2	4.8	8.0	3.7	3.8	3.9	6.0	3.0	3.0	3.2	4.5
500	4.9	5.6	7.7	8.8	5.0	5.5	6.5	7.6	4.4	4.8	6.1	7.0
2000	5.2	6.6	7.2	7.0	4.8	5.9	6.2	6.2	4.7	5.7	5.8	6.1
5000	5.2	6.1	7.8	6.5	4.9	5.3	6.6	5.9	4.9	5.2	6.2	5.6
	Panel B: Heteroskedastic data											
100	4.3	4.3	5.5	7.9	3.5	3.7	4.1	5.5	2.8	3.0	3.2	3.7
500	5.5	6.3	8.2	8.0	4.5	5.5	6.7	6.6	4.5	4.8	5.6	5.6
2000	5.0	6.3	8.8	7.3	5.0	6.0	7.9	6.2	5.2	5.7	6.9	5.7
5000	5.3	7.0	8.5	6.5	5.0	5.9	7.5	6.0	4.9	5.8	7.2	5.8
	Panel C: Autoregressive data											
100	4.1	4.2	4.8	8.0	4.2	4.4	4.8	6.6	3.5	3.7	3.5	5.3
500	5.5	5.6	7.8	8.9	5.4	5.2	7.0	7.6	5.1	4.9	6.4	7.1
2000	5.0	6.1	8.6	7.1	5.4	5.7	8.0	6.2	5.2	5.6	7.3	5.7
5000	5.3	6.6	7.6	6.6	5.2	6.1	6.8	5.8	4.9	5.8	6.4	5.5
	Panel D: AR-GARCH data											
100	4.0	3.8	5.2	7.5	3.9	4.3	4.9	5.7	3.5	3.8	4.1	5.0
500	5.4	6.0	7.8	8.1	5.4	5.9	6.7	7.6	4.7	5.4	5.9	6.5
2000	5.5	6.4	7.9	6.9	5.4	5.5	7.4	6.1	5.3	5.2	6.7	5.8
5000	5.3	6.3	7.6	6.7	5.2	6.2	6.7	5.9	5.1	6.0	5.9	6.0

Notes: This table presents the empirical size of the mode rationality test using various sample sizes, various levels of skewness in the residual distribution, different choices of instruments, and the four DGPs described in equation (4.1). The nominal level of significance level is 5%.

The first type of misspecification introduces (deterministically) biased forecasts, where the degree of misspecification depends on the misspecification parameter κ . We standardize the bias through the unconditional standard deviation of the forecasts, $\sqrt{\text{Var}(X_t)}$. The second type of misspecification introduces independent noise to the forecasts. The magnitude of the noise is regulated through the parameter κ : for $\kappa = 1$, the signal-to-noise ratio is one, as the standard deviation of the signal equals the standard deviation of the independent noise, and as κ shrinks to zero the noise vanishes.

Figure 1 presents power plots for the biased forecasts and Figure 2 presents power plots for the “noisy” forecasts. In each of the plots, we plot the rejection rate against the degree of misspecification κ . For all plots, we use the instrument choice $(1, X_t)$, a Gaussian kernel, and a nominal test significance level of 5%. Notice that the empirical test size is shown in the figures for $\kappa = 0$.

Figure 1 and Figure 2 reveal that the proposed mode rationality test exhibits, as expected, increasing power for an increasing degree of misspecification. Also as expected, larger sample sizes lead to tests with greater power, although even the two smaller sample sizes exhibit reasonable power, particular in the case of biased forecasts. The figures also reveal that increasing degree of skewness yields to a slight loss of power. This is driven through the bandwidth choice, where larger values of the (empirical) skewness result in a smaller bandwidth, and consequently a lower test power (which is comparable to the bias-variance trade-off in the nonparametric estimation literature).

4.2 Rationality tests for an unknown measure of central tendency

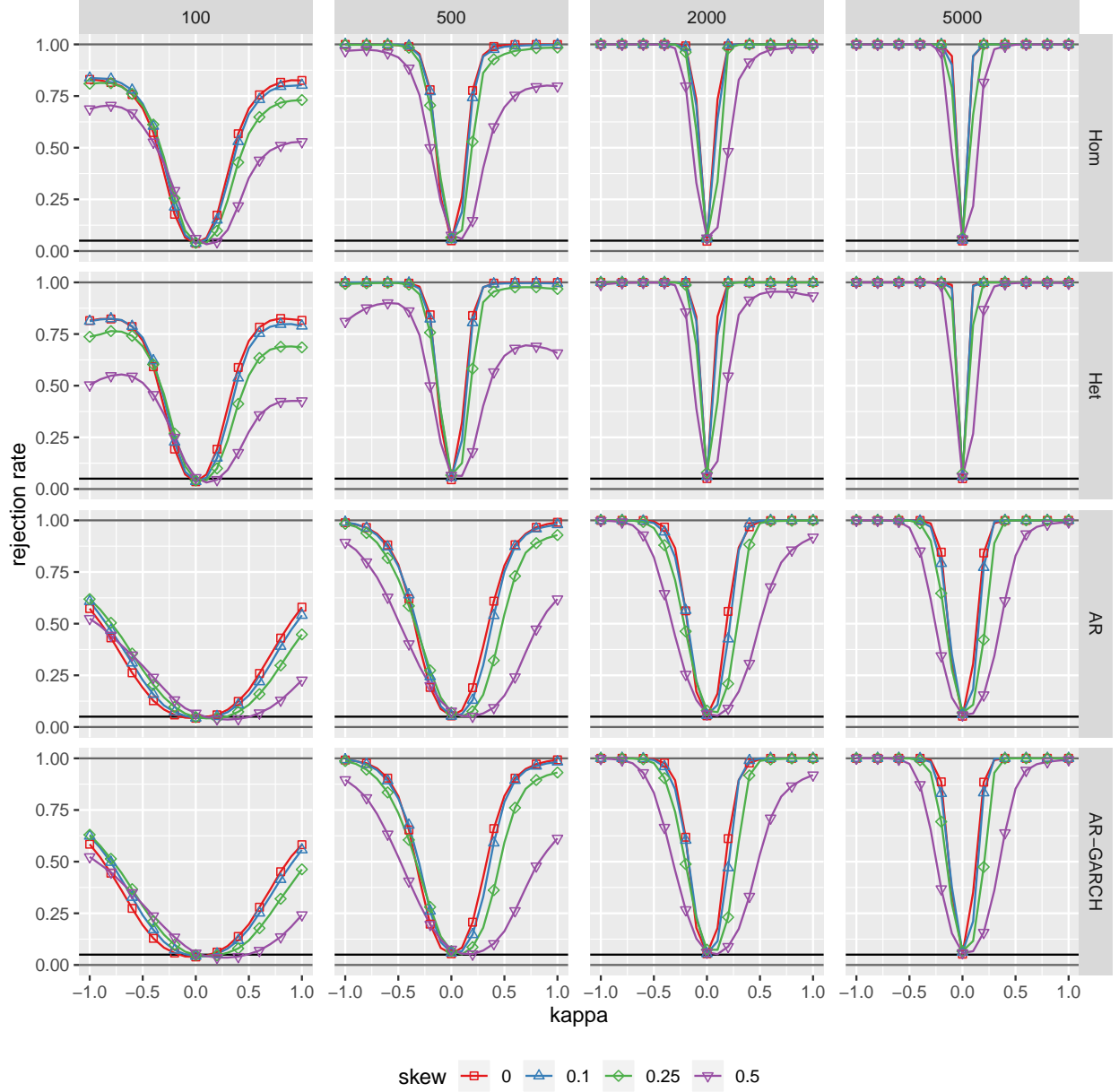
In this section we examine the small sample behavior of the asymptotic confidence sets for the measures of central tendency, described in Section 3. As in the previous section, we consider the four DGPs described in and after equation (4.1) and the same varying sample sizes T , skewness parameters γ , and instruments \mathbf{h}_t . We generate optimal one-step ahead forecasts for the mean, median and mode as the true conditional mean, median and mode of Y_{t+1} given \mathcal{F}_t :

$$X_t^{Mean} = 0.5Y_t + \sigma_{t+1} \text{Mean}(\varepsilon_{t+1}), \quad (4.3)$$

$$X_t^{Med} = 0.5Y_t + \sigma_{t+1} \text{Median}(\varepsilon_{t+1}), \quad (4.4)$$

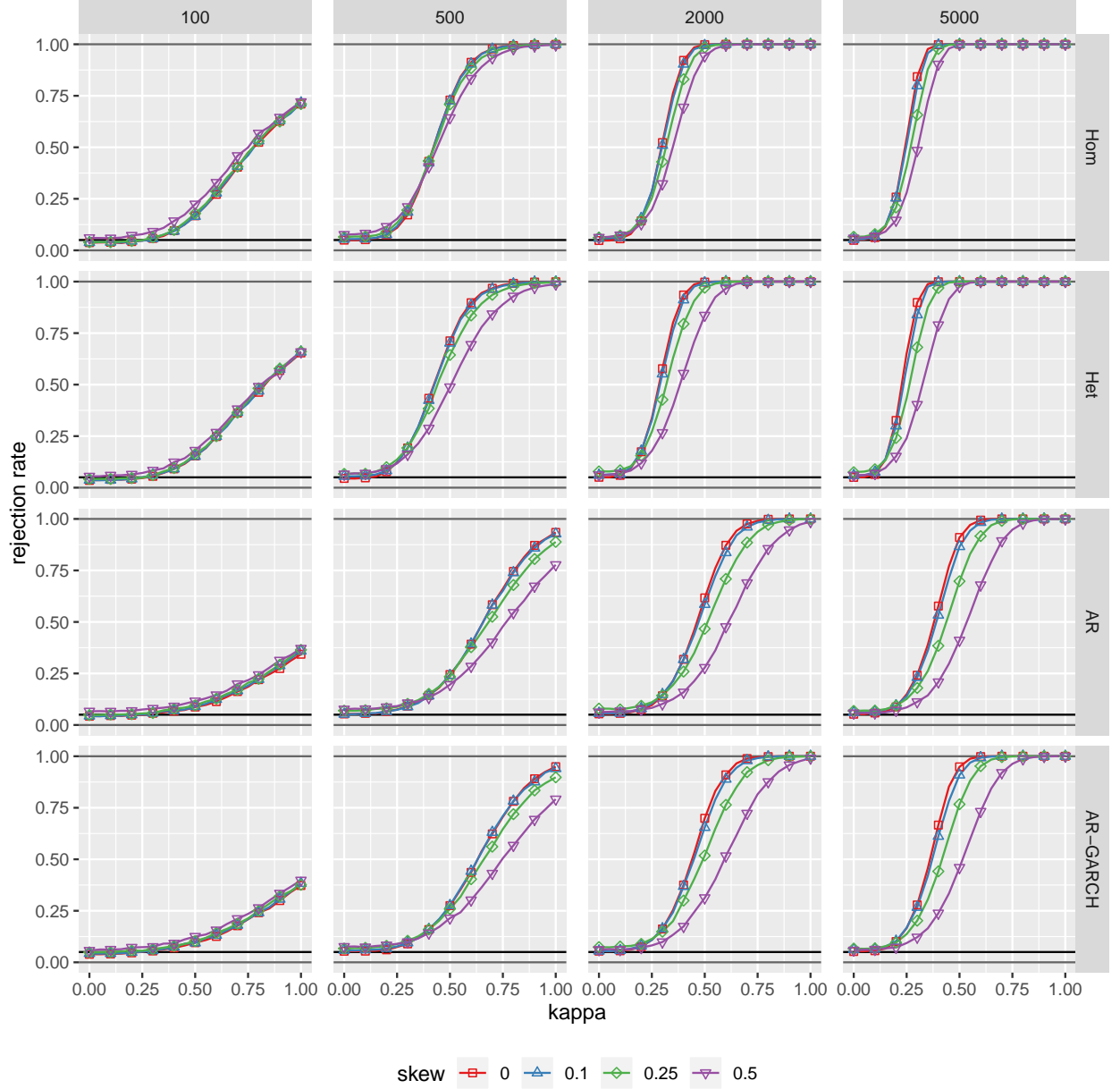
$$X_t^{Mode} = 0.5Y_t + \sigma_{t+1} \text{Mode}(\varepsilon_{t+1}). \quad (4.5)$$

Figure 1: Test Power for the Bias Simulation Setup



Notes: This figure plots the empirical rejection frequencies against the degrees of misspecification κ for different sample sizes in the vertical panels and for the four DGPs in the horizontal panels. The misspecification follows the *bias* setup and we utilize the instrument vector $(1, X_t)$ and a nominal significance level of 5%.

Figure 2: Test Power for the Noise Simulation Setup



Notes: This figure plots the empirical rejection frequencies against the degrees of misspecification κ for different sample sizes in the vertical panels and for the four DGPs in the horizontal panels. The misspecification follows the *noise* setup and we utilize the instrument vector $(1, X_t)$ and a nominal significance level of 5%.

We use the notation $\mathbf{X}_t = (X_t^{Mean}, X_t^{Med}, X_t^{Mode})^\top$ and consider convex combinations of these functionals through $X_t = \mathbf{X}_t^\top \beta$, where we consider the following specifications: (a) Mean: $\beta = (1, 0, 0)^\top$, (b) Mode: $\beta = (0, 0, 1)^\top$, (c) Median: $\beta = (0, 1, 0)^\top$, (d) Mean-Mode: $\beta = (1/2, 0, 1/2)^\top$, (e) Mean-Median: $\beta = (1/2, 1/2, 0)^\top$, (f) Median-Mode: $\beta = (0, 1/2, 1/2)^\top$, (g) Mean-Median-Mode: $\beta = (1/3, 1/3, 1/3)^\top$.

For the interpretation of simulation results below, notice that the functional identified by a convex combination of identification functions for the mean, median and the mode (with weights θ) is some convex combination of the mean, median and mode forecasts, but with possibly different combination weights, $\beta \neq \theta$. Hence, an equal-weighted combination of the mean and the mode forecasts, for example, is not necessarily identified by an equal-weighted combination of the mean and mode identification functions, rather it will generally be some other weighted combination of these functions.

Furthermore, for any fixed forecast combination weight vector β , there are possibly infinitely many corresponding identification function weights θ . For example, in the right-skewed DGP used here, the three centrality measures are ordered $\text{Mode} < \text{Median} < \text{Mean}$, and given the functional forms of the optimal forecasts for this DGP presented in equations (4.3)-(4.5), this implies that when the true forecast is the median (and so the forecast combination weight vector is $\beta = (0, 1, 0)^\top$), any identification function combination weight vector $\theta = [\theta_{Mean}, \theta_{Median}, \theta_{Mode}] \in \Theta$ that satisfies

$$\theta_{Mean} = \frac{\text{Median}(\varepsilon_{t+1}) - \text{Mode}(\varepsilon_{t+1})}{\text{Mean}(\varepsilon_{t+1}) - \text{Median}(\varepsilon_{t+1})} \cdot \theta_{Mode} \quad (4.6)$$

will lead to a combination forecast that coincides with the median forecast.⁷ This again highlights the identification problems that can arise in our analysis of forecasts of measures of central tendency. On the other hand, the mean and mode centrality measures in this DGP each have a unique identification function combination weight vector, equal to the associated forecast combination weight vector.

⁷When the DGP is conditionally location-scale, one of the three centrality measures can always be expressed as a (constant) convex combination of the other two. In this DGP, this is the median, but in other applications it may be any of the three measures. When the conditional distribution exhibits variation in higher-order moments or other “shape” parameters, this restriction will generally not hold, and the variation may or may not be sufficient to separately identify the three centrality measures.

Analyzing the coverage properties of this method requires knowledge of the set of identification function weights θ corresponding to the forecast weights β used to construct the forecast. In general, θ is not known in closed-form; in our simulation study we use one thousand draws from each DGP, sample size and skewness level to obtain the set of identification weights corresponding to each forecast combination weight vector.

Table 2 shows the empirical coverage rates for the confidence sets of centrality measures for the seven simulated convex combinations of functionals, different sample sizes, skewness parameters, and DGPs. When the set of identification function weights corresponding to a particular forecast combination weight vector is not a singleton, we choose the mid-point of the line that defines this set.⁸ In the left panel of Table 2 the data is unimodal and symmetric, and the measures of central tendency coincide, making all seven forecasts identical. The test outcomes, however, can differ as each row uses a different set of moment conditions to evaluate forecast rationality. We see that in all cases the coverage rates are very close to the nominal 90% level. In the right panel of Table 2 the data is asymmetric and the measures of central tendency differ. The coverage rates remain close to the nominal 90% level, especially for larger sample sizes.

Figure 3 illustrates the average rejection rates based on 90% confidence sets for the central tendency measures across a richer set of combination weights. (We omit the mean-median combination forecast from this figure in the interest of space.) This figure uses the AR-GARCH DGP; equivalent results for the homoskedastic cross-sectional DGP are shown in Figure 10 in the Supplemental Appendix. Each point in the triangles corresponds to a tested centrality measure, i.e. to one choice of the convex combination weights θ . We depict a coverage rate between 85% and 100% by a black point, a coverage rate between 50% and 85% by a dark grey point and anything below 50% by a light grey point. We use a cut-off of 85% to include points with coverage rates “close” to the nominal rate of 90%. We fix the sample size $T = 2000$, the instruments $\mathbf{h}_t = (1, X_t)$ and use a Gaussian kernel. The upper panel of the plots shows results for the DGPs with zero skewness DGP whereas the lower panel considers a skewness of $\gamma = 0.5$.

⁸For this DGP, θ is a singleton only when the forecast is the mean or the mode. Table S.9 and Table S.10 in the supplemental appendix show finite-sample rejection rates for three values of θ : the end-points of the line defining the set, and the mid-point reported in Table 2. In all cases we find very similar results for all three points.

Table 2: Coverage of the central tendency confidence sets in finite samples

Sample size	Symmetric data				Skewed data			
	100	500	2000	5000	100	500	2000	5000
Centrality measure	Panel A: Homoskedastic iid data							
Mean	91.4	90.5	89.5	90.5	90.2	88.7	88.7	90.8
Mode	91.4	89.1	90.2	90.0	88.2	88.9	88.1	88.3
Median	92.0	89.1	89.5	90.2	91.4	92.4	91.7	92.4
Mean-Mode	91.1	88.9	89.8	90.0	92.0	93.2	91.4	92.7
Mean-Median	92.1	88.7	89.7	90.6	90.8	91.3	90.0	91.2
Median-Mode	91.1	89.4	90.0	89.9	91.3	92.8	90.2	91.2
Mean-Median-Mode	91.1	89.1	89.9	89.6	91.6	93.2	92.7	93.1
Panel B: Heteroskedastic data								
Mean	91.9	90.5	90.8	90.7	91.9	91.9	90.1	90.0
Mode	90.7	91.6	88.9	90.2	87.5	87.4	88.9	87.4
Median	90.9	90.0	88.8	89.9	91.2	92.4	90.4	90.4
Mean-Mode	91.1	90.7	88.4	90.2	90.9	91.0	89.8	92.7
Mean-Median	91.2	90.7	89.0	89.6	91.1	90.6	88.1	87.3
Median-Mode	90.6	90.9	89.1	90.3	89.9	91.4	89.8	90.9
Mean-Median-Mode	91.7	90.2	88.3	90.4	91.1	91.3	91.0	92.7
Panel C: Autoregressive data								
Mean	89.6	88.5	91.0	90.5	87.6	89.8	89.2	90.8
Mode	91.0	89.4	90.9	89.0	86.6	87.7	87.4	86.9
Median	88.8	88.7	90.2	90.3	88.2	92.1	90.1	92.5
Mean-Mode	90.1	88.1	89.9	88.9	90.9	92.6	91.4	92.3
Mean-Median	88.5	89.3	90.6	89.5	87.8	91.0	89.8	91.8
Median-Mode	90.6	88.5	90.2	89.4	90.7	91.7	90.3	90.6
Mean-Median-Mode	90.1	88.4	89.7	89.6	90.1	92.7	91.0	93.7
Panel D: AR-GARCH data								
Mean	88.7	87.9	90.6	90.6	88.1	89.7	88.8	90.2
Mode	91.2	90.3	90.9	90.1	88.8	87.3	88.5	90.1
Median	88.9	90.4	89.5	89.8	91.0	91.6	92.6	91.6
Mean-Mode	90.0	90.1	90.5	90.5	91.3	91.7	93.6	92.1
Mean-Median	89.6	90.1	90.0	89.4	90.1	91.4	90.2	90.8
Median-Mode	90.8	90.6	90.8	90.3	91.7	90.9	92.5	90.5
Mean-Median-Mode	89.4	90.0	90.3	90.6	91.7	92.6	93.3	92.3

Notes: This table presents empirical coverage rates of nominal 90% confidence sets for the forecasts of central tendency. We report the results for symmetric and skewed data ($\gamma = 0$ or 0.5), for various sample sizes and the four DGPs described in equation (4.1). As instruments we use $\mathbf{h}_t = (1, X_t)$.

Panel A of Figure 3 uses a unimodal DGP with zero skewness, and so all measures of central tendency and all convex combinations thereof coincide. This implies that all six of these triangles are identical; we include them here for ease of comparison with the lower panel, where the optimal forecasts differ. Under symmetry and unimodality, every point in the triangle should be contained in the confidence set with probability 90%, and this figure is consistent with this, thus confirming the procedure’s coverage level in this simulation design.

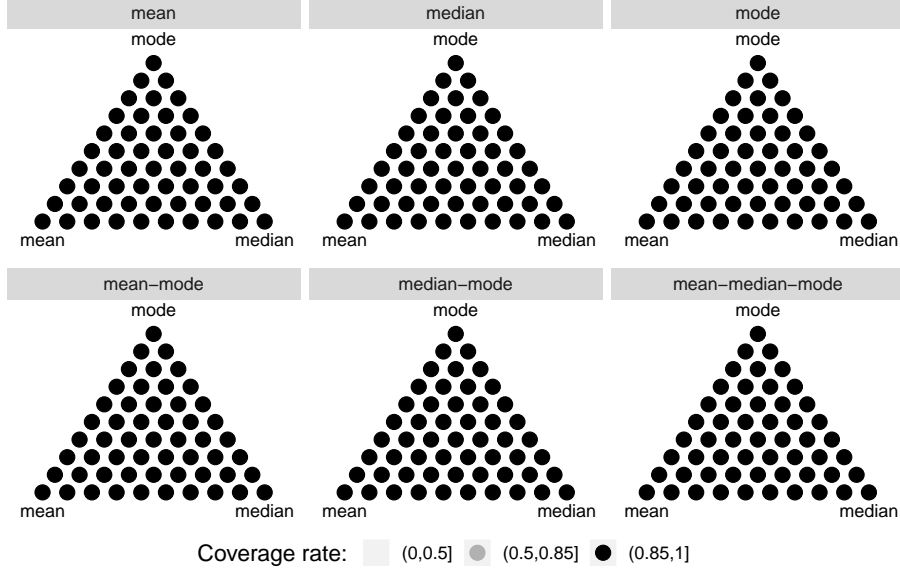
Panel B of Figure 3 uses a skewness parameter of $\gamma = 0.5$, and so the three measures of central tendency differ. The upper left plot of Panel B considers ideal mean forecasts and exhibits the expected behavior: the mean, and convex combinations close to the mean, are usually contained in the confidence set, whereas points far away are usually excluded. A similar, but more pronounced, picture can be observed for ideal mode forecasts in the upper right plot.

The median plot in Panel B of Figure 3 reveals, as expected, that the ideal median forecast is generally not rejected when testing using the identification function for the median (revealed by the dot at the median vertex being black). This plot further shows that the convex combinations of mean, median and mode that coincide with the median (see equation 4.6) are also generally included in the confidence interval.

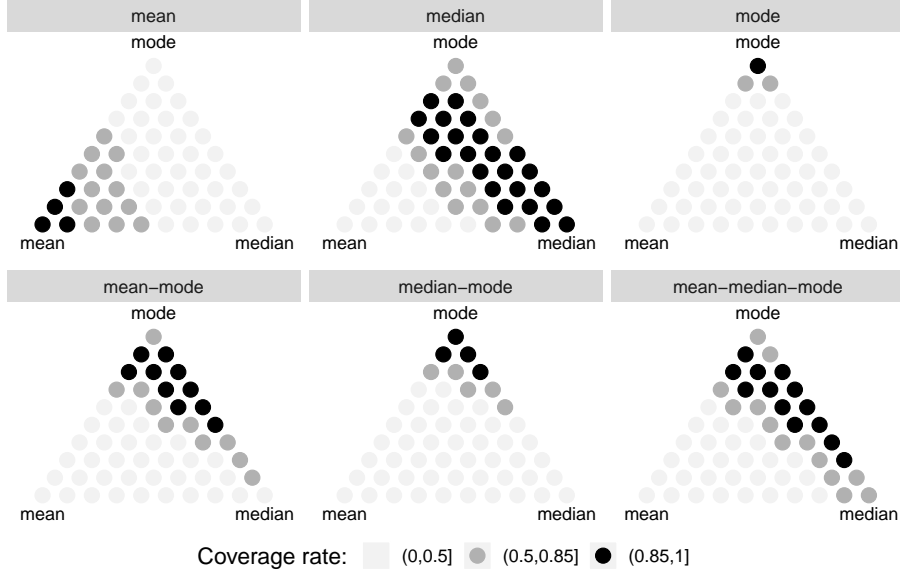
For the interpretation of the three convex combination plots in the bottom row of Panel B, recall that the functional identified by a convex combination of identification functions for the mean, median and the mode results again in some convex combination of the mean, median and mode, however, with possibly different combination weights. Further, as the median is itself a convex combination of the mean and mode in this simulation design, the set of combination weights consistent with rationality is a line from one edge of the triangle to another. In this design the line always connects the mean-mode edge to the mode-median edge. In all three cases we note that this line is nicely contained inside the region of dark dots, indicating correct coverage in these unidentified cases.

**Figure 3: Confidence Regions for Central Tendency Measures:
AR-GARCH DGP**

(a) AR-GARCH DGP with skewness $\gamma = 0$



(b) AR-GARCH DGP with skewness $\gamma = 0.5$



Notes: This figure shows (average) 90% confidence bounds for the possible measures of central tendency for the AR-GARCH DGP. The individual plots correspond to the (true) forecasted functional stated in the text above the triangle. The individual points correspond to the respective convex combinations, and the vertex points correspond to the mean, median and mode functionals. The upper panel shows results for the unskewed DGP, the lower panel for a skewness of $\gamma = 0.5$. We fix the sample size $T = 2000$, the instruments $\mathbf{h}_t = (1, X_t)$ and use a Gaussian kernel.

5 Evaluating Economic Forecasts

5.1 Survey forecasts of individual income

We now apply the tests developed above in three economic forecasting applications. Firstly, we consider data from Labor Market Survey component of the Survey of Consumer Expectations⁹, conducted by the Federal Reserve Bank of New York in March, July, and November of each year. Our sample runs from March 2015 to July 2017. In this survey participants are asked a variety of questions, including about their current earnings and their beliefs about their earnings in four months' time (i.e., the date of the next survey). Using adjacent surveys we obtain a sample 3,145 pairs of forecasts (X_t) and realizations (Y_{t+1}).¹⁰ In testing the rationality of these forecasts we assume that all participants report the same, unknown, measure of centrality as their forecast. In the next subsection we explore potential heterogeneity in the measure of centrality used by different respondents.

Table 3 presents the results of rationality tests for three measures of central tendency, for a variety of instrument sets. The first instrument set includes just a constant, and the rationality test simply tests whether the forecast errors have unconditional mean, median or mode, respectively, of zero. The other instrument sets additionally include the forecast (X_t) itself, and other information about the respondent collected in the survey. We consider the respondent's income at the time of making the forecast, indicators for the respondent's type of employer,¹¹ and whether the respondent received any job offers in the past four months.

The first row of Table 3 shows that when only a constant is used, rationality of the survey forecasts can be rejected for the mean, but cannot be rejected for the other two measures of central tendency. When we additionally include the forecast as an instrument, we can reject rationality as

⁹Source: Survey of Consumer Expectations, 2013-2019 Federal Reserve Bank of New York (FRBNY). The SCE data are available without charge at <http://www.newyorkfed.org/microeconomics/sce> and may be used subject to license terms posted there. FRBNY disclaims any responsibility or legal liability for this analysis and interpretation of Survey of Consumer Expectations data.

¹⁰We drop observations that include forecasts or realizations of annualized income below \$1,000 or above \$1 million, which represent less than 1% of the raw sample. We also drop observations where the ratio of the realization to the forecast, or its inverse, is between 9 and 13, to avoid our results being affected by misplaced decimal points (leading to an proportional error of around 10) or by the failure to consistently report annualized or non-annualized income.

¹¹The survey includes the categories government, private (for-profit), non-profit, family business, and "other." The first two categories dominate the responses and so we only consider indicators for those.

Table 3: Evaluating income survey forecasts. This table presents p -values from tests of rationality of individual income forecasts from the New York Federal Reserve’s Survey of Consumer Expectations. The columns present test results when interpreting the point forecasts as forecasts of the mean, median or mode. The rows present results for different choices of instruments used in the test: 1 is the constant, X is the forecast, “lag income” is the respondent’s income at the time of the forecast, “government” and “private” are indicators for the self-reported industry in which the survey respondent works, “job offers” is an indicator for whether the respondent received any job offers in the previous four months. p -values less than 0.10, indicating a rejection of rationality, are marked in bold.

Instruments	Centrality measure		
	Mean	Median	Mode
1	0.031	0.513	0.445
1, X	0.044	0.000	0.719
1, X , lag income	0.083	0.000	0.911
1, X , government	0.127	0.004	0.804
1, X , private	0.075	0.003	0.768
1, X , job offers	0.064	0.000	0.879

mean or median forecasts, but we cannot reject them as rational mode forecasts. We are similarly able to reject rationality as mean and median forecasts when we include additional covariates, with the exception of the mean when using the “government” industry indicator.

Figure 4 shows the convex combinations of mean, median and mode forecasts that lie in the confidence set constructed using the methods for weakly-identified GMM estimation in [Stock and Wright \(2000\)](#).¹² In the left panel we see that when using only a constant as the instrument, we are able to reject rationality for the mean, and for measures of centrality “close” to the mean, but we are unable to reject rationality for most measures of centrality. This is consistent with the entries in the first row of Table 3, which correspond directly to the three vertices in Figure 4. In the right panel of Figure 4, when the instrument set includes a constant and the forecast, we see that only

¹²The interpretation of this figure is slightly different to that of Figure 3: in that figure the shade of each dot indicated the proportion of times, across simulations, that point was included in the confidence set, allowing us to study the finite-sample coverage rates of our procedure. In Figure 4 the shade of each dot indicates whether, for this sample, that point is included in the 90% confidence set, the 95% confidence set, or is outside the 95% confidence set, the latter indicating a rejection of rationality at the 5% significance level.

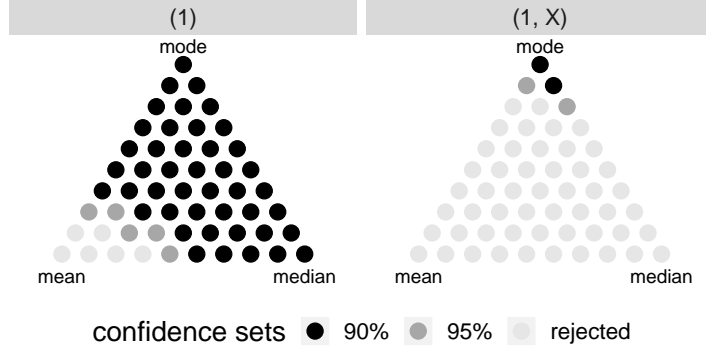


Figure 4: Confidence sets for income survey forecasts. This figure shows the measures of centrality that rationalize the New York Federal Reserve income survey forecasts. Black dots indicate that the measure is inside the Stock-Wright 90% confidence set, dark grey dots indicate that the measure is inside the 95% confidence set, light grey dots indicate that rationality for that measure can be rejected at the 5% level. The left panel uses just a constant as the instrument; the right panel uses a constant and the forecast.

the mode and centrality measures very close to the mode are included in the confidence set; all other forecasts can be rejected at the 5% level.

When interpreting the results in Figure 4, and similar figures below, it is worth keeping in mind that the power to detect sub-optimal forecasts is not uniform across values of θ : the mean and median are estimable at rate $T^{1/2}$, while the mode is only estimable at rate approximately $T^{2/7}$. This implies that for comparably sub-optimal forecasts, power will be lower at the mode vertex than at the mean or median vertices.¹³ This unavoidable variation in power means that the information conveyed by inclusion in the confidence set differs across values of θ .¹⁴

Overall, we conclude that the responses to the New York Fed’s income survey, taken on aggregate, are consistent with rationality when interpreted as mode forecasts, but not when interpreted as forecasts of the mean, median, or convex combinations of these measures.

¹³We find that we are able to reject rationality at the mode vertex in some applications, discussed below, and so it is not the case that forecasts are always rationalizable as mode forecasts; i.e., power at the mode vertex is not zero.

¹⁴Stock and Wright (2000) suggest caution when interpreting a small but nonempty confidence set, as such an outcome is consistent with both a correctly-specified model (a rational forecast, in our case) estimated precisely *and also* with a misspecified model (irrational forecast) facing low power. These two interpretations clearly have very different economic implications, but cannot be disentangled empirically. Given the lower power at the mode vertex, the latter explanation may be relevant here.

5.2 Heterogeneity in individual income forecasts

The analysis of individual income survey forecasts above used 3,145 pairs of forecasts and realizations from a total of 2,119 unique survey respondents. This naturally raises the question of whether there is heterogeneity in the measure of centrality used by different respondents. Given that our survey respondents generally only appear once or twice in our sample, allowing for arbitrary heterogeneity is not empirically feasible, however by exploiting other information on covariates contained in the survey we may shed some light on this question.

Firstly, we consider stratifying our sample by income. This is motivated by the possibility that, in addition to a different *level* of future income, low-income respondents face a different *shape* of distribution of future income, compared with high-income respondents. This analysis may also reveal that respondents at different income levels use different centrality measures to summarize their predictive distribution. Figure 5 presents confidence sets for forecast rationality of measures of centrality for low-, middle-, and high-income respondents based on terciles of the distribution of reported incomes.¹⁵ We see that for low-income respondents, only the mode is contained in the 90% confidence set. For middle- and high-income respondents, the mode, mean, and centrality measures broadly close to the mean and mode are included in the confidence set. This finding is consistent with all respondents using the mode, and only the distribution for low-income respondents allowing for separate identification of the mode and the mean. It is also consistent with low-income respondents reporting the mode as their forecast, while other respondents report the mean.

Next we consider a two-way sort, where we stratify the sample both by income and by the industry in which the respondent works. Stratifying by industry is motivated by the possibility that workers in the government and non-profit sectors may have more predictable future earnings than those in the private sector.

Figure 6 presents the striking result that forecasts from low-income workers in the private sector cannot be rationalized using *any* measure of centrality; all points lie outside the 95% confidence set. In contrast, high-income workers in the private sector, and all workers in the non-private sector (which includes the government, non-profit, family business, and “other” sectors), issue forecasts

¹⁵Qualitatively similar results are found if we stratify the sample into just two groups based on the median reported income.

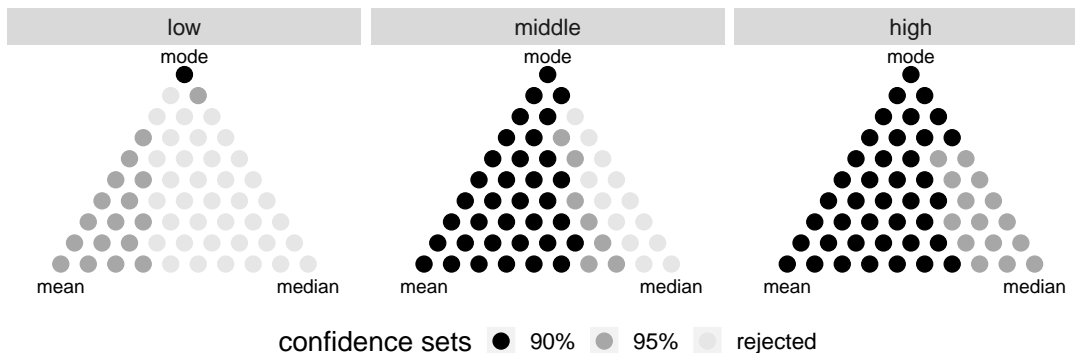


Figure 5: Confidence sets for income survey forecasts, stratified by income. This figure shows the measures of centrality that rationalize the New York Federal Reserve income survey forecasts, for low-, middle- and high-income respondents. Groups are formed using terciles of lagged reported income. Black dots indicate that the measure is inside the Stock-Wright 90% confidence set, dark grey dots indicate that the measure is inside the 95% confidence set, light grey dots indicate that rationality for that measure can be rejected at the 5% level. All panels tests a constant and the forecast as instruments.

that can be rationalized as many measures of central tendency.¹⁶ For high-income private sector workers, we can only reject the mean, and measures close to the mean, while for non-private sector workers, we can only reject the median, and measures close to the median. This figure suggests that low-income workers in the private sector have difficulty predicting their income over the coming four months, and make systematic errors when doing so.

Finally we consider a sort based on whether the respondent reported having received a job offer in the previous four months. Such respondents are more likely to change jobs in the coming period, and therefore face a more uncertain distribution of future income.¹⁷ Figure 7 reveals that forecasts from low-income respondents who reported receiving a job offer in the past four months cannot be rationalized using any measure of central tendency, at the 5% significance level. Forecasts from low-income respondents who did not receive a job offer in the previous four months, thereby presumably having more predictable future earnings, are rationalizable as mean, mode and many other centrality

¹⁶We find very similar results when we sort respondents into government and non-government, or government+non-profit and not government+non-profit: we reject rationality for whichever segment contains low-income workers from the private sector.

¹⁷We find very similar results when we segment respondents by their estimated probability of receiving a job offer in the next four months, or by their estimated probability of staying in the same job in the next four months.

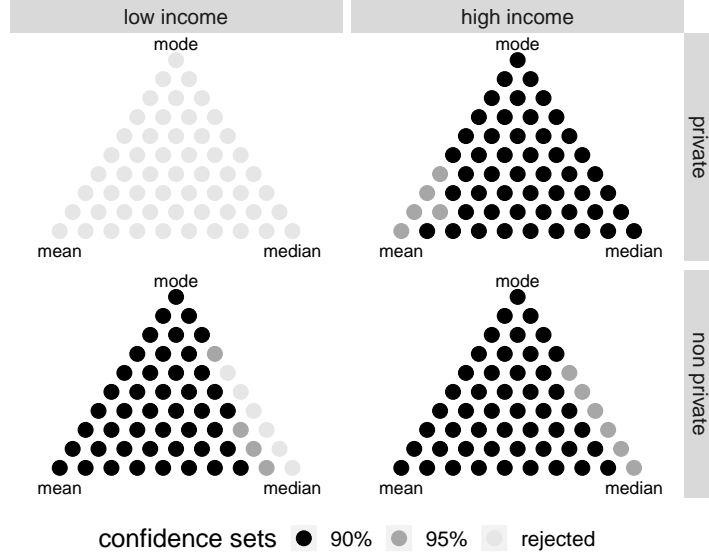


Figure 6: Confidence sets for income survey forecasts, stratified by income and industry. This figure shows the measures of centrality that rationalize the New York Federal Reserve income survey forecasts, for low- and high-income respondents in the private sector or not. Income groups are formed using the median lagged reported income. Black dots indicate that the measure is inside the Stock-Wright 90% confidence set, dark grey dots indicate that the measure is inside the 95% confidence set, light grey dots indicate that rationality for that measure can be rejected at the 5% level. All panels tests a constant and the forecast as instruments.

measures, though not the median and measures close to it. For high-income respondents with no recent job offer, *all* measures of central tendency can be rationalized, while the high-income respondents who recently received a job offer, all measures except those close to the median can be rationalized.

Overall, the results in this section indicate some important heterogeneity in both the rationality of point forecasts, and the measure of central tendency employed. We find that forecasts from survey respondents with income below the median and who are either employed in the private sector (as opposed to the government, non-profit or other sectors) or who are likely to change jobs in the coming period cannot be rationalized using any measure of central tendency. In contrast, forecasts from respondents with income above the median, regardless of the industry in which they work or their likelihood of changing jobs, can be rationalized using many different centrality measures.

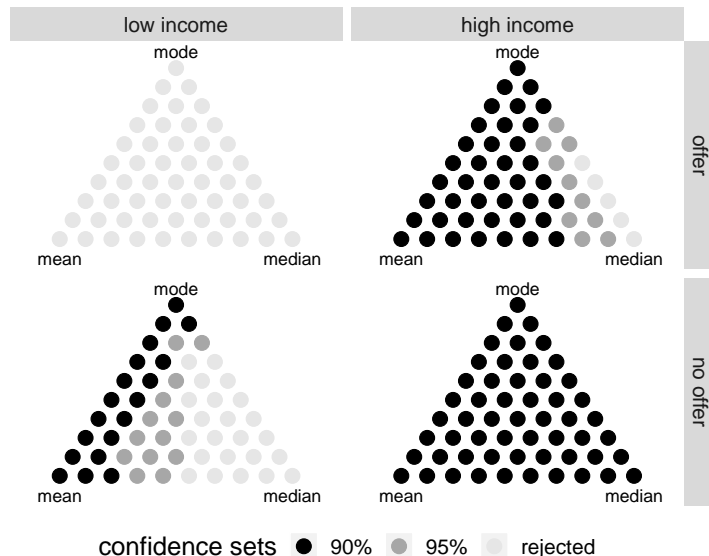


Figure 7: Confidence sets for income survey forecasts, stratified by income and job offer. This figure shows the measures of centrality that rationalize the New York Federal Reserve income survey forecasts, for low- and high-income respondents in the private sector or not. Groups are formed using the median lagged reported income, and whether or not the respondent reported received at least one job offer in the past four months. Black dots indicate that the measure is inside the Stock-Wright 90% confidence set, dark grey dots indicate that the measure is inside the 95% confidence set, light grey dots indicate that rationality for that measure can be rejected at the 5% level. All panels tests a constant and the forecast as instruments.

5.3 Greenbook forecasts of U.S. GDP

We now consider one-quarter-ahead forecasts of U.S. GDP growth produced by economists working at the Board of Governors of the Federal Reserve (the so-called “Greenbook” forecasts), from 1967Q2 until 2014Q1, a total of 187 observations.¹⁸ These forecasts are prepared in preparation for each meeting of the Federal Open Market Committee, and substantial resources are devoted to them. Greenbook forecasts are available several times each quarter; for this analysis we take the single forecast closest to the middle date in each quarter. Broadly similar results are found when using the first, or last, forecast within each quarter.

Figure 8 presents the confidence set for the measures of centrality that can be rationalized for these forecasts. Noting that GDP growth is measured with error and official values are often

¹⁸Greenbook forecasts are only available to the public after a five-year lag.

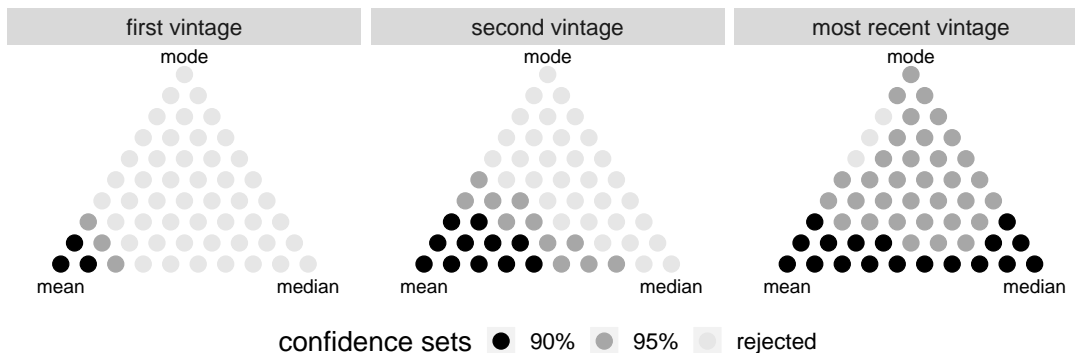


Figure 8: Confidence sets for Greenbook GDP forecasts. This figure shows the measures of centrality that rationalize the Federal Reserve Board’s “Greenbook” forecasts of U.S. GDP growth. The three panels use three different measures of GDP growth in a given quarter. Black dots indicate that the measure is inside the Stock-Wright 90% confidence set, dark grey dots indicate that the measure is inside the 95% confidence set, light grey dots indicate that rationality for that measure can be rejected at the 5% level. All panels use a constant and the forecast as instruments.

revised, we present results for three different “vintages” of the realized value: the first, second and most recent release. For the first and second vintages, we see that only measures of centrality “close to” the mean can be rationalized as optimal, while the mode, median and similar measures can all be rejected. Using the most recent vintage for GDP growth, both the mean and median, and centrality measures near those, are included in the confidence set. That the Greenbook GDP forecasts are rational when interpreted as mean forecasts, but generally not when taken as mode or median forecasts, is consistent with the Fed staff using econometric models for these forecasts, as such models almost invariably focus on the mean.

5.4 Random walk forecasts of exchange rates

For our final empirical application we revisit the famous result of [Meese and Rogoff \(1983\)](#), that exchange rates movements are approximately unpredictable when evaluated by the squared-error loss function, implying that the lagged exchange rate is an optimal mean forecast. We use daily

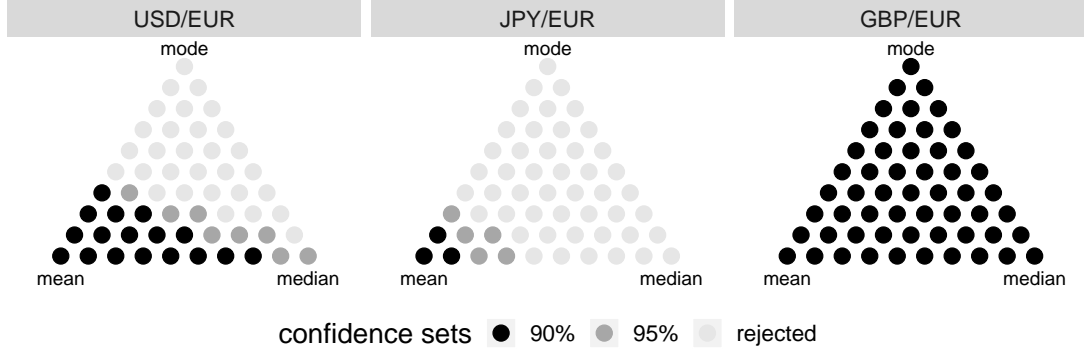


Figure 9: Confidence sets for random walk forecasts of exchange rates. This figure shows the measures of centrality that rationalize the random walk forecast of daily exchange rates movements. Black dots indicate that the measure is inside the Stock-Wright 90% confidence set, dark grey dots indicate that the measure is inside the 95% confidence set, light grey dots indicate that rationality for that measure can be rejected at the 5% level. All panels use a constant and the forecast as instruments.

data on the USD/EUR, JPY/EUR and GBP/EUR exchange rates over the period May 2000 to June 2019, a total of 4,978 trading days. Note that our sample period has no overlap with that of [Meese and Rogoff \(1983\)](#), and so their conclusions about the mean-optimality of the random walk forecast need not hold in our data.

Figure 9 presents the results of our tests for rationality, all of which use a constant and the forecast as the instrument set. The left and middle panels reveal that for the USD/EUR and JPY/EUR exchange rates the lagged exchange rate is not rejected as a mean forecast, while it is rejected when taken as a mode or median forecast. Thus the rationality of the random walk forecast critically depends, for these exchange rates, on whether it is interpreted as a mean, median or mode forecast. For the GBP/EUR exchange rate we find we cannot reject rationality with respect to *any* of convex combination of these measures of central tendency, implying that the random walk forecast is consistent with rationality under any of these measures. The mean vertex being included in the confidence set for all three exchange rates, indicating no of evidence against rationality of the random walk model when interpreted as a mean forecast, is consistent with the conclusion of [Meese and Rogoff \(1983\)](#).

6 Conclusion

Reasonable people can interpret a request for their prediction of a random variable in a variety of ways. Some, including perhaps most economists, will report their expectation of the value of the variable (i.e., the mean of their predictive distribution), others might report the value such that the observed outcome is equally likely to be above or below it (i.e., the median), and others may report the value most likely to be observed (i.e., the mode). Still others might solve a loss minimization problem and report a forecast that is not a measure of central tendency. Economic surveys generally request a *point* forecast, despite calls for surveys to solicit distributional forecasts, see [Manski \(2004\)](#) for example, and the specific type of point forecast (mean, median, etc.) to be reported is generally not made explicit in the survey.

This paper proposes new methods to test the rationality of forecasts of some unknown measure of central tendency. Similar to [Elliott et al. \(2005\)](#), we propose a testing framework that nests the mean forecast as a special case, but unlike [Elliott et al. \(2005\)](#) we allow for alternative forecasts within the class of measures of central tendency, rather than measures that represent other aspects of the predictive distribution (such as non-central quantiles or expectiles). We consider the class of central tendency measures generated by convex combinations of the mean, median and mode. Our approach faces a weak identification problem in economic applications, as the optimal weights in the convex combination are weakly- or un-identified when the distribution of the target variable is weakly asymmetric or symmetric, as can be the case for economic variables. We overcome this by using the work of [Stock and Wright \(2000\)](#) on GMM inference under weak identification.

As a building block for the above tests, we also present new tests for the rationality of mode forecasts. Mode regression has received some attention in the recent literature (see, e.g., [Kemp and Silva, 2012](#) and [Kemp et al., 2019](#)), however tests for mode forecast rationality similar to those available for the mean and median (e.g., [Mincer and Zarnowitz, 1969](#) and [Gaglianone et al., 2011](#)) are lacking. Direct analogs of existing tests are infeasible because the mode is not elicitable ([Heinrich, 2014](#)). We introduce the concept of *asymptotic elicibility* and show it applies to the mode by considering a generalized modal midpoint with asymptotically vanishing length. We then present results that allow for tests similar to the famous Mincer-Zarnowitz regression for mean forecasts.

The concept of asymptotic elicitability is of interest in its own right. Beyond the rationality tests proposed here, asymptotic elicitability may facilitate forecast comparison and elicitation of novel measures of uncertainty. See for example [Eyting and Schmidt \(2018\)](#) for an elicitation procedure for the maximum, a functional that generally is not elicitable ([Bellini and Bignozzi, 2015](#)).

We apply our tests in three economic forecasting applications. Using individual income expectations survey data collected by the New York Federal Reserve, we reject forecast rationality with respect to the mean or median, however we cannot reject rationality when interpreting these as mode forecasts. We also find evidence of heterogeneity in this sample: forecasts from low-income respondents who are likely to soon change jobs are not rationalizable using *any* measure of centrality, while forecasts from high-income respondents, regardless of their likelihood to change jobs, are rationalizable for many, though not all, measures of centrality. Next we study the Federal Reserve’s “Greenbook” forecasts of U.S. GDP, and we find that we cannot reject rationality with respect to the mean, however we can reject with respect to the median and mode. This is consistent with the Greenbook forecasts being made using econometric models, which almost invariably focus on the mean as a measure of central tendency. Finally, we revisit the famous result of [Meese and Rogoff \(1983\)](#) that random walk forecasts for exchange rates are rational. For the GBP/EUR exchange rate, we find we cannot reject rationality with respect to *any* of convex combination of the mean, median and mode, indicating the random walk forecast is rational under any of these measures. For the USD/EUR and JPY/EUR exchange rates, however, we find the random walk forecast is only rational for centrality measures “close” to the mean; rationality with respect to the median and mode is rejected.

References

- Barendse, S. (2017). Interquantile expectation regression. Tinbergen Institute Discussion Paper 2017-034/III.
- Bellini, F. and Bignozzi, V. (2015). On elicitable risk measures. *Quantitative Finance*, 15(5):725–733.
- Charness, G. and Dufwenberg, M. (2006). Promises and partnership. *Econometrica*, 74(6):1579–1601.
- Christoffersen, P. F. (1998). Evaluating Interval Forecasts. *International Economic Review*, 39(4):841–62.
- Christoffersen, P. F. and Diebold, F. X. (1997). Optimal prediction under asymmetric loss. *Econometric Theory*, 13(06):808–817.
- Davidson, J. (1994). *Stochastic Limit Theory: An Introduction for Econometricians*. Advanced Texts in Econometrics. OUP Oxford.
- Dearborn, K. and Frongillo, R. (2019). On the indirect elicibility of the mode and modal interval. *Annals of the Institute of Statistical Mathematics*.
- Dufwenberg, M. and Gneezy, U. (2000). Measuring beliefs in an experimental lost wallet game. *Games and Economic Behavior*, 30(2):163–182.
- Eddy, W. F. (1980). Optimum kernel estimators of the mode. *Ann. Statist.*, 8(4):870–882.
- Elliott, G., Komunjer, I., and Timmermann, A. (2005). Estimation and testing of forecast rationality under flexible loss. *The Review of Economic Studies*, 72(4):1107–1125.
- Elliott, G., Komunjer, I., and Timmermann, A. (2008). Biases in macroeconomic forecasts: irrationality or asymmetric loss? *Journal of the European Economic Association*, 6(1):122–157.
- Elliott, G. and Timmermann, A. (2016). *Economic Forecasting*. Princeton University Press.
- Eyting, M. and Schmidt, P. (2018). Belief elicitation with multiple point predictions. Working paper.
- Fissler, T. and Ziegel, J. F. (2016). Higher order elicibility and Osband’s principle. *Annals of Statistics*, 44(4):1680–1707.
- Gaglianone, W. P., Lima, L. R., Linton, O., and Smith, D. R. (2011). Evaluating value-at-risk models via quantile regression. *Journal of Business & Economic Statistics*, 29(1):150–160.
- Gneiting, T. (2011). Making and evaluating point forecasts. *Journal of the American Statistical Association*, 106(494):746–762.
- Granger, C. W. J. (1969). Prediction with a generalized cost of error function. *Journal of the Operational Research Society*, 20:199–207.
- Heinrich, C. (2014). The mode functional is not elicitable. *Biometrika*, 101(1):245–251.

- Hossain, T. and Okui, R. (2013). The binarized scoring rule. *Review of Economic Studies*, 80(3):984–1001.
- Huber, P. J. (1964). Robust estimation of a location parameter. *Annals of Statistics*, 53(1):73–101.
- Ibragimov, I. A. (1956). On the composition of unimodal distributions. *Theory of Probability and Its Applications*, 1:255–260.
- Kemp, G. C., Parente, P. M., and Silva, J. S. (2019). Dynamic vector mode regression. *Journal of Business & Economic Statistics*. forthcoming.
- Kemp, G. C. and Silva, J. S. (2012). Regression towards the mode. *Journal of Econometrics*, 170(1):92 – 101.
- Kirchkamp, O. and Reiß, J. P. (2011). Out-of-equilibrium bids in first-price auctions: Wrong expectations or wrong bids. *The Economic Journal*, 121(557):1361–1397.
- Li, Q. and Racine, J. S. (2006). *Nonparametric Econometrics: Theory and Practice*. Number 8355 in Economics Books. Princeton University Press.
- Manski, C. F. (2004). Measuring expectations. *Econometrica*, 72(5):1329–1376.
- McClave, J. T., Benson, P. G., and Sincich, T. (2017). *Statistics for Business and Economics, 13th Edition*. Pearson, New York.
- Meese, R. and Rogoff, K. (1983). Empirical exchange rate models of the seventies: Do they fit out of sample? *Journal of International Economics*, 14:3–24.
- Mincer, J. and Zarnowitz, V. (1969). The Evaluation of Economic Forecasts. In *Economic Forecasts and Expectations: Analysis of Forecasting Behavior and Performance*, pages 3–46. National Bureau of Economic Research, Inc.
- Nolde, N. and Ziegel, J. F. (2017). Elicitability and backtesting: Perspectives for banking regulation. *The Annals of Applied Statistics*, 11(4):1833–1874.
- Patton, A. J. (2018). Comparing possibly misspecified forecasts. *Journal of Business & Economic Statistics*. Forthcoming.
- Patton, A. J. and Timmermann, A. (2007). Testing forecast optimality under unknown loss. *Journal of the American Statistical Association*, 102(480):1172–1184.
- Peterson, C. and Miller, A. (1964). Mode, median, and mean as optimal strategies. *Journal of Experimental Psychology*, 68(4):363–367.
- Sapienza, P., Toldra-Simats, A., and Zingales, L. (2013). Understanding trust. *The Economic Journal*, 123(573):1313–1332.
- Stock, J. H. and Wright, J. H. (2000). GMM with weak identification. *Econometrica*, 68(5):1055–1096.
- von Bahr, B. and Esseen, C.-G. (1965). Inequalities for the r th absolute moment of a sum of random variables, $1 \leq r \leq 2$. *Ann. Math. Statist.*, 36(1):299–303.

- White, H. (1994). *Estimation, Inference and Specification Analysis*. Econometric Society Monographs. Cambridge University Press.
- White, H. (2001). *Asymptotic Theory for Econometricians*. Academic Press, San Diego.

A Proofs

Proof of Proposition 2.4. Let $Y \sim P \in \mathcal{P}$ and let $\tilde{K}_\delta(e) = \frac{1}{\delta} K\left(\frac{e}{\delta}\right)$. Then, it holds that

$$L_\delta^K(x, P) = \mathbb{E}[L_\delta^K(x, Y)] = - \int \frac{1}{\delta} K\left(\frac{x-y}{\delta}\right) f(y) dy = - \int \tilde{K}_\delta(x-y) f(y) dy = -(f * K_\delta)(x),$$

where $f * K_\delta$ denotes the convolution of the functions f and K_δ . [Ibragimov \(1956\)](#) shows that for any log-concave density, its convolution with any other unimodal distribution function is again unimodal.¹⁹ Thus, $L_\delta^K(x, P)$ exhibits a unique minima which shows that Γ_δ is well-defined by (2.6).

We now show that $\Gamma_\delta(P) \rightarrow \text{Mode}(P)$ for all $P \in \mathcal{P}$. For this, notice that

$$L_\delta^K(x, P) = - \int \frac{1}{\delta} K\left(\frac{x-y}{\delta}\right) f(y) dy = - \int K(u) f(x+u\delta) du, \quad (\text{A.1})$$

by applying integration by substitution with the transformation $y \mapsto u(y) = (x-y)/\delta$. Interpreting the kernel $K(\cdot)$ as the density of the probability measure \mathcal{K} , we get that

$$L_\delta^K(x, P) = - \int f(x+u\delta) d\mathcal{K}(u). \quad (\text{A.2})$$

Notice that the functional $\Gamma_\delta(P)$ induced by the loss function L_δ^K is given as $\arg \min_x L_\delta^K(x, P)$. As the density f is bounded from above by assumption, we can apply dominated convergence in order to conclude that

$$\lim_{\delta \rightarrow 0} L_\delta^K(x, P) = - \int \lim_{\delta \rightarrow 0} f(x+u\delta) d\mathcal{K}(u) = - \int f(x) d\mathcal{K}(u) = -f(x) \quad (\text{A.3})$$

for all $x \in \mathbb{R}$ as $\int d\mathcal{K}(u) = 1$. By assumption, it holds that there exists some $x \in \text{supp}(P)$ such that $-f(x) < -f(\tilde{x})$ for all $\tilde{x} \in \mathbb{R}$, where $x = \Gamma(P)$ is the mode of the distribution P by definition. As $L_\delta^K(x, P)$ is a continuous function in x and δ , we get that

$$\Gamma(P) = \lim_{\delta \rightarrow 0} \Gamma_\delta(P) = \lim_{\delta \rightarrow 0} \left(\arg \min_x L_\delta^K(x, P) \right) = \arg \min_x \left(\lim_{\delta \rightarrow 0} L_\delta^K(x, P) \right). \quad (\text{A.4})$$

¹⁹[Ibragimov \(1956\)](#) calls densities satisfying this property *strongly unimodal*. It is important to note that his notion of strong unimodality is different from ours introduced in Definition 2.1.

□

Proof of Theorem 2.6. We define

$$g_{t,T} := \delta_T^{3/2} T^{-1/2} \psi(Y_{t+1}, X_t, \mathbf{h}_t, \delta_T) = (T\delta_T)^{-1/2} K' \left(\frac{X_t - Y_{t+1}}{\delta_T} \right) \mathbf{h}_t, \quad (\text{A.5})$$

$$g_{t,T}^e := \mathbb{E}_t[g_{t,T}], \quad \text{and} \quad (\text{A.6})$$

$$g_{t,T}^* := g_{t,T} - g_{t,T}^e, \quad (\text{A.7})$$

such that

$$\delta_T^{3/2} T^{-1/2} \sum_{t=1}^T \psi(Y_{t+1}, X_t, \mathbf{h}_t, \delta_T) = \sum_{t=1}^T g_{t,T}^e + \sum_{t=1}^T g_{t,T}^*. \quad (\text{A.8})$$

Lemma S.3.1 shows that $\sum_{t=1}^T g_{t,T}^e \xrightarrow{P} 0$. Thus, it remains to show that $\sum_{t=1}^T g_{t,T}^* \xrightarrow{d} \mathcal{N}(0, \Omega_{Mode})$.

For some arbitrary, but fixed $\lambda \in \mathbb{R}^k$, $\|\lambda\|_2 = 1$, we define

$$z_{t,T} = \lambda^\top g_{t,T}^*, \quad \bar{\omega}_T^2 = \sum_{t=1}^T \text{Var}(z_{t,T}), \quad \text{and} \quad h_{t,T} = \frac{z_{t,T}}{\bar{\omega}_T}. \quad (\text{A.9})$$

In the following, we show that a univariate CLT for MDS holds for $\sum_{t=1}^T h_{t,T}$. It obviously holds that $(g_{t,T}^*, \mathcal{F}_{t+1})$ is a MDS as $g_{s,T}^* \in \mathcal{F}_{t+1}$ for all $s \leq t$ and by definition, $\mathbb{E}[g_{t,T}^* | \mathcal{F}_t] = \mathbb{E}_t[g_{t,T}^*] = \mathbb{E}_t[g_{t,T}] - \mathbb{E}_t[g_{t,T}^e] = g_{t,T}^e - g_{t,T}^e = 0$, almost surely. Thus, $(z_{t,T}, \mathcal{F}_{t+1})$ and $(h_{t,T}, \mathcal{F}_{t+1})$ are also MDS.

We verify the following three conditions of Theorem 24.3 of Davidson (1994),

$$(a) \quad \sum_{t=1}^T \text{Var}(h_{t,T}) = 1,$$

$$(b) \quad \sum_{t=1}^T h_{t,T}^2 \xrightarrow{P} 1, \quad \text{and}$$

$$(c) \quad \max_{1 \leq t \leq T} |h_{t,T}| \xrightarrow{P} 0.$$

Lemma S.3.2 shows that $\bar{\omega}_T^2 = \sum_{t=1}^T \text{Var}[z_{t,T}] \rightarrow \bar{\omega}^2 = \lambda^\top \Omega_{Mode} \lambda$ as $T \rightarrow \infty$. Thus, for all T sufficiently large enough, $\bar{\omega}_T^2$ is strictly positive and thus, $h_{t,T}$ is well-defined and $\sum_{t=1}^T \text{Var}(h_{t,T}) = 1$, which shows condition (a). Lemma S.3.3 shows that $\sum_{t=1}^T z_{t,T}^2 \xrightarrow{P} \bar{\omega}^2$ as $T \rightarrow \infty$ which implies

condition (b), i.e. $\sum_{t=1}^T h_{t,T}^2 = \sum_{t=1}^T \frac{z_{t,T}^2}{\bar{\omega}_T^2} \xrightarrow{P} 1$. Eventually, Lemma S.3.4 shows condition (c). Consequently, we apply Theorem 24.3 of Davidson (1994) in order to conclude that for all $\lambda \in \mathbb{R}^k, \|\lambda\|_2 = 1$, it holds that $\sum_{t=1}^T h_{t,T} \xrightarrow{d} \mathcal{N}(0, 1)$. As $\bar{\omega}_T^2 \rightarrow \bar{\omega}^2$, Slutsky's theorem implies that $\sum_{t=1}^T z_{t,T} = \sum_{t=1}^T \lambda^\top g_{t,T}^* \xrightarrow{d} \mathcal{N}(0, \bar{\omega}^2)$. Eventually, as this holds for all $\lambda \in \mathbb{R}^k, \|\lambda\|_2 = 1$, we apply the Cramer-Wold theorem and get that $\sum_{t=1}^T g_{t,T}^* \xrightarrow{d} \mathcal{N}(0, \Omega_{Mode})$, which concludes the proof of this theorem. \square

Proof of Theorem 2.7. Let $\lambda \in \mathbb{R}^k, \|\lambda\|_2 = 1$ be a fixed and deterministic vector. Then,

$$\begin{aligned}
& \lambda^\top \hat{\Omega}_{T, Mode} \lambda - \lambda^\top \Omega_{Mode} \lambda \\
&= \frac{1}{T} \sum_{t=1}^T \delta_T^{-1} K' \left(\frac{X_t - Y_{t+1}}{\delta_T} \right)^2 (\lambda^\top \mathbf{h}_t)^2 - \mathbb{E} \left[(\lambda^\top \mathbf{h}_t)^2 f_t(0) \int K'(u)^2 du \right] \\
&= \frac{1}{T} \sum_{t=1}^T \delta_T^{-1} K' \left(\frac{X_t - Y_{t+1}}{\delta_T} \right)^2 (\lambda^\top \mathbf{h}_t)^2 - \frac{1}{T} \sum_{t=1}^T \mathbb{E}_t \left[\delta_T^{-1} K' \left(\frac{X_t - Y_{t+1}}{\delta_T} \right)^2 (\lambda^\top \mathbf{h}_t)^2 \right] \\
&+ \frac{1}{T} \sum_{t=1}^T \mathbb{E}_t \left[\delta_T^{-1} K' \left(\frac{X_t - Y_{t+1}}{\delta_T} \right)^2 (\lambda^\top \mathbf{h}_t)^2 \right] - \mathbb{E} \left[(\lambda^\top \mathbf{h}_t)^2 f_t(0) \int K'(u)^2 du \right].
\end{aligned} \tag{A.10}$$

We start by showing that the first line in (A.10) is $o_P(1)$,

$$\frac{1}{T} \sum_{t=1}^T \mathbb{E}_t \left[\delta_T^{-1} K' \left(\frac{X_t - Y_{t+1}}{\delta_T} \right)^2 (\lambda^\top \mathbf{h}_t)^2 \right] = \frac{1}{T} \sum_{t=1}^T (\lambda^\top \mathbf{h}_t)^2 \delta_T^{-1} \int K' \left(\frac{e}{\delta_T} \right)^2 f_t(e) de \tag{A.11}$$

$$= \frac{1}{T} \sum_{t=1}^T (\lambda^\top \mathbf{h}_t)^2 \int K'(u)^2 f_t(\delta_T u) du \xrightarrow{P} \mathbb{E} \left[(\lambda^\top \mathbf{h}_t)^2 f_t(0) \int K'(u)^2 du \right], \tag{A.12}$$

as $f_t(\delta_T u) \rightarrow f_t(0) \leq c$, and by further applying a weak law of large numbers for stationary and ergodic data as $\mathbb{E} [\|\mathbf{h}_t\|^{2+\delta}] < \infty$. We further show that the second line in (A.10) converges to zero in L_p (p -th mean) for some $p > 1$ small enough. By applying the von Bahr and Esseen (1965) inequality for MDS, we get that

$$\begin{aligned}
& \mathbb{E} \left| \frac{1}{T} \sum_{t=1}^T \delta_T^{-1} K' \left(\frac{X_t - Y_{t+1}}{\delta_T} \right)^2 (\lambda^\top \mathbf{h}_t)^2 - \frac{1}{T} \sum_{t=1}^T \mathbb{E}_t \left[\delta_T^{-1} K' \left(\frac{X_t - Y_{t+1}}{\delta_T} \right)^2 (\lambda^\top \mathbf{h}_t)^2 \right] \right|^p \\
& \leq 2^{p+1} T^{-p} \sum_{t=1}^T \mathbb{E} \left| \delta_T^{-1} K' \left(\frac{X_t - Y_{t+1}}{\delta_T} \right)^2 (\lambda^\top \mathbf{h}_t)^2 \right|^p
\end{aligned}$$

$$\begin{aligned}
&= 2^{p+1} T^{-p} \sum_{t=1}^T \delta_T^{-p} \mathbb{E} \left[\left| \lambda^\top \mathbf{h}_t \right|^{2p} \mathbb{E}_t \left| K' \left(\frac{X_t - Y_{t+1}}{\delta_T} \right) \right|^2 \right] \\
&= 2^{p+1} T^{-p} \sum_{t=1}^T \delta_T^{-p} \mathbb{E} \left[\left| \lambda^\top \mathbf{h}_t \right|^{2p} \int \left| K' \left(\frac{e}{\delta_T} \right) \right|^2 f_t(e) de \right] \\
&= (T \delta_T)^{1-p} 2^{p+1} \frac{1}{T} \sum_{t=1}^T \mathbb{E} \left[\left| \lambda^\top \mathbf{h}_t \right|^{2p} \int |K'(u)|^2 f_t(\delta_T u) du \right] \rightarrow 0,
\end{aligned}$$

as $(T \delta_T)^{1-p} \rightarrow 0$ for any $p > 1$ and $\mathbb{E} [\|\mathbf{h}_t\|^{2p}] < \infty$ for $p > 1$ small enough. As L_p convergence for any $p > 1$ implies convergence in probability, the result of the theorem follows. \square

Proof of Theorem 2.9. As in the proof of Theorem 2.6, we split $\sum_{t=1}^T g_{t,T} = \sum_{t=1}^T g_{t,T}^e + \sum_{t=1}^T g_{t,T}^*$. It holds again that $\sum_{t=1}^T g_{t,T}^* \xrightarrow{d} \mathcal{N}(0, \Omega_{Mode})$, as this part of the proof does not depend on the assumption on $f_t'(0)$ made by the respective null and global alternative hypotheses. As in the proof of Lemma S.3.1, we obtain that

$$\sum_{t=1}^T g_{t,T}^e = -T^{-1/2} \delta_T^{3/2} \mathbf{h}_t \int K(u) f_t'(\delta_T u) du. \quad (\text{A.13})$$

From a Taylor expansion of $f_t'(\delta_T u)$ around zero, we obtain that for some $\zeta \in [0, 1]$, it holds that $f_t'(\delta_T u) = f_t'(0) + (\delta_T u) f_t''(0) + \frac{(\delta_T u)^2}{2} f_t'''(\zeta \delta_T u)$. Thus,

$$\sum_{t=1}^T g_{t,T}^e = -\frac{1}{T} \sum_{t=1}^T (T \delta_T^3)^{1/2} \mathbf{h}_t f_t'(0) \int K(u) du \quad (\text{A.14})$$

$$- \frac{1}{T} \sum_{t=1}^T (T \delta_T^5)^{1/2} \mathbf{h}_t f_t''(0) \int u K(u) du \quad (\text{A.15})$$

$$- \frac{1}{T} \sum_{t=1}^T (T \delta_T^7)^{1/2} \mathbf{h}_t \int u^2 K(u) f_t'''(\zeta \delta_T u) du, \quad (\text{A.16})$$

for some $\zeta \in [0, 1]$. The second term equals zero as $\int u K(u) du = 0$ by assumption. Furthermore, the third term converges to zero as \mathbf{h}_t is stationary and ergodic and thus a weak law of large numbers applies and furthermore, $T \delta_T^7 \rightarrow 0$ by assumption. However, for the first term we get that $\int K(u) du = 1$ and $\frac{1}{T} \sum_{t=1}^T \mathbf{h}_t \xrightarrow{P} \mathbb{E}[\mathbf{h}_t]$. As furthermore $(T \delta_T^3)^{1/2} \rightarrow \infty$ and $\mathbb{E}[\mathbf{h}_t] \neq 0$ by assumption and $|f_t'(0)| \geq \varepsilon > 0$ almost surely under the global alternative, we obtain that the

first term diverges in probability. This implies that for any $c \in \mathbb{R}$, $\mathbb{P}\left(\left|\sum_{t=1}^T g_{t,T}^e\right| \geq c\right) \rightarrow 1$, and consequently also $\mathbb{P}\left(\left|\sum_{t=1}^T g_{t,T}\right| \geq c\right) \rightarrow 1$. As furthermore $\widehat{\Omega}_{T,Mode} \xrightarrow{P} \Omega_{Mode}$, which is uniformly positive definite and $J_T = \left(\sum_{t=1}^T g_{t,T}\right)^\top \widehat{\Omega}_{T,Mode}^{-1} \left(\sum_{t=1}^T g_{t,T}\right)$, the conditions of Theorem 8.13 of [White \(1994\)](#) are satisfied and we can conclude that for any $c \in \mathbb{R}$, $\mathbb{P}(|J_T| \geq c) \rightarrow 1$, which concludes the proof of this theorem. \square

Proof of Theorem 3.3. For all fixed $\lambda \in \mathbb{R}^k$ such that $\|\lambda\|_2 = 1$, we define

$$\sigma^2 = \lambda^\top \Sigma(\theta_0) \lambda \quad (\text{A.17})$$

$$= \mathbb{E} \left[\theta_{10}^2 \left(\mathbf{h}_t^\top \mathbf{W}_{\text{Mean}} \lambda \right)^2 \varepsilon_t^2 + \theta_{20}^2 \left(\mathbf{h}_t^\top \mathbf{W}_{\text{Med}} \lambda \right)^2 \left(\mathbb{1}_{\{\varepsilon_t > 0\}} - \mathbb{1}_{\{\varepsilon_t < 0\}} \right)^2 \right. \quad (\text{A.18})$$

$$\left. + \theta_{30}^2 \left(\mathbf{h}_t^\top \mathbf{W}_{\text{Mode}} \lambda \right)^2 f_t(0) \int K'(u)^2 du \right. \quad (\text{A.19})$$

$$\left. + 2\theta_{10}\theta_{20} \left(\mathbf{h}_t^\top \mathbf{W}_{\text{Mean}} \lambda \right) \left(\mathbf{h}_t^\top \mathbf{W}_{\text{Med}} \lambda \right) \varepsilon_t \left(\mathbb{1}_{\{\varepsilon_t > 0\}} - \mathbb{1}_{\{\varepsilon_t < 0\}} \right) \right], \quad (\text{A.20})$$

and $\sigma_T^2 = \sum_{t=1}^T \text{Var}(\phi_{t,T}^*(\theta_0)\lambda)$ for the MDS $\phi_{t,T}^*(\theta_0)$. Lemma S.3.5 shows that $\sigma_T^2 \rightarrow \sigma^2$ and thus, σ_T^2 is strictly positive for T large enough and consequently, $\sigma_T^{-1} \sum_{t=1}^T \phi_{t,T}^*(\theta_0)\lambda$ is well-defined. In the following, we show that $\sigma_T^{-1} \sum_{t=1}^T \phi_{t,T}^*(\theta_0)\lambda \xrightarrow{d} \mathcal{N}(0, 1)$ by applying Theorem 24.3 in [Davidson \(1994\)](#). For this, we check that the respective regularity conditions hold.

Lemma S.3.6 shows that $\sum_{t=1}^T (\phi_{t,T}^*(\theta_0)\lambda)^2 \xrightarrow{P} \sigma^2$, which implies condition (a) of Theorem 24.3 of [Davidson \(1994\)](#), i.e. that $\sigma_T^{-1} \sum_{t=1}^T (\phi_{t,T}^*(\theta_0)\lambda)^2 \xrightarrow{P} 1$. Lemma S.3.7 shows condition (b), i.e. that $\max_{t=1, \dots, T} |\sigma_T^{-1} \phi_{t,T}^*(\theta_0)\lambda| \xrightarrow{P} 0$. Thus, we can apply Theorem 24.3 of [Davidson \(1994\)](#) and conclude that $\sigma_T^{-1} \sum_{t=1}^T \phi_{t,T}^*(\theta_0)\lambda \xrightarrow{d} \mathcal{N}(0, 1)$.

As $\sigma_T^2 \rightarrow \sigma^2$, Slutsky's theorem implies that $\sum_{t=1}^T \phi_{t,T}^*(\theta_0)\lambda \xrightarrow{d} \mathcal{N}(0, \sigma^2)$. As this holds for all $\lambda \in \mathbb{R}^k$ such that $\|\lambda\|_2 = 1$, we can conclude that

$$\sum_{t=1}^T \phi_{t,T}^*(\theta_0) \xrightarrow{d} \mathcal{N}(0, \Sigma(\theta_0)). \quad (\text{A.21})$$

Furthermore, $\|\sum_{t=1}^T \phi_{t,T}^*(\theta_0) - \tilde{\phi}_{t,T}(\theta_0)\| = \|\sum_{t=1}^T u_{t,T}(\theta_0)\| \xrightarrow{P} 0$ by Assumption 3.1 and

$$\sum_{t=1}^T \|\tilde{\phi}_{t,T}(\theta) - \phi_{t,T}(\theta)\| = \sum_{t=1}^T \left\| \theta \cdot \begin{pmatrix} T^{-1/2} \mathbf{h}_t^\top (\widehat{\mathbf{W}}_{T,\text{Mean}} - \mathbf{W}_{\text{Mean}}) \varepsilon_t \\ T^{-1/2} \mathbf{h}_t^\top (\widehat{\mathbf{W}}_{T,\text{Med}} - \mathbf{W}_{\text{Med}}) (\mathbb{1}_{\{\varepsilon_t > 0\}} - \mathbb{1}_{\{\varepsilon_t < 0\}}) \\ T^{-1/2} \mathbf{h}_t^\top (\widehat{\mathbf{W}}_{T,\text{Mode}} - \mathbf{W}_{\text{Mode}}) \delta_T^{-1/2} K' \left(\frac{\varepsilon_t}{\delta_T} \right) \end{pmatrix} \right\| \xrightarrow{P} 0$$

as it holds that $\widehat{\mathbf{W}}_{T,\text{Mean}} \xrightarrow{P} \mathbf{W}_{\text{Mean}}$, $\widehat{\mathbf{W}}_{T,\text{Med}} \xrightarrow{P} \mathbf{W}_{\text{Med}}$ and $\widehat{\mathbf{W}}_{T,\text{Mode}} \xrightarrow{P} \mathbf{W}_{\text{Mode}}$ by assumption.

Hence we can conclude that

$$\sum_{t=1}^T \phi_{t,T}(\theta_0) \xrightarrow{d} \mathcal{N}(0, \Sigma(\theta_0)), \quad (\text{A.22})$$

which concludes the proof of this theorem. \square

Proof of Theorem 3.4. For notational simplicity, we show consistency of the covariance estimator by considering the bilinear forms $\lambda^\top \left(\frac{1}{T} \sum_{t=1}^T \phi_{t,T}(\theta_0) \phi_{t,T}(\theta_0)^\top \right) \lambda$ and $\lambda^\top \Sigma(\theta_0) \lambda$ for some arbitrary but fixed $\lambda \in \mathbb{R}^k$ such that $\|\lambda\|_2 = 1$. For this, we define

$$\sigma^2 = \lambda^\top \Sigma(\theta_0) \lambda \quad (\text{A.23})$$

$$= \mathbb{E} \left[\theta_{10}^2 \left(\mathbf{h}_t^\top \mathbf{W}_{\text{Mean}} \lambda \right)^2 \varepsilon_t^2 + \theta_{20}^2 \left(\mathbf{h}_t^\top \mathbf{W}_{\text{Med}} \lambda \right)^2 (\mathbb{1}_{\{\varepsilon_t > 0\}} - \mathbb{1}_{\{\varepsilon_t < 0\}})^2 \right] \quad (\text{A.24})$$

$$+ \theta_{30}^2 \left(\mathbf{h}_t^\top \mathbf{W}_{\text{Mode}} \lambda \right)^2 f_t(0) \int K'(u)^2 du \quad (\text{A.25})$$

$$+ 2\theta_{10}\theta_{20} \left(\mathbf{h}_t^\top \mathbf{W}_{\text{Mean}} \lambda \right) \left(\mathbf{h}_t^\top \mathbf{W}_{\text{Med}} \lambda \right) \varepsilon_t (\mathbb{1}_{\{\varepsilon_t > 0\}} - \mathbb{1}_{\{\varepsilon_t < 0\}}) \Big], \quad (\text{A.26})$$

and

$$\lambda^\top \left(\frac{1}{T} \sum_{t=1}^T \phi_{t,T}(\theta_0) \phi_{t,T}(\theta_0)^\top \right) \lambda \quad (\text{A.27})$$

$$= \frac{1}{T} \sum_{t=1}^T \theta_{10}^2 \left(\mathbf{h}_t^\top \widehat{\mathbf{W}}_{T,\text{Mean}} \lambda \right)^2 \varepsilon_t^2 \quad (\text{A.28})$$

$$+ \theta_{20}^2 \left(\mathbf{h}_t^\top \widehat{\mathbf{W}}_{T,\text{Med}} \lambda \right)^2 (\mathbb{1}_{\{\varepsilon_t > 0\}} - \mathbb{1}_{\{\varepsilon_t < 0\}})^2 \quad (\text{A.29})$$

$$+ \theta_{30}^2 \left(\mathbf{h}_t^\top \widehat{\mathbf{W}}_{T,\text{Mode}} \lambda \right)^2 \delta_T^{-1} K' \left(\frac{\varepsilon_t}{\delta_T} \right)^2 \quad (\text{A.30})$$

$$+ 2\theta_{10}\theta_{20} \left(\mathbf{h}_t^\top \widehat{\mathbf{W}}_{T,\text{Mean}} \lambda \right) \left(\mathbf{h}_t^\top \widehat{\mathbf{W}}_{T,\text{Med}} \lambda \right) \varepsilon_t (\mathbb{1}_{\{\varepsilon_t > 0\}} - \mathbb{1}_{\{\varepsilon_t < 0\}}) \quad (\text{A.31})$$

$$+ 2\theta_{10}\theta_{30} \left(\mathbf{h}_t^\top \widehat{\mathbf{W}}_{T,\text{Mean}} \lambda \right) \left(\mathbf{h}_t^\top \widehat{\mathbf{W}}_{T,\text{Mode}} \lambda \right) \varepsilon_t \delta_T^{-1/2} K' \left(\frac{\varepsilon_t}{\delta_T} \right) \quad (\text{A.32})$$

$$+ 2\theta_{20}\theta_{30} \left(\mathbf{h}_t^\top \widehat{\mathbf{W}}_{T,\text{Med}} \lambda \right) \left(\mathbf{h}_t^\top \widehat{\mathbf{W}}_{T,\text{Mode}} \lambda \right) (\mathbb{1}_{\{\varepsilon_t > 0\}} - \mathbb{1}_{\{\varepsilon_t < 0\}}) \delta_T^{-1/2} K' \left(\frac{\varepsilon_t}{\delta_T} \right). \quad (\text{A.33})$$

We start to show convergence in probability component-wisely for the first line,

$$\frac{1}{T} \sum_{t=1}^T \theta_{10}^2 \left(\mathbf{h}_t^\top \widehat{\mathbf{W}}_{T,\text{Mean}} \lambda \right)^2 \varepsilon_t^2 \quad (\text{A.34})$$

$$= \frac{1}{T} \sum_{t=1}^T \theta_{10}^2 \sum_{i,j,\iota,l} \mathbf{h}_{t,i} \widehat{\mathbf{W}}_{T,\text{Mean},ij} \lambda_j \widehat{\mathbf{W}}_{T,\text{Mean},ij} \mathbf{h}_{t,\iota} \widehat{\mathbf{W}}_{T,\text{Mean},\iota l} \lambda_l \varepsilon_t^2 \quad (\text{A.35})$$

$$= \sum_{i,j,\iota,l} \widehat{\mathbf{W}}_{T,\text{Mean},ij} \widehat{\mathbf{W}}_{T,\text{Mean},\iota l} \frac{1}{T} \sum_{t=1}^T \theta_{10}^2 \mathbf{h}_{t,i} \lambda_j \mathbf{h}_{t,\iota} \lambda_l \varepsilon_t^2 \quad (\text{A.36})$$

$$\xrightarrow{P} \sum_{i,j,\iota,l} \mathbf{W}_{\text{Mean},ij} \mathbf{W}_{\text{Mean},\iota l} \mathbb{E} \left[\theta_{10}^2 \mathbf{h}_{t,i} \lambda_j \mathbf{h}_{t,\iota} \lambda_l \varepsilon_t^2 \right] \quad (\text{A.37})$$

$$= \mathbb{E} \left[\theta_{10}^2 \left(\mathbf{h}_t^\top \mathbf{W}_{\text{Mean}} \lambda \right)^2 \varepsilon_t^2 \right]. \quad (\text{A.38})$$

Convergence of the remaining terms follows analogously by considering the terms component-wisely and by applying the logic of Lemma S.3.6 and by using the decomposition in S.3.64.

□

Testing Forecast Rationality for Measures of Central Tendency

Timo Dimitriadis and Andrew J. Patton and Patrick Schmidt

This Version: May 24, 2022

S.1 Kernel Choice

The asymptotic results presented in Section 2.3 rely on an adequately chosen Kernel K as captured in Assumption (A5). Besides the normalization $\int K(u)du = 1$ and boundedness assumptions, we impose the *first-order kernel* condition $\int uK(u)du = 0$, which is naturally fulfilled for symmetric and bounded kernel functions. Following Li and Racine (2006), kernels of order $\nu > 0$ fulfill the following conditions

$$\int u^l K(u)du = 0 \quad \forall l \leq \nu \quad \text{and} \quad \int u^\nu K(u)du = \kappa_\nu \neq 0. \quad (\text{S.1.1})$$

By the use of higher-order kernels, one can apply a Taylor expansion of higher order in the proofs (see e.g. (S.3.6) in the proof of Lemma S.3.1) and can therefore obtain faster rates of convergence, which could in theory be made arbitrarily close to \sqrt{T} . This however comes at the cost of stronger smoothness assumptions on the underlying density function. Consequently, the rate $\delta_T \approx T^{-1/7}$ obtained from Theorem 2.6 is a strict bound given that we do not want to impose additional smoothness assumptions on the density f_t .

Furthermore, in our specific application of kernel functions, the definition of the generalized modal midpoint in Definition 2.3 is based on the argmin, where we have to guarantee that it is well-defined and unique. For this, we assume in Proposition 2.4 that the kernel function is log-concave. This assumption is automatically violated for any inevitably partly negative higher-order kernel and thus, we cannot guarantee well-definiteness and uniqueness of the generalized modal midpoint functional. Consequently, we stick to first order kernels in this work.

It is well-known in the literature on nonparametric statistics that kernels with bounded support

can be more efficient. However, strict identifiability of the generalized modal midpoint only holds for kernel functions with unbounded support, which supports the usage of unbounded kernel functions such as the Gaussian kernel.

S.2 Bandwidth Choice

Throughout the paper, we choose the bandwidth according to the following formula

$$\delta_T = k_1 \cdot k_2 \cdot T^{-0.143}, \quad (\text{S.2.1})$$

where

$$k_1 = \widehat{\text{Med}}_t[(X_t - Y_{t+1}) - \widehat{\text{Med}}_s(X_s - Y_{s+1})], \quad \text{and} \quad (\text{S.2.2})$$

$$k_2 = 3.2 \exp(-3.2|\hat{\gamma}|), \quad \text{where} \quad (\text{S.2.3})$$

$$\hat{\gamma} = \left| \frac{3\left(\frac{1}{T} \sum_t (X_t - Y_{t+1}) - \widehat{\text{Med}}_t[X_t - Y_{t+1}]\right)}{\hat{\sigma}(X_t - Y_{t+1})} \right|. \quad (\text{S.2.4})$$

As discussed in the Section 2.3, in order to obtain an optimal convergence for our nonparametric test (for first-order kernels), we choose $\delta_T \approx T^{-1/7}$. Following [Kemp and Silva \(2012\)](#), we choose $\delta_T = O(T^{-0.143})$, which is almost $-1/7$. While this choice follows the theoretical deviations from the previous section, the following choices of the constants k_1 and k_2 stem from intuitive reasoning and numerical experiments.

The constant k_1 equals the median absolute deviation which is a robust measure for the scale (standard deviation) of the data and follows the suggestion of [Kemp and Silva \(2012\)](#) and [Kemp et al. \(2019\)](#). The choice of the bandwidth parameter should be proportional to the scale of the underlying data such that test results are robust to linear re-scaling. The constant k_2 adjusts for the empirical skewness $\hat{\gamma}$ of the forecast error and generalizes the approach of [Kemp and Silva \(2012\)](#). For perfectly symmetric distributions, the generalized modal midpoint equals the mode (assuming symmetric kernels). Increasing the skewness increases the distance between the mode and the generalized modal midpoint. Consequently, we choose smaller bandwidth values for increasing

empirical skewness of the underlying distribution.

A popular option for bandwidth choice in the classical literature on nonparametric estimation is *cross-validation* (Li and Racine, 2006). This means that we choose the bandwidth which empirically minimizes some out-of-sample evaluation criteria in a rotating evaluation sample. However, implementation of such a procedure is infeasible in our setup of rationality testing as we cannot use such an evaluation criteria as in nonparametric estimation.

S.3 Technical Proofs

Lemma S.3.1. *Given Assumption 2.5 and under the null hypothesis in (2.8), it holds that*

$$\sum_{t=1}^T g_{t,T}^e \xrightarrow{P} 0. \quad (\text{S.3.1})$$

Proof. Applying integration by parts yields that

$$g_{t,T}^e = \mathbb{E}_t \left[(T\delta_T)^{-1/2} K' \left(\frac{\varepsilon_t}{\delta_T} \right) \mathbf{h}_t \right] = (T\delta_T)^{-1/2} \mathbf{h}_t \int K' \left(\frac{e}{\delta_T} \right) f_t(e) \, de \quad (\text{S.3.2})$$

$$= -T^{-1/2} \delta_T^{1/2} \mathbf{h}_t \int K \left(\frac{e}{\delta_T} \right) f_t'(e) \, de + T^{-1/2} \delta_T^{1/2} \mathbf{h}_t \left[K \left(\frac{e}{\delta_T} \right) f_t(e) \right]_{e=-\infty}^{e=\infty}. \quad (\text{S.3.3})$$

As $\lim_{e \rightarrow \pm\infty} K(e) = 0$ and $f_t(e) \leq c$ for all $e \in \mathbb{R}$ by assumption, we get that

$$T^{-1/2} \delta_T^{1/2} \mathbf{h}_t \left[K \left(\frac{e}{\delta_T} \right) f_t(e) \right]_{e=-\infty}^{e=\infty} = 0 \quad (\text{S.3.4})$$

almost surely for all $T \in \mathbb{N}$. By transformation of variables, it further holds that

$$g_{t,T}^e = -T^{-1/2} \delta_T^{1/2} \mathbf{h}_t \int K \left(\frac{e}{\delta_T} \right) f_t'(e) \, de = -T^{-1/2} \delta_T^{3/2} \mathbf{h}_t \int K(u) f_t'(\delta_T u) \, du. \quad (\text{S.3.5})$$

A Taylor expansion of $f_t'(\delta_T u)$ around zero is given by

$$f_t'(\delta_T u) = f_t'(0) + (\delta_T u) f_t''(0) + \frac{(\delta_T u)^2}{2} f_t'''(\zeta \delta_T u), \quad (\text{S.3.6})$$

for some $\zeta \in [0, 1]$ and $f'_t(0) = 0$ holds under the null hypothesis specified in (2.8). Consequently,

$$\sum_{t=1}^T g_{t,T}^e = -T^{-1/2} \delta_T^{5/2} \sum_{t=1}^T \mathbf{h}_t \int u K(u) f_t''(0) du \quad (\text{S.3.7})$$

$$-0.5T^{-1/2} \delta_T^{7/2} \sum_{t=1}^T \mathbf{h}_t \int u^2 K(u) f_t'''(\zeta \delta_T u) du. \quad (\text{S.3.8})$$

As $\int u K(u) du = 0$ by assumption (A5), we obtain for the first term that for all $T \in \mathbb{N}$,

$$-T^{-1/2} \delta_T^{5/2} \sum_{t=1}^T \mathbf{h}_t f_t''(0) \int u K(u) du = 0. \quad (\text{S.3.9})$$

As $\sup_x f_t'''(x) \leq c$ by Assumption (A4) and $\int u^2 K(u) du \leq c < \infty$ by Assumption (A5), we obtain for the second term that

$$-0.5T^{-1/2} \delta_T^{7/2} \sum_{t=1}^T \mathbf{h}_t \int u^2 K(u) f_t'''(\zeta \delta_T u) du \quad (\text{S.3.10})$$

$$\leq -0.5(T\delta_T^7)^{1/2} \frac{1}{T} \sum_{t=1}^T \mathbf{h}_t \sup_x f_t'''(x) \int u^2 K(u) du \quad (\text{S.3.11})$$

$$\leq -0.5c^2(T\delta_T^7)^{1/2} \frac{1}{T} \sum_{t=1}^T \mathbf{h}_t \xrightarrow{P} 0, \quad (\text{S.3.12})$$

as $T\delta_T^7 \rightarrow 0$ for $T \rightarrow \infty$ by Assumption (A6) and $\frac{1}{T} \sum_{t=1}^T \mathbf{h}_t \xrightarrow{P} \mathbb{E}[\mathbf{h}_t]$ by a law of large numbers for stationary and ergodic sequences. The result of the lemma follows. \square

Lemma S.3.2. *Given Assumption 2.5 and under the null hypothesis in (2.8), it holds that*

$$\sum_{t=1}^T \text{Var}(z_{t,T}) \rightarrow \bar{\omega}^2, \quad \text{as } T \rightarrow \infty. \quad (\text{S.3.13})$$

Proof. We first observe that

$$\text{Var}[z_{t,T}] = \text{Var}\left[\lambda^\top (g_{t,T} - g_{t,T}^e)\right] = \mathbb{E}\left[(\lambda^\top (g_{t,T} - g_{t,T}^e))^2\right] - \mathbb{E}\left[\lambda^\top (g_{t,T} - g_{t,T}^e)\right]^2. \quad (\text{S.3.14})$$

The second term vanishes as $\mathbb{E}\left[\lambda^\top (g_{t,T} - g_{t,T}^e)\right] = \mathbb{E}\left[\lambda^\top (\mathbb{E}_t[g_{t,T}] - g_{t,T}^e)\right] = 0$. For the first term,

we get that

$$\mathbb{E} \left[(\lambda^\top (g_{t,T} - g_{t,T}^e))^2 \right] = \mathbb{E} \left[(\lambda^\top g_{t,T})^2 \right] + \mathbb{E} \left[(\lambda^\top g_{t,T}^e)^2 \right] - 2\mathbb{E} \left[(\lambda^\top g_{t,T}^e) \cdot (\lambda^\top g_{t,T}) \right] \quad (\text{S.3.15})$$

$$= \mathbb{E} \left[(\lambda^\top g_{t,T})^2 \right] - \mathbb{E} \left[(\lambda^\top g_{t,T}^e)^2 \right], \quad (\text{S.3.16})$$

as

$$\mathbb{E} \left[(\lambda^\top g_{t,T}^e) \cdot (\lambda^\top g_{t,T}) \right] = \mathbb{E} \left[(\lambda^\top g_{t,T}^e) \cdot \mathbb{E}_t [\lambda^\top g_{t,T}] \right] = \mathbb{E} \left[(\lambda^\top g_{t,T}^e)^2 \right]. \quad (\text{S.3.17})$$

Thus, we get that

$$\text{Var} [z_{t,T}] = \mathbb{E} \left[(\lambda^\top g_{t,T})^2 \right] - \mathbb{E} \left[(\lambda^\top g_{t,T}^e)^2 \right]. \quad (\text{S.3.18})$$

For the first term in (S.3.18), we get that

$$\mathbb{E} \left[(\lambda^\top g_{t,T})^2 \right] = \mathbb{E} \left[(T\delta_T)^{-1} (\lambda^\top \mathbf{h}_t)^2 K' \left(\frac{X_t - Y_{t+1}}{\delta_T} \right)^2 \right] \quad (\text{S.3.19})$$

$$= \frac{1}{T} \int \int \delta_T^{-1} (\lambda^\top h)^2 K' \left(\frac{e}{\delta_T} \right)^2 dP_t(e) dP_{\mathbf{h}_t}(h) \quad (\text{S.3.20})$$

$$= \frac{1}{T} \int \int \delta_T^{-1} (\lambda^\top h)^2 K' \left(\frac{e}{\delta_T} \right)^2 f_t(e) de dP_{\mathbf{h}_t}(h) \quad (\text{S.3.21})$$

$$= \frac{1}{T} \int \int (\lambda^\top h)^2 K'(u)^2 f_t(\delta_T u) du dP_{\mathbf{h}_t}(w) \quad (\text{S.3.22})$$

$$= \frac{1}{T} \int (\lambda^\top h)^2 \left(\int K'(u)^2 f_t(\delta_T u) du \right) dP_{\mathbf{h}_t}(h). \quad (\text{S.3.23})$$

As the distribution of ε_t given \mathbf{h}_t is time-invariant as we assume stationarity, by letting $\delta_T \rightarrow 0$, we obtain that $\int K'(u)^2 f_t(\delta_T u) du \rightarrow \int K'(u)^2 f_t(0) du = f_t(0) \int K'(u)^2 du$. Thus,

$$\sum_{t=1}^T \mathbb{E} \left[(\lambda^\top g_{t,T})^2 \right] \rightarrow \mathbb{E} \left[f_t(0) (\lambda^\top \mathbf{h}_t)^2 \right] \int K'(u)^2 du = \lambda^\top \mathbb{E} \left[f_t(0) \mathbf{h}_t \mathbf{h}_t^\top \right] \lambda \int K'(u)^2 du. \quad (\text{S.3.24})$$

For the second term in (S.3.18), inserting the equality in (S.3.5) yields

$$\left(\lambda^\top g_{t,T}^e\right)^2 = \left(\delta_T^{3/2} T^{-1/2} (\lambda^\top \mathbf{h}_t) \int K'(u) f'_t(\delta_T u) du\right)^2 \leq \delta_T^3 T^{-1} \|\lambda\|^2 \|\mathbf{h}_t\|^2 \left| \int K'(u) f'_t(u \delta_T) du \right|^2.$$

As $\sup_x |f'_t(x)| \leq c$ and $\int K'(u) du \leq c$ by assumption, it holds that

$$\sum_{t=1}^T \mathbb{E} \left[\left(\lambda^\top g_{t,T}^e \right)^2 \right] \leq \delta_T^3 c \|\lambda\|^2 \left(\frac{1}{T} \sum_{t=1}^T \mathbb{E} [\|\mathbf{h}_t\|^2] \right) \rightarrow 0, \quad (\text{S.3.25})$$

as $\delta_T^3 \rightarrow 0$ as $T \rightarrow \infty$. The result of the lemma eventually follows by combining (S.3.24) and (S.3.25). □

Lemma S.3.3. *Given Assumption 2.5 and under the null hypothesis in (2.8), it holds that*

$$\sum_{t=1}^T z_{t,T}^2 - \bar{\omega}^2 \xrightarrow{P} 0, \quad \text{as } T \rightarrow \infty. \quad (\text{S.3.26})$$

Proof. We define

$$h_{1,T} = \sum_{t=1}^T (z_{t,T}^2 - \mathbb{E}_t [z_{t,T}^2]) \quad \text{and} \quad h_{2,T} = \sum_{t=1}^T \mathbb{E}_t [z_{t,T}^2] - \bar{\omega}^2, \quad (\text{S.3.27})$$

such that $\sum_{t=1}^T z_{t,T}^2 - \bar{\omega}^2 = h_{1,T} + h_{2,T}$. We first show that $h_{1,T} \xrightarrow{L_p} 0$ for some $1 < p < 2$ sufficiently small enough and thus $h_{1,T} \xrightarrow{P} 0$. For this, first notice that $z_{t,T}^2 - \mathbb{E}_t [z_{t,T}^2]$ is a \mathcal{F}_{t+1} -MDS by definition. Thus, we can apply the von Bahr and Esseen (1965)-inequality (for $p \in (1, 2)$) for MDS in order to conclude that

$$\mathbb{E} [|h_{1,T}|^p] = \mathbb{E} \left[\left| \sum_{t=1}^T z_{t,T}^2 - \mathbb{E}_t [z_{t,T}^2] \right|^p \right] \quad (\text{S.3.28})$$

$$\leq 2 \sum_{t=1}^T \mathbb{E} [|z_{t,T}^2 - \mathbb{E}_t [z_{t,T}^2]|^p] \quad (\text{S.3.29})$$

$$\leq 2 \sum_{t=1}^T 2^{p-1} (\mathbb{E} [|z_{t,T}^2|^p] + \mathbb{E} [|\mathbb{E}_t [z_{t,T}^2]|^p]) \quad (\text{S.3.30})$$

$$\leq 2^p \sum_{t=1}^T \left(\mathbb{E} \left[|z_{t,T}|^{2p} \right] + \mathbb{E} \left[\mathbb{E}_t \left[|z_{t,T}|^{2p} \right] \right] \right) \quad (\text{S.3.31})$$

$$= 2^{p+1} \sum_{t=1}^T \mathbb{E} \left[|z_{t,T}|^{2p} \right]. \quad (\text{S.3.32})$$

Furthermore,

$$\mathbb{E} \left[|z_{t,T}|^{2p} \right] = (T\delta_T)^{-p} \mathbb{E} \left[\left| \lambda^\top \mathbf{h}_t K' \left(\frac{\varepsilon_t}{\delta_T} \right) \right|^{2p} \right] \quad (\text{S.3.33})$$

$$\leq (T\delta_T)^{-p} \mathbb{E} \left[\left| \lambda^\top \mathbf{h}_t \right|^{2p} \mathbb{E}_t \left[\left| K' \left(\frac{\varepsilon_t}{\delta_T} \right) \right|^{2p} \right] \right] \quad (\text{S.3.34})$$

$$= (T\delta_T)^{-p} \mathbb{E} \left[\left| \lambda^\top \mathbf{h}_t \right|^{2p} \int \left| K' \left(\frac{e}{\delta_T} \right) \right|^{2p} f_t(e) de \right] \quad (\text{S.3.35})$$

$$= (T\delta_T)^{-p} \delta_T \mathbb{E} \left[\left| \lambda^\top \mathbf{h}_t \right|^{2p} \int |K'(u)|^{2p} f_t(\delta_T u) du \right]. \quad (\text{S.3.36})$$

Consequently,

$$\mathbb{E} [|h_{1,T}|^p] \leq 2^{p+1} \sum_{t=1}^T (T\delta_T)^{-p} \delta_T \mathbb{E} \left[\left| \lambda^\top \mathbf{h}_t \right|^{2p} \int |K'(u)|^{2p} f_t(\delta_T u) du \right] \quad (\text{S.3.37})$$

$$\leq (T\delta_T)^{1-p} 2^{p+1} \|\lambda\|^{2p} \left(\frac{1}{T} \sum_{t=1}^T \mathbb{E} [|h_t|^{2p}] \right) \left(\int |K'(u)|^{2p} f_t(\delta_T u) du \right) \rightarrow 0, \quad (\text{S.3.38})$$

as $(T\delta_T)^{1-p} \rightarrow 0$ for all $p \in (1, 2)$ and

$$\int |K'(u)|^{2p} f_t(\delta_T u) du \leq c \int |K'(u)|^{2p} du \leq c c^{2p-1} \int |K'(u)| du < \infty, \quad (\text{S.3.39})$$

as $\int |K'(u)| du < \infty$, $\sup_u |K'(u)| \leq c$ and $\sup_x f_t(x) \leq c$ almost surely by assumption. Thus, we have shown that $h_{1,T} \xrightarrow{L_p} 0$ for $1 < p < 2$ sufficiently small enough which implies that $h_{1,T} \xrightarrow{P} 0$.

We continue by showing that $h_{2,T} \xrightarrow{P} 0$. For this, we split

$$h_{2,T} = \sum_{t=1}^T \mathbb{E}_t [z_{t,T}^2] - \bar{\omega}^2 = \sum_{t=1}^T \mathbb{E}_t \left[(\lambda^\top g_{t,T})^2 \right] - \sum_{t=1}^T (\lambda^\top g_{t,T}^e)^2 - \bar{\omega}^2. \quad (\text{S.3.40})$$

In the following, we first show that $\sum_{t=1}^T (\lambda^\top g_{t,T}^e)^2 \xrightarrow{P} 0$. For this we apply a transformation of

variables,

$$\sum_{t=1}^T (\lambda^\top g_{t,T}^e)^2 = (T\delta_T)^{-1} \sum_{t=1}^T (\lambda^\top \mathbf{h}_t)^2 \mathbb{E}_t \left[K' \left(\frac{\varepsilon_t}{\delta_T} \right) \right]^2 \quad (\text{S.3.41})$$

$$= (T\delta_T)^{-1} \sum_{t=1}^T (\lambda^\top \mathbf{h}_t)^2 \left(\int \delta_T K'(u) f_t(\delta_T u) du \right)^2 \quad (\text{S.3.42})$$

$$= \delta_T \frac{1}{T} \sum_{t=1}^T (\lambda^\top \mathbf{h}_t)^2 \left(\int K'(u) f_t(\delta_T u) du \right)^2 \quad (\text{S.3.43})$$

$$\leq \delta_T \left(\frac{1}{T} \sum_{t=1}^T (\lambda^\top \mathbf{h}_t)^2 \right) \left(c \int |K'(u)| du \right)^2 \xrightarrow{P} 0, \quad (\text{S.3.44})$$

as $\delta_T \rightarrow 0$, $\frac{1}{T} \sum_{t=1}^T (\lambda^\top \mathbf{h}_t)^2 = \mathbb{E} [(\lambda^\top \mathbf{h}_t)^2] + o_P(1)$ and $(\int |K'(u)| du)^2 \leq \int |K'(u)|^2 du < \infty$ by assumption. In addition, it holds that

$$\sum_{t=1}^T \mathbb{E}_t \left[(\lambda^\top g_{t,T})^2 \right] = (T\delta_T)^{-1} \sum_{t=1}^T (\lambda^\top \mathbf{h}_t)^2 \mathbb{E}_t \left[K' \left(\frac{\varepsilon_t}{\delta_T} \right)^2 \right] \quad (\text{S.3.45})$$

$$= (T\delta_T)^{-1} \sum_{t=1}^T (\lambda^\top \mathbf{h}_t)^2 \int K' \left(\frac{e}{\delta_T} \right)^2 f_t(e) de \quad (\text{S.3.46})$$

$$= (T\delta_T)^{-1} \sum_{t=1}^T (\lambda^\top \mathbf{h}_t)^2 \int \delta_T K'(u)^2 f_t(\delta_T u) du \quad (\text{S.3.47})$$

$$= \left(\frac{1}{T} \sum_{t=1}^T (\lambda^\top \mathbf{h}_t)^2 \right) \int K'(u)^2 f_t(\delta_T u) du \quad (\text{S.3.48})$$

$$\xrightarrow{P} \mathbb{E} \left[f_t(0) (\lambda^\top \mathbf{h}_t)^2 \right] \int K'(u)^2 du \quad (\text{S.3.49})$$

$$= \lambda^\top \mathbb{E} \left[f_t(0) \mathbf{h}_t \mathbf{h}_t^\top \right] \lambda \int K'(u)^2 du = \bar{\omega}^2. \quad (\text{S.3.50})$$

Thus, we get that $h_{2,T} \xrightarrow{P} 0$ and consequently $\sum_{t=1}^T z_{t,T}^2 - \bar{\omega}^2 \xrightarrow{P} 0$, which concludes the proof of this lemma. \square

Lemma S.3.4. *Given Assumption 2.5 and under the null hypothesis in (2.8), it holds that*

$$\max_{1 \leq t \leq T} |h_{t,T}| \xrightarrow{P} 0. \quad (\text{S.3.51})$$

Proof. Let $\zeta > 0$ and $\delta > 0$ (sufficiently small such that $\mathbb{E} [||\mathbf{h}_t||^{2+\delta}] < \infty$ by assumption still holds). Then,

$$\mathbb{P} \left(\max_{1 \leq t \leq T} |h_{t,T}| > \zeta \right) = \mathbb{P} \left(\max_{1 \leq t \leq T} |h_{t,T}|^{2+\delta} > \zeta^{2+\delta} \right) \leq \sum_{t=1}^T \mathbb{P} \left(|h_{t,T}|^{2+\delta} > \zeta^{2+\delta} \right) \quad (\text{S.3.52})$$

$$\leq \zeta^{-2-\delta} \sum_{t=1}^T \mathbb{E} \left[|h_{t,T}|^{2+\delta} \right] = \zeta^{-2-\delta} \bar{\omega}_T^{-2-\delta} \sum_{t=1}^T \mathbb{E} \left[|z_{t,T}|^{2+\delta} \right], \quad (\text{S.3.53})$$

by the Markov inequality. We further get by the c_r -inequality that for all $t = 1, \dots, T$,

$$\mathbb{E} \left[|z_{t,T}|^{2+\delta} \right] = \mathbb{E} \left[\left| \lambda^\top (g_{t,T} - g_{t,T}^e) \right|^{2+\delta} \right] \quad (\text{S.3.54})$$

$$\leq 2^{1+\delta} \left(\mathbb{E} \left[\left| \lambda^\top g_{t,T} \right|^{2+\delta} \right] + \mathbb{E} \left[\left| \lambda^\top g_{t,T}^e \right|^{2+\delta} \right] \right) \quad (\text{S.3.55})$$

$$\leq 2^{2+\delta} \mathbb{E} \left[\left| \lambda^\top g_{t,T} \right|^{2+\delta} \right] \quad (\text{S.3.56})$$

$$\leq 2^{2+\delta} (T\delta_T)^{-(2+\delta)/2} \mathbb{E} \left[\left| \lambda^\top \mathbf{h}_t \right|^{2+\delta} \mathbb{E}_t \left[\left| K' \left(\frac{X_t - Y_{t+1}}{\delta_T} \right) \right|^{2+\delta} \right] \right]. \quad (\text{S.3.57})$$

It further holds that

$$\mathbb{E}_t \left[\left| K' \left(\frac{X_t - Y_{t+1}}{\delta_T} \right) \right|^{2+\delta} \right] = \int \left| K' \left(\frac{e}{\delta_T} \right) \right|^{2+\delta} f_t(e) de \quad (\text{S.3.58})$$

$$= \delta_T \int |K'(u)|^{2+\delta} f_t(\delta_T u) du \quad (\text{S.3.59})$$

$$\leq \delta_T c \int |K'(u)|^{2+\delta} du, \quad (\text{S.3.60})$$

and as $\sup_u |K'(u)| < c$, we get that

$$\int |K'(u)|^{2+\delta} du = c^{2+\delta} \int \left| \frac{K'(u)}{c} \right|^{2+\delta} du \leq c^{2+\delta} \int \left| \frac{K'(u)}{c} \right|^2 du \leq c^{3+\delta}. \quad (\text{S.3.61})$$

Thus,

$$\mathbb{P} \left(\max_{1 \leq t \leq T} |h_{t,T}| > \zeta \right) \leq \zeta^{-2-\delta} \bar{\omega}_T^{-2-\delta} \sum_{t=1}^T \mathbb{E} |z_{t,T}|^{2+\delta} \quad (\text{S.3.62})$$

$$\leq (T\delta_T)^{-\delta/2} \zeta^{-2-\delta} \bar{\omega}_T^{-2-\delta} 2^{2+\delta} c^{4+\delta} \frac{1}{T} \sum_{t=1}^T \mathbb{E} \left[|\lambda^\top \mathbf{h}_t|^{2+\delta} \right] \rightarrow 0, \quad (\text{S.3.63})$$

as $(T\delta_T)^{-\delta/2} \rightarrow 0$ for all $\delta > 0$ by assumption and $\frac{1}{T} \sum_{t=1}^T \mathbb{E} [||\mathbf{h}_t||^{2+\delta}] < \infty$ for some sufficiently small $\delta > 0$.

□

Lemma S.3.5. *Given Assumption 3.1 and Assumption 3.2, for all $\lambda \in \mathbb{R}^k$ such that $||\lambda||_2 = 1$, it holds that $\sum_{t=1}^T \text{Var}(\phi_{t,T}^*(\theta_0)\lambda) \rightarrow \sigma^2$.*

Proof. As $\phi_{t,T}^*$ is a \mathcal{F}_{t+1} -MDS, it holds that $\mathbb{E}[\phi_{t,T}^*(\theta_0)\lambda] = 0$ and thus, $\text{Var}(\phi_{t,T}^*(\theta_0)\lambda) = \mathbb{E}[(\phi_{t,T}^*(\theta_0)\lambda)^2]$.

We further get that

$$\begin{aligned}
& \sum_{t=1}^T \mathbb{E} \left[(\phi_{t,T}^*(\theta_0) \lambda)^2 \right] \\
&= \sum_{t=1}^T \mathbb{E} \left[\left\{ \theta_{10} T^{-1/2} \left(\lambda^\top \mathbf{W}_{\text{Mean}} \mathbf{h}_t \right) \varepsilon_t + \theta_{20} T^{-1/2} \left(\lambda^\top \mathbf{W}_{\text{Med}} \mathbf{h}_t \right) (\mathbb{1}_{\{\varepsilon_t > 0\}} - \mathbb{1}_{\{\varepsilon_t < 0\}}) \right. \right. \\
&\quad \left. \left. + \theta_{30} T^{-1/2} \left(\lambda^\top \mathbf{W}_{\text{Mode}} \mathbf{h}_t \right) \delta_T^{-1/2} K' \left(\frac{\varepsilon_t}{\delta_T} \right) + u_{t,T}(\theta_0) \right\}^2 \right] \\
&= \frac{1}{T} \sum_{t=1}^T \mathbb{E} \left[\theta_{10}^2 \left(\lambda^\top \mathbf{W}_{\text{Mean}} \mathbf{h}_t \right)^2 \varepsilon_t^2 \right] \\
&+ \frac{1}{T} \sum_{t=1}^T \mathbb{E} \left[\theta_{20}^2 \left(\lambda^\top \mathbf{W}_{\text{Med}} \mathbf{h}_t \right)^2 (\mathbb{1}_{\{\varepsilon_t > 0\}} - \mathbb{1}_{\{\varepsilon_t < 0\}})^2 \right] \\
&+ \frac{1}{T} \sum_{t=1}^T \mathbb{E} \left[\theta_{30}^2 \left(\lambda^\top \mathbf{W}_{\text{Mode}} \mathbf{h}_t \right)^2 \delta_T^{-1} K'^2 \left(\frac{\varepsilon_t}{\delta_T} \right) \right] \tag{S.3.64} \\
&+ \sum_{t=1}^T \mathbb{E} \left[(\lambda^\top u_{t,T}(\theta_0))^2 \right] \\
&+ \frac{2}{T} \sum_{t=1}^T \mathbb{E} \left[\theta_{10} \theta_{20} \left(\lambda^\top \mathbf{W}_{\text{Mean}} \mathbf{h}_t \right) \left(\lambda^\top \mathbf{W}_{\text{Med}} \mathbf{h}_t \right) \varepsilon_t (\mathbb{1}_{\{\varepsilon_t > 0\}} - \mathbb{1}_{\{\varepsilon_t < 0\}}) \right] \\
&+ \frac{2}{T} \sum_{t=1}^T \mathbb{E} \left[\theta_{10} \theta_{30} \left(\lambda^\top \mathbf{W}_{\text{Mean}} \mathbf{h}_t \right) \left(\lambda^\top \mathbf{W}_{\text{Mode}} \mathbf{h}_t \right) \varepsilon_t \delta_T^{-1/2} K' \left(\frac{\varepsilon_t}{\delta_T} \right) \right] \\
&+ \frac{2}{T} \sum_{t=1}^T \mathbb{E} \left[\theta_{20} \theta_{30} \left(\lambda^\top \mathbf{W}_{\text{Med}} \mathbf{h}_t \right) \left(\lambda^\top \mathbf{W}_{\text{Mode}} \mathbf{h}_t \right) (\mathbb{1}_{\{\varepsilon_t > 0\}} - \mathbb{1}_{\{\varepsilon_t < 0\}}) \delta_T^{-1/2} K' \left(\frac{\varepsilon_t}{\delta_T} \right) \right] \\
&+ 2 \sum_{t=1}^T \mathbb{E} \left[(u_{t,T}(\theta_0) \lambda) (\tilde{\phi}_{t,T}(\theta_0) \lambda) \right].
\end{aligned}$$

For the fourth and last term, we obtain that

$$\sum_{t=1}^T \mathbb{E} \left[(u_{t,T}(\theta_0) \lambda)^2 \right] \rightarrow 0, \quad \text{and} \quad \sum_{t=1}^T \mathbb{E} \left[(u_{t,T}(\theta_0) \lambda) (\tilde{\phi}_{t,T}(\theta_0) \lambda) \right] \rightarrow 0, \tag{S.3.65}$$

by assumption. For the sixth term,

$$\frac{2}{T} \sum_{t=1}^T \mathbb{E} \left[\theta_{10} \theta_{30} \left(\lambda^\top \mathbf{W}_{\text{Mean}} \mathbf{h}_t \right) \left(\lambda^\top \mathbf{W}_{\text{Mode}} \mathbf{h}_t \right) \varepsilon_t \delta_T^{-1/2} K' \left(\frac{\varepsilon_t}{\delta_T} \right) \right] \tag{S.3.66}$$

$$= \frac{2}{T} \sum_{t=1}^T \mathbb{E} \left[\theta_{10} \theta_{30} \left(\lambda^\top \mathbf{W}_{\text{Mean}} \mathbf{h}_t \right) \left(\lambda^\top \mathbf{W}_{\text{Mode}} \mathbf{h}_t \right) \varepsilon_t \delta_T^{1/2} \int K'(u) f_t(\delta_T u) du \right] \rightarrow 0, \quad (\text{S.3.67})$$

as $\delta_T^{1/2} \rightarrow 0$ and the respective moments are finite. The seventh term converges to zero by the same argument. For the third term, it holds that

$$\frac{1}{T} \sum_{t=1}^T \mathbb{E} \left[\theta_{30}^2 \left(\lambda^\top \mathbf{W}_{\text{Mode}} \mathbf{h}_t \right)^2 \delta_T^{-1} K' \left(\frac{\varepsilon_t}{\delta_T} \right)^2 \right] \quad (\text{S.3.68})$$

$$= \frac{1}{T} \sum_{t=1}^T \mathbb{E} \left[\theta_{30}^2 \left(\lambda^\top \mathbf{W}_{\text{Mode}} \mathbf{h}_t \right)^2 \delta_T^{-1} \int \delta_T K'(u)^2 f_t(\delta_T u) du \right] \quad (\text{S.3.69})$$

$$\rightarrow \mathbb{E} \left[\theta_{30}^2 \left(\lambda^\top \mathbf{W}_{\text{Mode}} \mathbf{h}_t \right)^2 f_t(0) \int K'(u)^2 du \right]. \quad (\text{S.3.70})$$

The remaining first, second and fifth term obviously converge to the equivalent quantities of σ^2 , which concludes the proof of the lemma. \square

Lemma S.3.6. *Given Assumption 3.1 and Assumption 3.2, for all $\lambda \in \mathbb{R}^k$ such that $\|\lambda\|_2 = 1$, it holds that*

$$\sum_{t=1}^T (\phi_{t,T}^*(\theta_0) \lambda)^2 \xrightarrow{P} \sigma^2 \quad (\text{S.3.71})$$

Proof. We apply the same factorization as in (S.3.64) (however without the expectation operator). By applying a law of large numbers for stationary and ergodic sequences (Theorem 3.34 in [White \(2001\)](#)), we obtain that

$$\frac{1}{T} \sum_{t=1}^T \left(\theta_{10} \left(\mathbf{h}_t^\top \mathbf{W}_{\text{Mean}} \lambda \right) \varepsilon_t \right)^2 \xrightarrow{P} \mathbb{E} \left[\left(\theta_{10} \left(\mathbf{h}_t^\top \mathbf{W}_{\text{Mean}} \lambda \right) \varepsilon_t \right)^2 \right], \quad (\text{S.3.72})$$

$$\frac{1}{T} \sum_{t=1}^T \left(\theta_{20} \left(\mathbf{h}_t^\top \mathbf{W}_{\text{Med}} \lambda \right) (\mathbb{1}_{\{\varepsilon_t > 0\}} - \mathbb{1}_{\{\varepsilon_t < 0\}}) \right)^2 \xrightarrow{P} \mathbb{E} \left[\left(\theta_{20} \left(\mathbf{h}_t^\top \mathbf{W}_{\text{Med}} \lambda \right) (\mathbb{1}_{\{\varepsilon_t > 0\}} - \mathbb{1}_{\{\varepsilon_t < 0\}}) \right)^2 \right], \quad (\text{S.3.73})$$

$$\frac{2}{T} \sum_{t=1}^T \left(\theta_{10} \theta_{20} \left(\mathbf{h}_t^\top \mathbf{W}_{\text{Mean}} \lambda \right) \left(\mathbf{h}_t^\top \mathbf{W}_{\text{Med}} \lambda \right) \varepsilon_t (\mathbb{1}_{\{\varepsilon_t > 0\}} - \mathbb{1}_{\{\varepsilon_t < 0\}}) \right)^2 \quad (\text{S.3.74})$$

$$\xrightarrow{P} 2 \mathbb{E} \left[\left(\theta_{10} \theta_{20} \left(\mathbf{h}_t^\top \mathbf{W}_{\text{Mean}} \lambda \right) \left(\mathbf{h}_t^\top \mathbf{W}_{\text{Med}} \lambda \right) \varepsilon_t (\mathbb{1}_{\{\varepsilon_t > 0\}} - \mathbb{1}_{\{\varepsilon_t < 0\}}) \right)^2 \right]. \quad (\text{S.3.75})$$

Furthermore, from Lemma S.3.3, we get that

$$\frac{1}{T} \sum_{t=1}^T \theta_{30}^2 \left(\mathbf{h}_t^\top \mathbf{W}_{\text{Mode}} \lambda \right)^2 \delta_T^{-1} K' \left(\frac{\varepsilon_t}{\delta_T} \right)^2 \xrightarrow{P} \mathbb{E} \left[\theta_{30}^2 \left(\mathbf{h}_t^\top \mathbf{W}_{\text{Mode}} \lambda \right)^2 f_t(0) \int K'(u)^2 du \right]. \quad (\text{S.3.76})$$

We now show that the remaining four terms vanish asymptotically (in probability). For the mixed mean/mode term, we apply the same addition of a zero as in the proof of Lemma S.3.3. We first note that

$$\frac{2}{T} \sum_{t=1}^T \theta_{10} \theta_{30} \left(\mathbf{h}_t^\top \mathbf{W}_{\text{Mean}} \lambda \right) \left(\mathbf{h}_t^\top \mathbf{W}_{\text{Mode}} \lambda \right) \delta_T^{-1/2} \mathbb{E}_t \left[\varepsilon_t K' \left(\frac{\varepsilon_t}{\delta_T} \right) \right] \quad (\text{S.3.77})$$

$$= \frac{2}{T} \sum_{t=1}^T \theta_{10} \theta_{30} \left(\mathbf{h}_t^\top \mathbf{W}_{\text{Mean}} \lambda \right) \left(\mathbf{h}_t^\top \mathbf{W}_{\text{Mode}} \lambda \right) \delta_T^{-1/2} \int e K' \left(\frac{e}{\delta_T} \right) f_t(e) de \quad (\text{S.3.78})$$

$$= \frac{2}{T} \sum_{t=1}^T \theta_{10} \theta_{30} \left(\mathbf{h}_t^\top \mathbf{W}_{\text{Mean}} \lambda \right) \left(\mathbf{h}_t^\top \mathbf{W}_{\text{Mode}} \lambda \right) \delta_T^{3/2} \int u K'(u) f_t(\delta_T u) du \xrightarrow{P} 0, \quad (\text{S.3.79})$$

as $\delta_T^{3/2} \rightarrow 0$. In the following, we further show that

$$\frac{2}{T} \sum_{t=1}^T \theta_{10} \theta_{30} \left(\mathbf{h}_t^\top \mathbf{W}_{\text{Mean}} \lambda \right) \left(\mathbf{h}_t^\top \mathbf{W}_{\text{Mode}} \lambda \right) \delta_T^{-1/2} \left\{ \varepsilon_t K' \left(\frac{\varepsilon_t}{\delta_T} \right) - \mathbb{E}_t \left[\varepsilon_t K' \left(\frac{\varepsilon_t}{\delta_T} \right) \right] \right\} \xrightarrow{L_p} 0, \quad (\text{S.3.80})$$

for any $p \in (1, 2)$. As in the proof of Lemma S.3.3, we apply the von Bahr and Esseen (1965) inequality in order to conclude that

$$\begin{aligned} & \mathbb{E} \left[\left| \frac{2}{T} \sum_{t=1}^T \theta_{10} \theta_{30} \left(\mathbf{h}_t^\top \mathbf{W}_{\text{Mean}} \lambda \right) \left(\mathbf{h}_t^\top \mathbf{W}_{\text{Mode}} \lambda \right) \delta_T^{-1/2} \left\{ \varepsilon_t K' \left(\frac{\varepsilon_t}{\delta_T} \right) - \mathbb{E}_t \left[\varepsilon_t K' \left(\frac{\varepsilon_t}{\delta_T} \right) \right] \right\} \right|^p \right] \\ & \leq 2^{p+1} \frac{2}{T} \sum_{t=1}^T \mathbb{E} \left[\left| \theta_{10} \theta_{30} \left(\mathbf{h}_t^\top \mathbf{W}_{\text{Mean}} \lambda \right) \left(\mathbf{h}_t^\top \mathbf{W}_{\text{Mode}} \lambda \right) \delta_T^{-1/2} \varepsilon_t K' \left(\frac{\varepsilon_t}{\delta_T} \right) \right|^p \right] \\ & \leq 2^p T^{-p} \sum_{t=1}^T \mathbb{E} \left[\left| \theta_{10} \theta_{30} \left(\mathbf{h}_t^\top \mathbf{W}_{\text{Mean}} \lambda \right) \left(\mathbf{h}_t^\top \mathbf{W}_{\text{Mode}} \lambda \right) \right|^p \delta_T^{-p/2} \int \left| e K' \left(\frac{e}{\delta_T} \right) \right|^p f_t(e) de \right] \\ & \leq 2^p \delta_T^{1+p/2} T^{1-p} \frac{1}{T} \sum_{t=1}^T \mathbb{E} \left[\left| \theta_{10} \theta_{30} \left(\mathbf{h}_t^\top \mathbf{W}_{\text{Mean}} \lambda \right) \left(\mathbf{h}_t^\top \mathbf{W}_{\text{Mode}} \lambda \right) \right|^p \int |u K'(u)|^p du f_t(0) \right] \rightarrow 0, \end{aligned}$$

as $\delta_T^{1+p/2} \rightarrow 0$ and $T^{1-p} \rightarrow 0$ for any $p > 1$. Applying the same line of reasoning for the mixed

median/mode terms shows that

$$\frac{2}{T} \sum_{t=1}^T \theta_{20} \theta_{30} \left(\mathbf{h}_t^\top \mathbf{W}_{\text{Med}} \lambda \right) \left(\mathbf{h}_t^\top \mathbf{W}_{\text{Mode}} \lambda \right) \delta_T^{-1/2} \mathbb{E}_t \left[\left(\mathbb{1}_{\{\varepsilon_t > 0\}} - \mathbb{1}_{\{\varepsilon_t < 0\}} \right) K' \left(\frac{\varepsilon_t}{\delta_T} \right) \right] \xrightarrow{P} 0. \quad (\text{S.3.81})$$

For the fourth and last term, we obtain that

$$\sum_{t=1}^T (u_{t,T}(\theta_0) \lambda)^2 \xrightarrow{P} 0, \quad \text{and} \quad \sum_{t=1}^T (u_{t,T}(\theta_0) \lambda) (\tilde{\phi}_{t,T}(\theta_0) \lambda) \xrightarrow{P} 0, \quad (\text{S.3.82})$$

by assumption, which concludes this proof. \square

Lemma S.3.7. *Given Assumption 3.1 and Assumption 3.2, for all $\lambda \in \mathbb{R}^k$ such that $\|\lambda\|_2 = 1$, it holds that*

$$\max_{1 \leq t \leq T} |\sigma^{-1} \phi_{t,T}^*(\theta_0) \lambda| \xrightarrow{P} 0. \quad (\text{S.3.83})$$

Proof. Let $\zeta > 0$ and $\delta > 0$ (sufficiently small such that $\mathbb{E} [\|\mathbf{h}_t\|^{2+\delta}] < \infty$ by assumption still holds). Then, as in the proof of Lemma S.3.4, we get that

$$\mathbb{P} \left(\max_{1 \leq t \leq T} |\sigma_T^{-1} \phi_{t,T}^*(\theta_0) \lambda| > \zeta \right) = \mathbb{P} \left(\max_{1 \leq t \leq T} |\sigma_T^{-1} \phi_{t,T}^*(\theta_0) \lambda|^{2+\delta} > \zeta^{2+\delta} \right) \quad (\text{S.3.84})$$

$$\leq \sum_{t=1}^T \mathbb{P} \left(|\sigma_T^{-1} \phi_{t,T}^*(\theta_0) \lambda|^{2+\delta} > \zeta^{2+\delta} \right) \leq \zeta^{-2-\delta} \sigma_T^{-2-\delta} \sum_{t=1}^T \mathbb{E} \left[|\phi_{t,T}^*(\theta_0) \lambda|^{2+\delta} \right], \quad (\text{S.3.85})$$

by the Markov inequality. Furthermore, we get that

$$\sum_{t=1}^T \mathbb{E} \left[|\phi_{t,T}^*(\theta_0) \lambda|^{2+\delta} \right] \quad (\text{S.3.86})$$

$$= \sum_{t=1}^T \mathbb{E} \left[\left| T^{-\frac{1}{2}} \left(\mathbf{h}_t^\top \mathbf{W}_{\text{Mean}} \lambda \right) \theta_{10} \varepsilon_t + T^{-\frac{1}{2}} \left(\mathbf{h}_t^\top \mathbf{W}_{\text{Med}} \lambda \right) \theta_{20} (\mathbb{1}_{\{\varepsilon_t > 0\}} - \mathbb{1}_{\{\varepsilon_t < 0\}}) \right. \right. \quad (\text{S.3.87})$$

$$\left. + T^{-\frac{1}{2}} \left(\mathbf{h}_t^\top \mathbf{W}_{\text{Mode}} \lambda \right) \theta_{30} \delta_T^{-1/2} K' \left(\frac{\varepsilon_t}{\delta_T} \right) + u_{t,T}(\theta_0) \right|^{2+\delta} \Big] \quad (\text{S.3.88})$$

$$\leq \theta_{10}^{2+\delta} T^{-\frac{2+\delta}{2}} \sum_{t=1}^T \mathbb{E} \left[\left| \mathbf{h}_t^\top \mathbf{W}_{\text{Mean}} \lambda \right|^{2+\delta} |\varepsilon_t|^{2+\delta} \right] \quad (\text{S.3.89})$$

$$+ \theta_{20}^{2+\delta} T^{-\frac{2+\delta}{2}} \sum_{t=1}^T \mathbb{E} \left[\left| \mathbf{h}_t^\top \mathbf{W}_{\text{Med}} \lambda \right|^{2+\delta} \left| \mathbb{1}_{\{\varepsilon_t > 0\}} - \mathbb{1}_{\{\varepsilon_t < 0\}} \right|^{2+\delta} \right] \quad (\text{S.3.90})$$

$$+ \theta_{30}^{2+\delta} T^{-\frac{2+\delta}{2}} \sum_{t=1}^T \mathbb{E} \left[\left| \mathbf{h}_t^\top \mathbf{W}_{\text{Mode}} \lambda \right|^{2+\delta} \delta_T^{-\frac{2+\delta}{2}} \left| K' \left(\frac{\varepsilon_t}{\delta_T} \right) \right|^{2+\delta} \right] \quad (\text{S.3.91})$$

$$+ \sum_{t=1}^T \mathbb{E} \left[|u_{t,T}(\theta_0)|^{2+\delta} \right]. \quad (\text{S.3.92})$$

In the following, we analyze these four terms separately. For the first term, we get that

$$\theta_{10}^{2+\delta} T^{-\frac{\delta}{2}} \frac{1}{T} \sum_{t=1}^T \mathbb{E} \left[\left| \mathbf{h}_t^\top \mathbf{W}_{\text{Mean}} \lambda \right|^{2+\delta} |\varepsilon_t|^{2+\delta} \right] \rightarrow 0 \quad (\text{S.3.93})$$

as $T^{-\frac{\delta}{2}} \rightarrow 0$ and the respective moment is bounded by assumption. Convergence in probability to zero of the second term is established equivalently. For the third term, we obtain convergence equivalently to the proof of Lemma S.3.4,

$$\theta_{30}^{2+\delta} T^{-\frac{2+\delta}{2}} \sum_{t=1}^T \mathbb{E} \left[\left| \mathbf{h}_t^\top \mathbf{W}_{\text{Mode}} \lambda \right|^{2+\delta} \delta_T^{-\frac{2+\delta}{2}} \left| K' \left(\frac{\varepsilon_t}{\delta_T} \right) \right|^{2+\delta} \right] \quad (\text{S.3.94})$$

$$\leq \theta_{30}^{2+\delta} T^{-\frac{2+\delta}{2}} \sum_{t=1}^T \mathbb{E} \left[\left| \mathbf{h}_t^\top \mathbf{W}_{\text{Mode}} \lambda \right|^{2+\delta} \delta_T^{-\frac{2+\delta}{2}} \int \left| K' \left(\frac{e}{\delta_T} \right) \right|^{2+\delta} f_t(e) de \right] \quad (\text{S.3.95})$$

$$\leq \theta_{30}^{2+\delta} T^{-\frac{\delta}{2}} \frac{1}{T} \sum_{t=1}^T \mathbb{E} \left[\left| \mathbf{h}_t^\top \mathbf{W}_{\text{Mode}} \lambda \right|^{2+\delta} \delta_T^{-\frac{\delta}{2}} \int |K'(u)|^{2+\delta} f_t(\delta_T u) du \right] \quad (\text{S.3.96})$$

$$\leq \theta_{30}^{2+\delta} (T\delta_T)^{-\frac{\delta}{2}} \frac{1}{T} \sum_{t=1}^T \mathbb{E} \left[\left| \mathbf{h}_t^\top \mathbf{W}_{\text{Mode}} \lambda \right|^{2+\delta} \int |K'(u)|^{2+\delta} f_t(0) du \right], \quad (\text{S.3.97})$$

which converges to zero as $(T\delta_T)^{-\frac{\delta}{2}} \rightarrow 0$. Finally, convergence of the last term follows by Assumption 3.1 and consequently, the result of the lemma follows. \square

S.4 Additional Plots and Tables

Table S.4: Empirical size of the mode rationality test: Gaussian kernel, 1% significance level.

	Instrument set 1				Instrument set 2				Instrument set 3			
Skewness	0	0.1	0.25	0.5	0	0.1	0.25	0.5	0	0.1	0.25	0.5
Sample size	Panel A: Homoskedastic iid data											
100	0.6	0.7	0.6	1.6	0.3	0.4	0.4	0.7	0.2	0.2	0.2	0.4
500	0.9	1.1	1.8	2.6	0.8	1.0	1.3	1.9	0.7	0.9	1.1	1.4
2000	1.1	1.2	2.0	1.7	1.0	1.3	1.5	1.5	0.9	1.1	1.2	1.3
5000	1.0	1.2	1.9	1.7	1.0	1.0	1.6	1.4	0.9	1.1	1.4	1.3
	Panel B: Heteroskedastic data											
100	0.6	0.6	0.8	1.5	0.3	0.3	0.4	0.6	0.1	0.2	0.2	0.4
500	0.9	1.3	2.0	2.1	0.9	1.1	1.4	1.4	1.0	1.0	1.3	1.2
2000	1.0	1.5	2.7	1.6	0.9	1.3	2.0	1.3	1.2	1.0	1.5	1.2
5000	1.0	1.8	2.7	1.7	0.9	1.4	2.1	1.3	1.1	1.4	2.0	1.2
	Panel C: Autoregressive data											
100	0.6	0.5	0.7	1.8	0.7	0.6	0.8	1.2	0.4	0.4	0.4	0.8
500	0.9	1.2	1.7	2.7	0.8	1.0	1.5	1.9	0.9	0.8	1.4	1.8
2000	1.1	1.3	2.4	1.8	1.3	1.3	1.8	1.5	0.8	1.1	1.7	1.4
5000	1.1	1.5	2.2	1.6	1.1	1.3	1.7	1.4	1.0	1.3	1.5	1.2
	Panel D: AR-GARCH data											
100	0.5	0.5	0.8	1.4	0.4	0.6	0.6	1.0	0.3	0.3	0.3	0.5
500	1.0	1.1	1.8	2.5	0.9	1.0	1.3	1.9	0.8	1.1	1.3	1.5
2000	1.1	1.2	2.1	1.9	1.1	1.0	1.7	1.4	1.1	1.0	1.5	1.3
5000	1.1	1.6	1.8	1.6	1.0	1.5	1.4	1.4	0.9	1.2	1.4	1.2

Notes: This table presents the empirical size of the mode rationality test for a Gaussian kernel, varying sample sizes, varying levels of skewness in the residual distribution and different instrument choices for a nominal significance level of 1%.

Table S.5: Empirical size of the mode rationality test: Gaussian kernel, 10% significance level

	Instrument set 1				Instrument set 2				Instrument set 3			
	0	0.1	0.25	0.5	0	0.1	0.25	0.5	0	0.1	0.25	0.5
Skewness												
Sample size	Panel A: Homoskedastic iid data											
100	9.2	9.6	10.4	15.1	8.8	9.0	8.9	12.5	8.1	8.2	8.0	10.5
500	10.4	11.1	14.1	15.1	10.0	10.8	12.4	13.4	9.6	10.3	11.8	12.8
2000	10.4	12.4	13.6	12.8	9.7	11.3	12.0	11.8	9.6	10.8	11.2	11.6
5000	10.5	11.9	13.7	12.2	10.3	11.1	12.4	11.8	10.1	10.4	11.7	10.8
	Panel B: Heteroskedastic data											
100	9.8	9.8	11.8	14.9	8.9	9.2	9.6	12.2	7.7	7.8	8.5	9.9
500	10.7	12.0	14.9	14.0	9.6	10.7	12.8	12.8	9.6	10.5	12.0	11.6
2000	10.4	11.7	15.3	13.9	10.4	11.8	13.7	11.6	10.5	11.1	12.6	11.4
5000	10.5	12.6	15.2	12.0	10.0	11.3	13.5	11.5	10.2	11.3	13.0	11.1
	Panel C: Autoregressive data											
100	9.5	9.5	10.7	14.7	9.4	9.8	10.1	12.8	8.4	8.9	8.9	11.7
500	11.6	11.6	14.1	14.5	11.1	10.8	12.9	13.6	11.1	10.4	12.4	13.0
2000	10.4	11.8	14.6	12.7	10.2	10.9	13.6	12.4	10.2	10.9	13.3	11.0
5000	10.5	12.4	13.9	12.2	10.5	11.4	12.6	11.3	10.2	11.1	12.0	11.0
	Panel D: AR-GARCH data											
100	9.1	9.4	11.3	14.6	9.1	9.3	10.4	12.9	8.4	9.0	9.2	10.7
500	11.3	11.9	14.1	14.3	10.8	11.0	13.1	13.0	10.2	10.7	11.8	12.5
2000	10.8	12.0	14.1	12.8	10.5	10.9	13.0	11.7	10.5	10.6	12.4	11.4
5000	10.3	11.5	13.9	12.4	10.2	11.4	12.2	11.5	10.3	11.2	11.5	11.0

Notes: This table presents the empirical size of the mode rationality test for a Gaussian kernel, varying sample sizes, varying levels of skewness in the residual distribution and different instrument choices for a nominal significance level of 10%.

Table S.6: Empirical size of the mode rationality test: biweight kernel, 1% significance level.

	Instrument set 1				Instrument set 2				Instrument set 3			
Skewness	0	0.1	0.25	0.5	0	0.1	0.25	0.5	0	0.1	0.25	0.5
Sample size	Panel A: Homoskedastic iid data											
100	0.5	0.6	0.7	1.9	0.2	0.3	0.4	0.9	0.1	0.1	0.2	0.4
500	1.0	1.2	1.8	2.3	0.8	1.0	1.4	1.7	0.7	0.8	1.2	1.4
2000	1.1	1.2	1.8	1.5	1.0	1.2	1.3	1.4	0.8	1.0	1.1	1.2
5000	1.0	1.3	1.7	1.4	1.1	1.1	1.4	1.2	0.9	1.1	1.3	1.2
	Panel B: Heteroskedastic data											
100	0.6	0.6	0.8	1.5	0.4	0.4	0.5	0.7	0.2	0.2	0.1	0.4
500	0.9	1.2	2.0	1.9	0.9	1.1	1.2	1.4	0.8	0.9	1.2	1.1
2000	1.1	1.4	2.6	1.4	1.0	1.2	1.8	1.1	1.1	1.2	1.6	1.2
5000	0.9	1.6	2.4	1.3	0.9	1.4	2.0	1.3	1.0	1.4	1.7	1.2
	Panel C: Autoregressive data											
100	0.6	0.5	0.7	1.9	0.6	0.6	0.6	1.3	0.4	0.4	0.4	0.8
500	1.0	1.0	1.7	2.5	0.9	1.1	1.7	1.8	1.0	0.8	1.4	1.7
2000	1.1	1.1	2.1	1.5	1.2	1.2	1.7	1.3	0.9	1.1	1.6	1.2
5000	1.1	1.5	2.0	1.4	1.1	1.3	1.6	1.2	0.9	1.2	1.5	1.1
	Panel D: AR-GARCH data											
100	0.4	0.5	0.8	1.5	0.4	0.6	0.7	1.1	0.2	0.3	0.3	0.6
500	0.9	1.1	1.9	2.3	0.9	1.0	1.5	1.8	0.9	0.8	1.2	1.4
2000	1.2	1.2	2.0	1.7	1.2	1.0	1.8	1.4	1.2	0.9	1.5	1.2
5000	1.1	1.4	1.5	1.4	1.0	1.4	1.2	1.2	0.9	1.3	1.2	1.2

Notes: This table presents the empirical size of the mode rationality test for a biweight kernel, varying sample sizes, varying levels of skewness in the residual distribution and different instrument choices for a nominal significance level of 1%.

Table S.7: Empirical size of the mode rationality test: biweight kernel, 5% significance level.

	Instrument set 1				Instrument set 2				Instrument set 3			
Skewness	0	0.1	0.25	0.5	0	0.1	0.25	0.5	0	0.1	0.25	0.5
Sample size	Panel A: Homoskedastic iid data											
100	4.4	4.4	5.1	8.2	3.9	3.8	4.0	6.2	2.9	2.8	3.1	4.4
500	5.3	5.9	7.6	8.0	5.0	5.5	6.4	6.9	4.8	4.8	5.9	6.6
2000	5.2	6.6	6.9	6.3	4.9	5.7	6.0	5.9	4.8	5.4	5.5	5.6
5000	5.2	6.0	7.1	6.2	5.0	5.3	6.4	5.6	4.9	5.1	5.8	5.2
	Panel B: Heteroskedastic data											
100	4.5	4.6	5.7	8.0	3.7	3.7	4.3	5.5	3.0	2.9	3.3	3.7
500	5.4	6.2	8.2	7.8	4.6	5.1	6.6	6.3	4.7	5.1	5.7	5.3
2000	5.1	6.5	8.6	6.6	5.5	6.1	7.3	5.4	5.4	5.6	6.4	5.2
5000	5.3	6.9	8.1	6.2	4.9	5.9	7.0	5.6	4.7	5.8	6.9	5.4
	Panel C: Autoregressive data											
100	4.2	4.2	5.0	8.4	4.2	4.3	4.8	6.7	3.5	3.5	3.6	5.2
500	5.6	5.7	7.6	8.2	5.3	5.3	6.6	7.4	5.2	5.0	6.1	6.6
2000	5.1	6.1	8.2	6.4	5.3	5.5	7.4	5.9	5.3	5.5	7.1	5.5
5000	5.5	6.7	7.3	5.9	5.2	6.0	6.5	5.5	4.9	5.9	6.2	5.5
	Panel D: AR-GARCH data											
100	4.1	4.1	5.5	7.8	3.9	4.1	4.8	6.2	3.4	3.6	3.9	4.6
500	5.6	6.0	7.7	7.7	5.4	5.8	6.7	7.0	5.0	5.4	6.0	6.5
2000	5.5	6.4	7.4	6.4	5.5	5.6	7.0	5.9	5.3	5.2	6.5	5.7
5000	5.2	6.0	6.9	6.0	5.3	6.0	5.6	5.6	5.2	5.6	5.5	5.4

Notes: This table presents the empirical size of the mode rationality test for a biweight kernel, varying sample sizes, varying levels of skewness in the residual distribution and different instrument choices for a nominal significance level of 5%.

Table S.8: Empirical size of the mode rationality test: biweight kernel, 10% significance level.

	Instrument set 1				Instrument set 2				Instrument set 3			
	0	0.1	0.25	0.5	0	0.1	0.25	0.5	0	0.1	0.25	0.5
Skewness												
Sample size	Panel A: Homoskedastic iid data											
100	9.8	9.9	10.5	15.2	8.8	8.9	9.0	12.5	8.2	8.2	8.0	10.5
500	10.9	11.4	14.0	14.0	10.5	10.8	12.3	13.0	10.0	10.2	11.4	12.3
2000	10.5	12.4	12.8	11.9	9.9	11.2	11.6	11.2	9.8	10.9	11.2	11.0
5000	10.4	11.9	12.8	11.6	10.4	10.9	11.8	11.1	9.8	10.6	11.3	10.6
	Panel B: Heteroskedastic data											
100	9.9	10.4	12.2	14.9	8.9	9.3	9.9	11.9	7.8	7.8	8.4	9.4
500	10.9	12.1	14.5	13.3	10.0	11.0	13.1	12.2	9.7	10.2	12.0	11.2
2000	10.5	11.9	14.5	12.8	10.3	11.9	13.3	11.1	10.5	11.1	12.2	10.5
5000	10.7	12.6	14.0	11.4	10.1	11.6	12.8	11.0	10.1	11.5	12.3	10.6
	Panel C: Autoregressive data											
100	9.6	9.7	10.8	15.0	9.4	9.8	10.3	12.9	8.3	8.7	9.1	11.7
500	11.8	12.0	13.9	13.9	11.3	10.7	12.7	13.2	10.7	10.3	12.2	12.6
2000	10.6	11.6	14.1	11.8	10.3	11.1	13.2	12.0	10.3	10.7	12.9	10.8
5000	10.7	12.2	13.2	11.6	10.2	11.4	12.4	10.7	9.9	11.2	11.7	10.8
	Panel D: AR-GARCH data											
100	9.7	9.6	11.5	14.6	9.2	9.4	10.6	13.0	8.5	9.0	9.2	11.2
500	11.3	12.0	13.9	13.1	10.8	11.3	12.7	12.7	10.3	10.8	12.1	11.8
2000	10.7	11.8	13.4	11.8	10.7	10.8	12.6	10.8	10.7	10.5	11.7	11.2
5000	10.2	11.4	12.8	11.6	10.3	11.4	11.3	11.1	10.2	10.9	10.8	10.8

Notes: This table presents the empirical size of the mode rationality test for a biweight kernel, varying sample sizes, varying levels of skewness in the residual distribution and different instrument choices for a nominal significance level of 10%.

**Table S.9: Empirical Coverage of the Confidence Sets for Central Tendency:
Cross-sectional data**

Centrality measure	θ_{Mean}	θ_{Med}	θ_{Mode}	Symmetric data				Skewed data			
				100	500	2000	5000	100	500	2000	5000
Panel A: Homoskedastic iid data											
Mean	1.00	0.00	0.00	91.4	90.5	89.5	90.5	90.2	88.7	88.7	90.8
Mode	0.00	0.00	1.00	91.4	89.1	90.2	90.0	88.2	88.9	88.1	88.3
Median	0.25	0.00	0.75	91.0	89.3	90.2	90.1	91.7	92.8	92.7	94.4
Median	0.14	0.50	0.36	92.0	89.1	89.5	90.2	91.4	92.4	91.7	92.4
Median	0.00	1.00	0.00	91.3	90.4	89.4	90.7	90.3	90.1	89.4	91.2
Mean-Mode	0.13	0.00	0.87	90.8	89.5	89.8	89.9	92.3	93.2	91.9	92.7
Mean-Mode	0.07	0.18	0.75	91.1	88.9	89.8	90.0	92.0	93.2	91.4	92.7
Mean-Mode	0.00	0.36	0.64	91.7	89.4	89.9	89.5	91.2	93.4	90.8	92.2
Mean-Median	0.45	0.00	0.55	91.2	88.5	89.8	90.2	92.1	91.9	92.6	93.5
Mean-Median	0.42	0.29	0.29	92.1	88.7	89.7	90.6	90.8	91.3	90.0	91.2
Mean-Median	0.41	0.59	0.00	91.7	89.5	90.4	91.1	90.7	89.5	88.3	89.9
Median-Mode	0.07	0.00	0.93	91.4	89.6	90.1	89.7	91.4	92.8	89.8	91.9
Median-Mode	0.04	0.08	0.88	91.1	89.4	90.0	89.9	91.3	92.8	90.2	91.2
Median-Mode	0.00	0.16	0.84	90.9	89.5	89.8	89.9	91.6	92.6	89.9	91.4
Mean-Median-Mode	0.17	0.00	0.83	90.1	89.2	89.5	90.2	92.6	93.6	92.9	93.4
Mean-Median-Mode	0.09	0.24	0.67	91.1	89.1	89.9	89.6	91.6	93.2	92.7	93.1
Mean-Median-Mode	0.00	0.48	0.52	91.8	89.3	89.8	90.3	91.8	93.1	90.8	92.1
Panel B: Heteroskedastic data											
Mean	1.00	0.00	0.00	91.9	90.5	90.8	90.7	91.9	91.9	90.1	90.0
Mode	0.00	0.00	1.00	90.7	91.6	88.9	90.2	87.5	87.4	88.9	87.4
Median	0.25	0.00	0.75	91.3	90.8	89.1	90.9	90.4	90.7	89.3	91.0
Median	0.14	0.50	0.36	90.9	90.0	88.8	89.9	91.2	92.4	90.4	90.4
Median	0.00	1.00	0.00	90.5	90.5	89.3	90.6	90.9	91.1	90.2	89.3
Mean-Mode	0.13	0.00	0.87	91.0	90.9	89.1	90.5	90.7	91.6	89.9	92.4
Mean-Mode	0.07	0.18	0.75	91.1	90.7	88.4	90.2	90.9	91.0	89.8	92.7
Mean-Mode	0.00	0.36	0.64	91.3	90.4	88.5	90.1	91.5	90.9	90.0	92.0
Mean-Median	0.45	0.00	0.55	91.9	90.7	89.3	90.2	90.7	89.7	88.2	88.4
Mean-Median	0.42	0.29	0.29	91.2	90.7	89.0	89.6	91.1	90.6	88.1	87.3
Mean-Median	0.41	0.59	0.00	92.6	90.0	89.8	91.3	90.7	91.1	89.2	88.8
Median-Mode	0.07	0.00	0.93	90.7	91.1	88.7	90.3	89.8	91.4	89.8	91.6
Median-Mode	0.04	0.08	0.88	90.6	90.9	89.1	90.3	89.9	91.4	89.8	90.9
Median-Mode	0.00	0.16	0.84	90.9	90.6	89.0	90.5	89.9	91.1	89.5	90.7
Mean-Median-Mode	0.17	0.00	0.83	91.4	90.9	89.1	90.7	90.5	91.7	90.5	92.6
Mean-Median-Mode	0.09	0.24	0.67	91.7	90.2	88.3	90.4	91.1	91.3	91.0	92.7
Mean-Median-Mode	0.00	0.48	0.52	91.4	90.4	88.4	90.0	91.5	92.2	90.5	91.8

Notes: This tables presents the empirical coverage rates of the confidence sets for the forecasts of central tendency with a nominal coverage rate of 90%. We report the results for symmetric ($\gamma = 0$) and skewed data ($\gamma = 0.5$), for four sample sizes and the two cross-sectional DGPs. We fix the instruments $\mathbf{h}_t = (1, X_t)$ and use a Gaussian kernel.

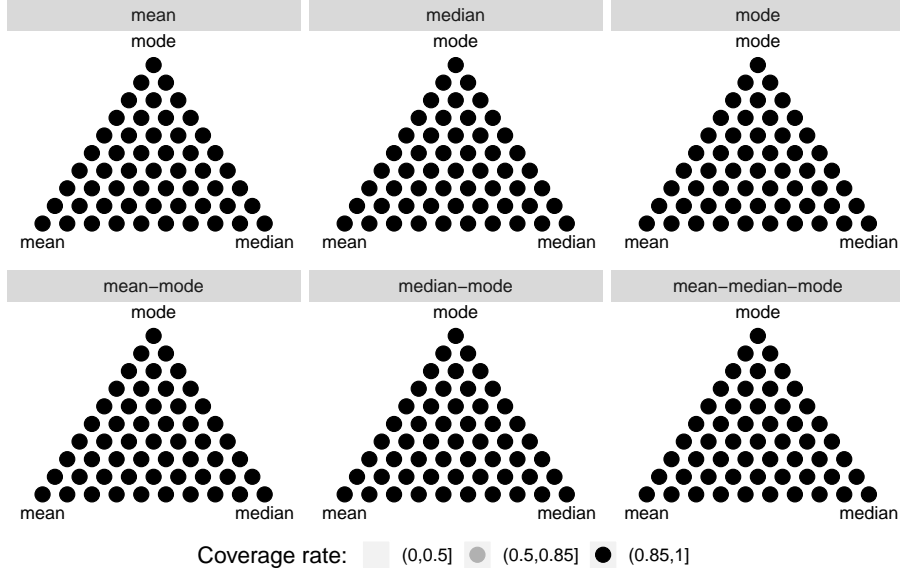
**Table S.10: Empirical Coverage of the Confidence Sets for Central Tendency:
Time Series Data**

Centrality measure	θ_{Mean}	θ_{Med}	θ_{Mode}	Symmetric data				Skewed data			
				100	500	2000	5000	100	500	2000	5000
Panel A: Autoregressive data											
Mean	1.00	0.00	0.00	89.6	88.5	91.0	90.5	87.6	89.8	89.2	90.8
Mode	0.00	0.00	1.00	91.0	89.4	90.9	89.0	86.6	87.7	87.4	86.9
Median	0.25	0.00	0.75	90.1	89.4	89.4	89.5	91.2	92.2	92.3	93.4
Median	0.14	0.50	0.36	88.8	88.7	90.2	90.3	88.2	92.1	90.1	92.5
Median	0.00	1.00	0.00	88.6	89.0	90.7	89.7	85.8	89.8	89.2	91.1
Mean-Mode	0.13	0.00	0.87	90.5	88.1	90.2	89.1	91.6	93.2	91.4	93.1
Mean-Mode	0.07	0.18	0.75	90.1	88.1	89.9	88.9	90.9	92.6	91.4	92.3
Mean-Mode	0.00	0.36	0.64	90.0	88.2	90.3	89.3	90.4	92.3	90.4	92.8
Mean-Median	0.45	0.00	0.55	89.3	88.9	90.5	89.8	89.8	92.2	90.6	93.0
Mean-Median	0.42	0.29	0.29	88.5	89.3	90.6	89.5	87.8	91.0	89.8	91.8
Mean-Median	0.41	0.59	0.00	88.5	89.8	90.9	89.7	86.1	90.0	89.1	91.2
Median-Mode	0.07	0.00	0.93	90.7	88.8	90.6	89.3	90.7	92.2	90.1	91.0
Median-Mode	0.04	0.08	0.88	90.6	88.5	90.2	89.4	90.7	91.7	90.3	90.6
Median-Mode	0.00	0.16	0.84	90.7	88.6	90.4	89.2	90.5	91.4	90.4	90.7
Mean-Median-Mode	0.17	0.00	0.83	90.6	88.2	89.9	89.4	91.3	92.8	91.9	93.2
Mean-Median-Mode	0.09	0.24	0.67	90.1	88.4	89.7	89.6	90.1	92.7	91.0	93.7
Mean-Median-Mode	0.00	0.48	0.52	89.8	88.6	90.4	90.2	89.0	91.6	90.4	93.2
Panel B: AR-GARCH data											
Mean	1.00	0.00	0.00	88.7	87.9	90.6	90.6	88.1	89.7	88.8	90.2
Mode	0.00	0.00	1.00	91.2	90.3	90.9	90.1	88.8	87.3	88.5	90.1
Median	0.25	0.00	0.75	88.9	90.3	89.8	90.3	92.4	92.0	93.6	92.5
Median	0.14	0.50	0.36	88.9	90.4	89.5	89.8	91.0	91.6	92.6	91.6
Median	0.00	1.00	0.00	89.0	90.1	90.3	89.9	89.4	90.1	91.0	89.0
Mean-Mode	0.13	0.00	0.87	90.3	90.8	90.1	90.6	91.6	92.0	93.3	92.3
Mean-Mode	0.07	0.18	0.75	90.0	90.1	90.5	90.5	91.3	91.7	93.6	92.1
Mean-Mode	0.00	0.36	0.64	89.8	90.2	90.6	90.2	90.9	91.0	93.1	91.6
Mean-Median	0.45	0.00	0.55	89.3	89.8	90.3	89.7	91.4	91.4	91.9	91.8
Mean-Median	0.42	0.29	0.29	89.6	90.1	90.0	89.4	90.1	91.4	90.2	90.8
Mean-Median	0.41	0.59	0.00	88.9	89.7	90.0	91.3	88.4	90.5	89.0	88.9
Median-Mode	0.07	0.00	0.93	90.9	90.7	90.7	90.4	91.9	90.8	92.2	91.2
Median-Mode	0.04	0.08	0.88	90.8	90.6	90.8	90.3	91.7	90.9	92.5	90.5
Median-Mode	0.00	0.16	0.84	90.5	90.8	90.6	89.8	91.7	90.8	92.5	90.3
Mean-Median-Mode	0.17	0.00	0.83	90.0	90.6	90.1	90.1	91.9	92.1	93.6	92.1
Mean-Median-Mode	0.09	0.24	0.67	89.4	90.0	90.3	90.6	91.7	92.6	93.3	92.3
Mean-Median-Mode	0.00	0.48	0.52	89.4	90.3	90.2	90.2	91.4	91.2	93.5	92.5

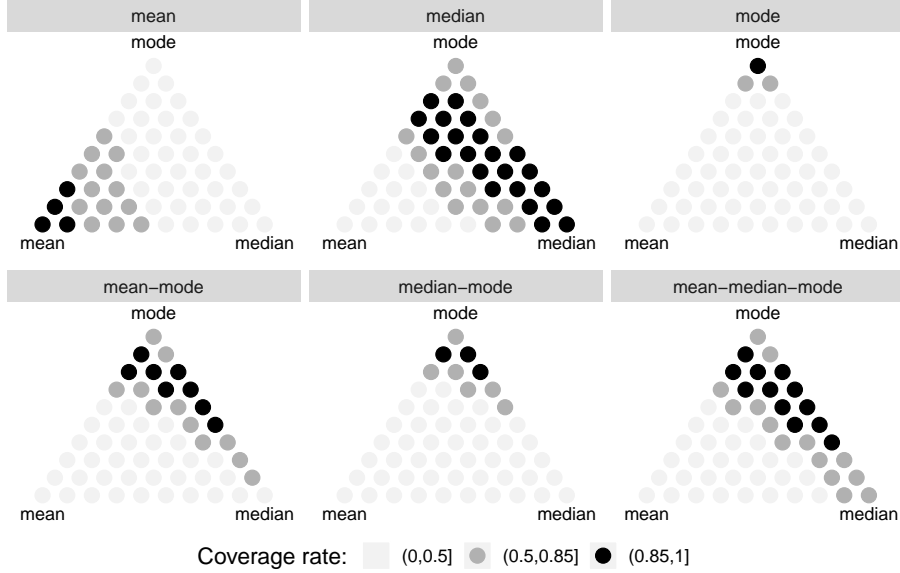
Notes: This tables presents the empirical coverage rates of the confidence sets for the forecasts of central tendency with a nominal coverage rate of 90%. We report the results for symmetric ($\gamma = 0$) and skewed data ($\gamma = 0.5$), for four sample sizes and the two time-series DGPs. We fix the instruments $\mathbf{h}_t = (1, X_t)$ and use a Gaussian kernel.

**Figure 10: Confidence Regions for Central Tendency Measures:
Homoskedastic DGP**

(a) Cross Sectional Homoskedastic DGP with skewness $\gamma = 0$



(b) Cross Sectional Homoskedastic DGP with skewness $\gamma = 0.5$



Notes: This figure shows (average) 90% confidence bounds for the possible measures of central tendency for the homoskedastic DGP. The individual plots correspond to the (true) forecasted functional stated in the text above the triangle. The individual points correspond to the respective convex combinations, and the vertex points correspond to the mean, median and mode functionals. The upper panel shows results for the unskewed DGP, the lower panel for a skewness of $\gamma = 0.5$. We fix the sample size $T = 2000$, the instruments $\mathbf{h}_t = (1, X_t)$ and use a Gaussian kernel.